POLYACETYLENE AND NOVEL CONJUGATED DERIVATIVES THROUGH THE METATHESIS POLYMERIZATION OF 1,3,5,7-CYCLOOCTATETRAENES

Thesis by
Floyd L. Klavetter

In Partial Fulfillment of the Requirements
for the Degree of
Doctor of Philosophy

California Institute of Technology
Pasadena, California
1989
(submitted May 26, 1989)

ACKNOWLEDGMENTS

I would like to acknowledge a number of people who have made my stay at Caltech enjoyable and educational. First, I'd like to thank Bob Grubbs for providing me with an opportunity to work in his laboratory. The diversity of research and talent in the group have played a valuable role in my graduate education.

I thank my lab mates, Tim Swager and Joon Won Park, for the constant encouragement, assistance, and friendship they provided. My gratitude and best wishes are extended to Scott Virgil — a synthetic powerhouse whose undergraduate stint in the Grubbs lab benefitted many of us — for his expertise during the synthesis of some of the tungsten catalyst used throughout my research. To Mike and Chris and Eric and Seth and Bruce, my thanks for your interest and efforts in continuing the poly-COT research, and I apologize for not being there more often to help out.

To Ernie and Paul . . . happy (ice-free) trails! Thanks so much guys, for everything.

I owe a lot to Theresa Daley for opening my eyes a little wider to the world, and for her never-ending smiles and enthusiasm.

Most importantly, I thank my parents, who are always a large part of my life.

ABSTRACT

A Diels-Alder adduct of cyclooctatetraene and benzyne has been polymerized through ring-opening metathesis by titanium methylidene sources to produce a soluble polyacetylene precursor. The polymerization proceeds through first order kinetics and linear increase in molecular weight, providing a route into conjugated polyene segments of various and controlled length.

A versatile and convenient route to polyacetylene has been developed through the condensed phase metathesis polymerization of cyclooctatetraene. Dissolution of catalyst in "neat" cyclooctatetraene provides a means of transforming the liquid into a highly lustrous film at ambient temperture and pressure. These films have physical and spectral properties very similar to films prepared by the Shirakawa methodology. Iodine-doped films exhibit conductivities greater than 300 Ω^{-1}/cm. New processing modes and novel morphologies for polyacetylene have been discovered. Novel polyacetylene derivatives have been prepared to demonstrate the versatility of the method. Both electron-releasing and electron-withdrawing groups have been attached to carbons in the π-conjugated system. These organic materials have been used in the fabrication of solid state devices.

The mechanism of metathesis polymerization with a well-defined tungsten carbene catalyst has been explored, using cyclooctatetraene and its soluble analogue 1,5-cyclooctadiene as monomers. A new phenomenon referred to as "cycloextrusion" has been discovered, and its influence upon the statistical distribution of isomers and the *cis-trans* polymer stereochemistry delineated. Cycloextrusion is a dilute solution phenomenon, limited to cycloolefins containing an unhindered diene moeity in the ring. The thermodynamics and kinetics of the catalyst in the presence of a reversibly binding ligand have been intensively researched. Tetrahydrofuran serves as the reversibly binding ligand which deactivates the catalyst to an extent dependent upon concentration of tetrahydrofuran present. The metathesis of cyclooctadiene with this tungsten carbene can thus be sufficiently retarded to show that the polymerization kinetics involves a catalyst-monomer bound complex, followed by regeneration of catalyst.

Linear copolymers are prepared in both random and block form from the metathesis polymerization of 1,5-cyclooctadiene/cyclooctatetraene and norbornene/cyclooctatetraene solutions, respectively. The average conjugation length in the random copolymers can be varied systematically by varying the mole fraction of cyclooctatetraene in the copolymerization solution. Raman spectroscopy, UV-Vis, NMR, electrical conductivity, and non-linear optical measurements all indicate a progression of conjugation length in the copolymer with increasing mole fraction cyclooctatetraene.

TABLE OF CONTENTS

LIST OF TABLES

CHAPTER 1. Introduction: Polyacetylene and Ring-Opening Metathesis Polymerization

CHAPTER 3. Cyclooctatetrane Liquid Polymerization: A Condensed Phase Route to High-Quality Polyacetylene

CHAPTER 4. Mechanistic Aspects of Metathesis Polymerization with a Well-defined Tungsten Carbene

CHAPTER 5. Novel Linear Polyacetylene Copolymers

LIST OF FIGURES AND SCHEMES

CHAPTER 1. Introduction: Polyacetylene and Ring-Opening Metathesis Polymerization

CHAPTER 2. Kinetic Control in the Polymerization of a Feast Monomer: A Route into Finite Polyenes

CHAPTER 3. Cyclooctatetrane Liquid Polymerization: A Condensed Phase Route to High-Quality Polyacetylene

CHAPTER 4. Mechanistic Aspects of Metathesis Polymerization with a Well-defined Tungsten Carbene

CHAPTER 5. Novel Linear Polyacetylene Copolymers

Chapter 1

Introduction:
Polyacetylene and Ring-Opening Metathesis Polymerization

CONCEPT

The prospect of combining the conductivity of metals with the light weight and processability of polymers has attracted considerable attention.[1] Whereas the vast majority of polymers are highly insulating, conducting polymers exhibit electrical and optical properties similar to those of metals. Unlike metals however, the conductivity in such polymers is highly anisotropic and spans over 15 orders of magnitude dependent upon dopant concentration.

Shown in Figure 1 are the most widely-researched conducting polymers, all of which possess the common structural feature of a conjugated backbone. Extended conjugation contributes to electronic conduction in two important aspects:

(1) Carrier mobility — conjugation delocalizes the p atomic orbitals into bands of spatially-extended molecular orbitals, providing a conduction pathway for the electrons.

(2) Carrier concentration — with increasing degree of conjugation the energy gap between electronically occupied and unoccupied states decreases (Figure 2). The lower this energy gap, the more valence electrons will be promoted into the conduction band.

Synthetic strategies continue to target backbone conjugation as the key to attaining highly conductive polymers.[2]

The greatest effort in the field of conducting polymers has been devoted to polyacetylene.[3] More theory, more characterization, more routes of preparation exist for polyacetylene than for any other conducting polymer. It is unique in its mechanism and magnitude of conduction. In fact, Naarmann and co-workers have recently reported doped polyacetylene films which have the highest room-temperature conductance/gram of any material known to man.[4]

This introduction discusses the progress and problems associated with polyacetylene, and the role that ring-opening metathesis polymerization offers to provide.

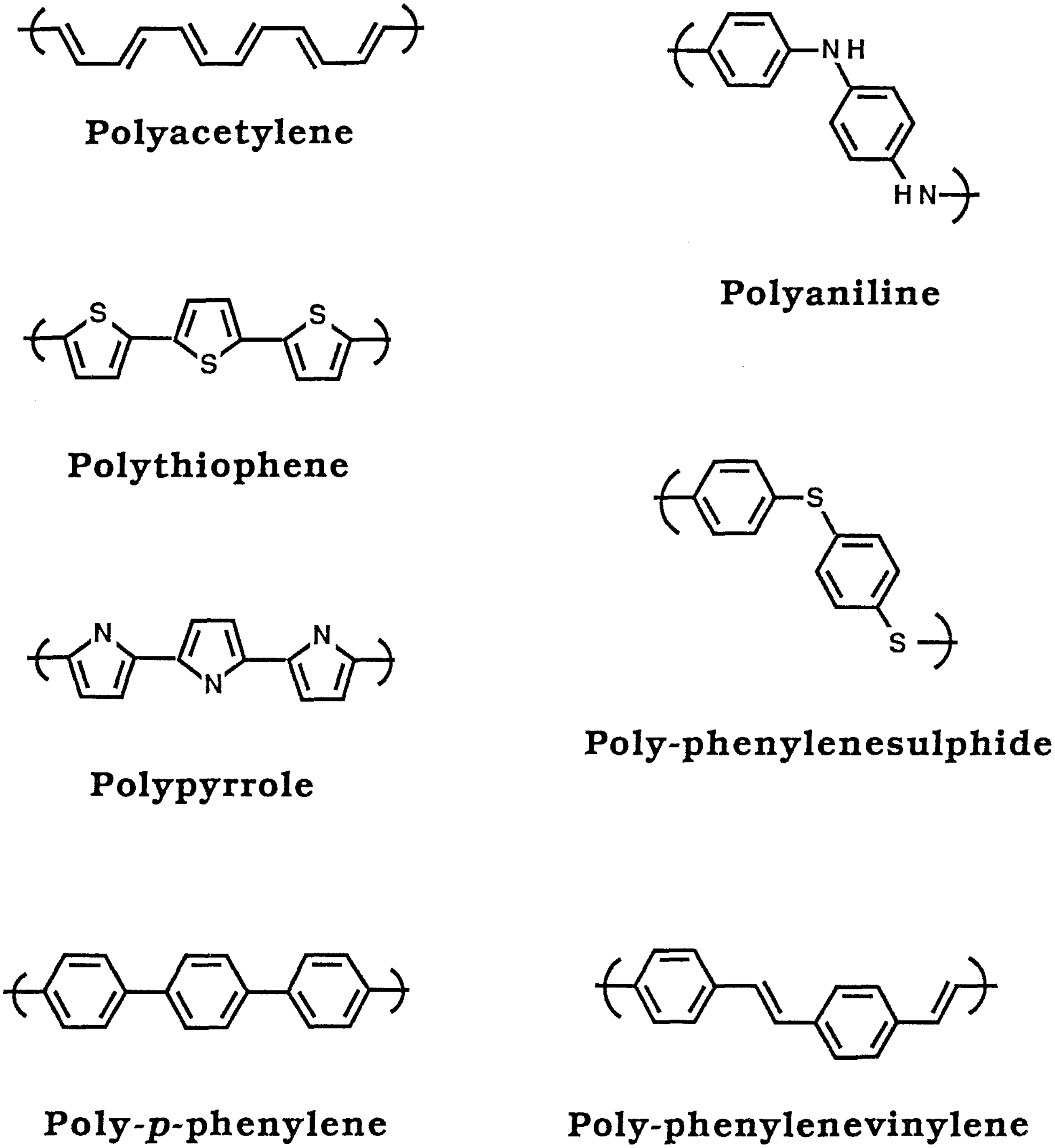

Polyacetylene

Polyaniline

Polythiophene

Poly-phenylenesulphide

Polypyrrole

Poly-*p*-phenylene

Poly-phenylenevinylene

Figure 1. Structures of widely-researched conducting polymers.

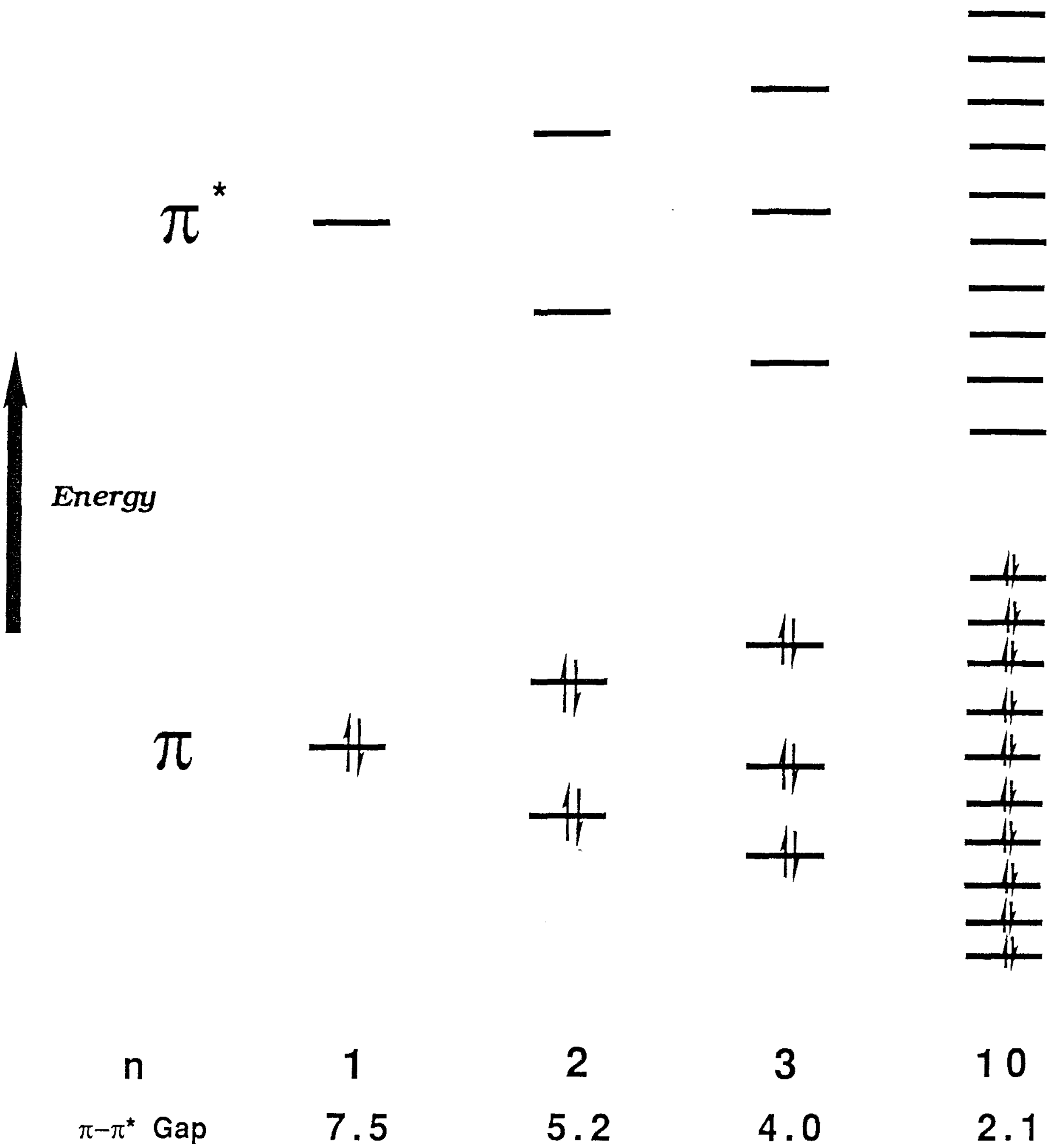

Figure 2: Energy gap *vs.* conjugation length. For each of four polyenes (-C=C-)$_n$ where **n** is the number of conjugated double bonds, the relative energy of the π-symmetry orbitals is depicted graphically. With increasing conjugation length the π–π* energy gap (in eV) decreases.

HISTORY

It was in the 1950's Natta *et al.* first polymerized acetylene by bubbling the gas into an organotitanium/trialkylaluminum catalyst solution.[5] The resulting black, powdery precipitate was found to be universally insoluble, air sensitive, and largely non-conductive. Subsequent experiments demonstrated that compressed pellets of this substance, upon exposure to Lewis acids, behaved as broad band semi-conductors.[6] However, the difficulty associated with handling and analyzing this insoluble powder did little to encourage further investigation.

A major breakthrough occurred in 1971 when H. Shirakawa and co-workers produced free-standing polyacetylene films.[7] Acetylene gas polymerized on the surface of a highly concentrated Ziegler-Natta catalyst solution resulted in semi-flexible, highly lustrous films. By 1974 conditions had been optimized:

> A slurry of triethylaluminum and titanium tetra-*n*-butoxide (4:1) in toluene is used to coat the inner walls of a Schlenk tube (inert atmosphere). Acetylene gas is introduced into the tube in 30-second intervals, polymerizing on the catalyst surface. The silvery film of polyacetylene can then be pried loose from the reactor wall, intact.[8]

Although conditions have been developed to polymerize acetylene as a low-density gel[9] or in protic solvents,[10] the vast majority of polyacetylene research continues to depend upon the Shirakawa method for producing films. Films so produced are air sensitive and highly intractable as is polyacetylene in powder form, but the physical continuity and optical reflectivity of these films provide the means for detailed investigation. Accordingly, numerous academic, industrial, and governmental laboratories have entered the field, resulting in a treasury of information on polyacetylene.[3]

PROGRESS

Exposing polyacetylene films to oxidizing agents (I_2, AsF_5, HNO_3) or reducing agents (sodium napthalide) has been found[11] to significantly increase the conductivity, imparting truly metallic transport properties to this organic polymer.[12] Naarmann's recent modification of the Shirakawa method has resulted in doped polyacetylene films having much improved environmental stability and conductivity near $10^6\ \Omega^{-1}/\text{cm}$.[4] Currently, polyacetylene exhibits a range of conductivities (depends on dopant concentration) unparalleled by other materials.

Table 1: Conductivities of Materials

Material	Log conductivity (Ω^{-1}/cm)
Ag, Cu	6.5
Pb	6
Fe, doped $(SN)_x$	5
Bi	4
Graphite, $(SN)_x$	3
Doped $(CH)_x$	-10 to 6
Doped Si	-4 to 0
Distilled water	-8
Diamond	-12
Polystyrene	-18

Moreover, partially aligned (stretched) polyacetylene films exhibit anisotropic electrical and optical properties, demonstrating features unique to 1-dimensional materials.[13] Polyacetylene has been successfully used in the fabrication of dc batteries,[14] photovoltaic cells,[15] and neutron flux detectors.[16] In *trans* polyacetylene, extensive electronic-vibrational coupling[17] and the saturation of photoexcited states (charged soliton pairs) at exceptionally low excitation intensities[18] presents the possibility of using this material in non-linear optics.[18-20] Nevertheless, problematic features limit both the understanding and the practicality of polyacetylene.

PROBLEMS

Intractability

The insoluble nature of polyacetylene complicates key aspects of its characterization. In addition, the absence of a glass transition (softening) point precludes melt processability. Does the same feature which conveys the electrical and optical attributes to polyacetylene — namely, a rigid pπ-pπ conjugated backbone — also limit the degree to which it can be physically manipulated?

In an attempt to produce soluble conductive polymers, numerous alkyl and dialkyl acetylenes (that is, terminal and internal alkynes) have been polymerized by the Shirakawa method.[1b] Of these derivatives, polypropyne exhibits the greatest conductivity ($10^{-3}\ \Omega^{-1}$/cm), though loses its solubility in the process of doping. Alkyl- or phenyl-substituted acetylenes have been copolymerized with acetylene.[21] As solubility of the copolymer increases (with decreasing percentage of acetylene in the mixture), conductivity decreases. Graft copolymers of polyacetylene on polybutadiene or polyisoprene have been prepared, with limited success.[22-26] Attempted copolymerizations of ethylene and acetylene have failed altogether to produce copolymer.[27]

Using the following strategy, Feast and Edwards have prepared a soluble precursor to polyacetylene:[28]

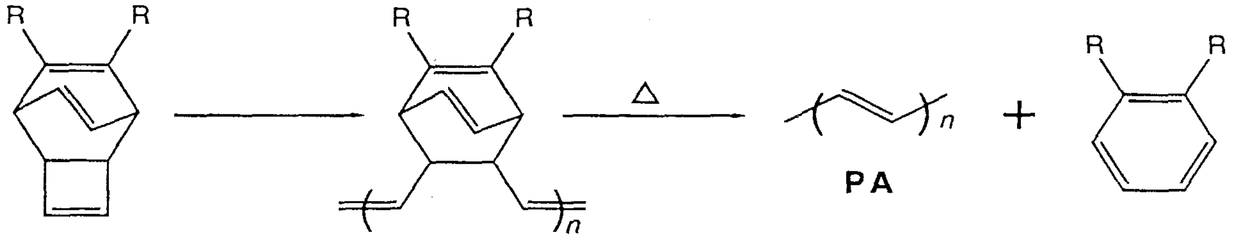

The soluble precursor can be analyzed by gel permeation chromatography for molecular weight, exhibits desirable viscoelastic properties, is readily purified from catalyst residue, and can be cast into films. Extrusion of aromatic molecules from a solution of this polymer yields polyacetylene only in powder form, and heating of the bulk precursor polymer results in incomplete extrusion of the aromatics. However, stretch-aligned films of the precursor, upon heating and subsequent doping, exhibit conductivities greater than $10^2\ \Omega^{-1}/\mathrm{cm}$.[29]

One investigation into the bulk processability of polyacetylene has employed a post-polymerization, "thermo-mechanical" fusion of polyacetylene powder.[30] No mention was made as to the doped conductivity of the heat-treated material. It is known, however, that such thermal treatment results in cross-linking and chain degradation.[31]

Although certain alternatives exist, the polyacetylene community still awaits a broadly applicable approach for the processing of this conducting polymer.

Stability

The greatest technical problem with polyacetylene lies in its instability towards atmospheric oxidation. Highest conductivities in doped Shirakawa polyacetylene correspond to those films with the lowest oxygen content (parts per thousand).[32] Oxidative degradation follows first-order kinetics

$$\left(\mathrm{CH}{=}\mathrm{CH}\right)_n + O_2 \underset{k_3}{\overset{k_1\ \text{(Rapid)}}{\rightleftharpoons}} [\text{PA / bound } O_2] \xrightarrow{k_2} \text{Products}$$

in which k_3 is very small.[33] After several days exposure of Shirakawa polyacetylene to atmosphere, the polyacetylene film is degraded irreversibly to an insulator, whereupon doping with iodine or arsenic pentafluoride is rendered ineffective.[34] Infrared bands appear in hydroxyl and ketone regions of polyacetylene that has undergone atmospheric degradation.[7]

Iodine-doped polyacetylene is somewhat more stable to oxidative degradation. After relatively rapid loss of one order magnitude in conductivity upon exposure to atmosphere, iodine-doped polyacetylene exhibits a conductivity loss of approximately one order magnitude per fifty days.[22,35] Doped polyacetylene stored in an inert atmosphere, after a slight initial loss, demonstrates a stable conductivity.[35]

Incorporation of anti-oxidants into doped films prolongs conductivity values by as much as a factor of four.[36,37] Encapsulation by polyethylene inhibits atmospheric oxidation, but is only short-term effective.[13] Silicone rubber protects films from atmospheric degradation for a longer period, but only non-porous materials (glass, metal) have proven to be entirely effective as encapsulants.[21]

Di-substituted polyacetylene derivatives containing no allylic or vinylic hydrogens, as well as mono-substituted *tert*-butyl polyacetylene $(\text{-HC=C(t-Bu)-})_n$, demonstrate exceptional atmospheric stability.[38] However, these same polymers have low doped conductivities, suggesting that the steric bulkiness of the substituents forces the backbone to twist out of conjugation.

Recently, much interest has been aroused by conjugated poly-heterocycles — most notably polyaniline, polythiophene, and polypyrrole.[39] These conducting polymers are processible to some degree in undoped form, and demonstrate good environmental stability in doped form. However, the increased stability of such materials is offset by their lower conductivity (three to five orders magnitude lower than polyacetylene) and the difficulty of preparation.

Mechanism of Conduction

Pristine polyacetylene is an extrinsic semi-conductor with band gap ~1.5 eV.[13] The relatively wide gap between π and π^* states was first explained by Peierls as due to a lattice distortion in which electrons localize into alternating double bonds.[40] This dimerization has subsequently been confirmed by experiment,[41] revealing that the alternating "double bonds" in polyacetylene are .04-.05 Å longer than the "single bonds."

Exposure of polyacetylene to iodine results in a positively charged (*p*-doped) polymer backbone, the counterions being primarily tri-iodide anions.[12] Exposure to arsenic pentafluoride also results in a *p*-doped polymer, with AsF_3 and (presumably) $[AsF_6]^-$ counterion. Reaction of polyacetylene with sodium napthalide results in an *n*-doped polymer and sodium cations.[42]

Both (1) chemical doping, independent of dopant, and (2) photoexcitation lead to formation of the same vibronic and electronic sates.[17] In confirmation of theory,[43] recent optical studies have provided direct evidence for the existence of a charged soliton band positioned energetically between the valence and conduction bands.[18,20] The soliton mechanism proposed for conductivity has proven effective in rationalizing the differing photoluminescent and photoconductive transport properties for *cis* and *trans* polyacetylene.[19] Thermopower and electron paramagnetic[12] resonance measurements are consistent with charged soliton conduction for moderately doped films. There is debate, however, regarding the sudden insulator to metal transition upon incremental increase of dopant.

The understanding of high conductivity in doped polyacetylene is more than an academic curiosity. Determining whether electronics (band gap) or lattice (interchain contact) is the limiting factor in polyacetylene's conductivity should lend insight into designing materials with even greater transport properties.

In summation, there is a need to probe the determinants of processability, stability, and conductivity. Intercorrelations of properties (density, crystallinity, conductivity, band gap, etc...) will become feasible only when an array of data has been amassed. New synthetic methodologies are required which will generate novel morphologies, yield new polyacetylene derivatives, and allow control of conjugation length. Hence, routes for the preparation of polyacetylene and its derviatives will now be considered.

ROLE OF METATHESIS POLYMERIZATION

Strategy First, Tactics Later*

Some methods used in the preparation of acetylenic polymers are illustrated below:

(1) Acetylene Polymerization

$$RC\equiv RC \xrightarrow[\text{or Free Radicals}]{\text{Transition Metal Catalysts}} \text{Polyacetylene}$$

(2) Polymer Backbone Transformations

$$\left(CH_2-CH(OH)\right)_n \xrightarrow[-H_2O]{H_2SO_4} \text{Polyacetylene}$$

$$\left(CH-CH_2-CHCl-CH\right)_n \xrightarrow{\text{Base / DMF}} \text{Polyacetylene}$$

$$\left(CH-CHCl-CHCl-CH\right)_n \xrightarrow{-Cl_2} \text{Polyacetylene}$$

(3) Ketone-mediated Polymerizations

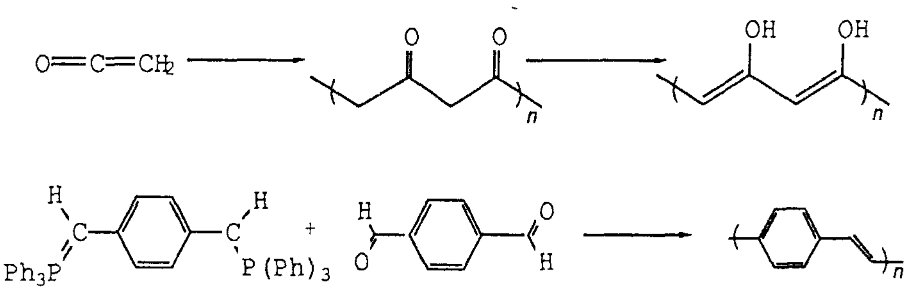

PPV

---

*Mikael Tal, former World Chess Champion (USSR)

While Ziegler-Natta catalysts (specifically, the Shirakwa system) have been employed extensively in preparing acetylenic polymers, methods (2)[2b-d] and (3)[2e,2f] have received little appreciation, largely due to the incompleteness of reaction resulting in oligomers and possible side reactions which interrupt backbone conjugation.

A more general, cleaner route to unsaturated polymers involves the ring-opening metathesis of cyclic olefins:[44]

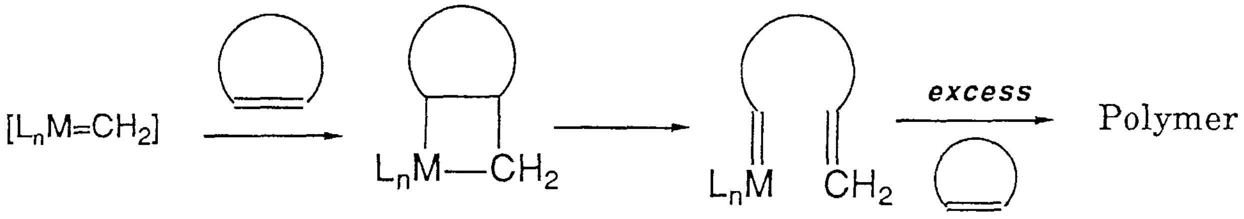

Metathesis polymerization occurs in olefins ring sizes of three, four, five, seven, and eight carbon atoms, as well as in larger rings. The six-membered ring's resistance to undergo polymerization probably stems from the low ring strain energy. Still, ring-opening metathesis polymerization (ROMP) offers a variety of possibilities for preparing conjugated polymers (see Table 2).

Those structures which might seem to be irresponsible suggestions for metathesis polymerization may, upon further consideration, prove to be more reasonable candidates. The reactivity or conjugation of a monomer can possibly be masked, resulting in a non-conjugated polyacetylene precursor. An advantage of such masking is that the non-conjugated precursor may be soluble and processable. The metathesis polymerization of such a monomer (masked cyclobutadiene) has been accomplished by Edwards and Feast.[28] Metathesis polymerization of the thermally unstable monomer benzvalene is known to yield a precursor polymer which can be partially isomerized to polyacetylene.[45]

The synthesis of conducting polymers is a field of research rich in science and technology. The research calls for an awareness of the possibilities and limitations in monomer and polymer synthesis, of morphology-property relationships, of catalytic control during the polymerization reaction. Once

TABLE 2

POTENTIAL RING-OPENING METATHESIS ROUTES TO CONJUGATED POLYMERS

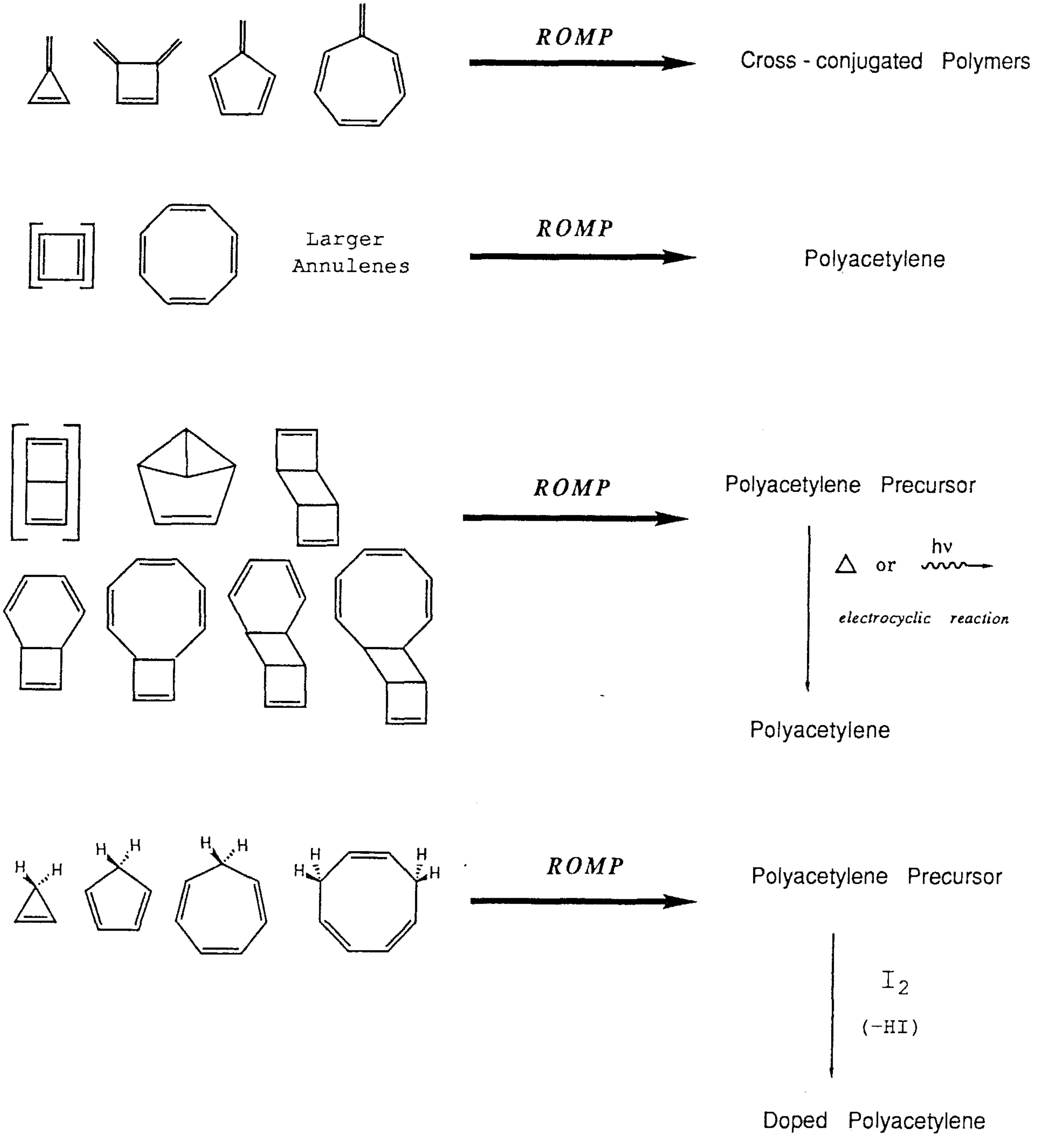

synthesized, analysis of the conducting polymers requires experimental competence in condensed-phase materials science; furthermore, knowledge in solid state physics (band structure, band bending, transport phenomena) is necessary for the correct interpretation of data. As with all science, the synthetic chemist must be aware of the problems existing in the field and must be prepared to direct his/her research to confront those challenges which are the most difficult, the most important, to the understanding and application of conducting polymers.

REFERENCES

(1) General reviews of conducting polymers: (a) Gill, W. D.; Clarke, T. C.; Street, G. B. *Appl. Phys. Comm.* **1982**, *2*(4), 211. (b) Gibson, H. W.; Pochan, J. M. *Encyclopedia of Polymer Science and Engineering*; Wiley-Interscience: New York, 1985; Vol. 1, pp 87-130. (c) Hermann, A. M. *Appl. Phys. Comm.* **1983**, *3*(1 & 2), 59. (d) Wudl, F.; Heeger, A. J.; Kobayashi, M.; Chen, J.; Chung, T. C.; Moraes, F. *Synth. Met.* **1984**, *9*, 77. (e) Wegner, G. *Angew. Chem, Int. Ed. Engl.* **1981**, *20*, 361. (f) *Handbook of Conducting Polymers*; Skotheim, T. A., Ed.; Marcel Dekker, Inc.: New York, 1986; Vols. 1 and 2.

(2) (a) Gibson, H. W.; Pochan, J. M. *Encyclopedia of Polymer Science and Engineering*; Wiley-Interscience: New York, 1985; Vol. 1, pp 87-130. (b) Lichtmann, L. S.; Fitchen, D. B. *Synth. Met.* **1979**, *1*, 139. (c) Minoura, Y.; Ikeda, H. *J. Appl. Polym. Sci.* **1971**, *15*, 2219. (d) Brunthaler, J. K.; Stelzer, F.; Leising, G. *J. Mol. Catal.* **1985**, *28*, 393. (e) Okamoto, Y.; Hwang, E.; Wang, M. *J. Polym. Sci., Polym. Lett. Ed.* **1985**, *23*, 285. (f) Gill, W. D.; Clarke, T. C.; Street, G. B. *Appl. Phys. Comm.* **1982**, *2*(4), 211. (g) Feast, W. J. In *Handbook of Conducting Polymers*; Skotheim, T. A., Ed.; Marcel Dekker, Inc.: New York, 1986; Vol. 1, pp 1-43.

(3) For an excellent compilation of polyacetylene research, see Chien, J. C. W. *Polyacetylene*; Academic Press: Orlando, FL, 1984.

(4) Basescu, N.; Liu, Z.-X.; Moses, D.; Heeger, A. J.; Naarmann, H.; Theophilou, N. *Nature* **1987**, *327*, 403.

(5) Natta, G.; Mazzanti, G. P.; Corrandi, P. *Atti. Naz. Lincei. Cl. Sci. Fis. Mat. Nat. Rend.* **1958**, *25*(8), 3.

(6) Berets, D. J.; Smith, D. S. *Trans. Far. Sci.* **1968**, *64*, 827.

(7) Shirakawa, H.; Ikeda, S. *Polym. J.* **1971**, *2*, 231.

(8) Ito, T.; Shirakawa, H.; Ikeda, S. *J. Polym. Sci, Polym. Chem. Ed.* **1974**, *12*, 11.

(9) Wnek, G. E.; Chien, J. C. W.; Karasz, F. E.; Druy, M. A.; Park, Y. W.; MacDiarmid, A. G.; Heeger, A. J. *J. Polym. Lett. Ed.* **1979**, *17*, 779.

(10) Lieser, G. E.; Wegner, G.; Mueller, W.; Enkelmann, V. *Makromol. Chem., Rapid Commun.* **1980**, *1*,621.

(11) Shirakawa, H.; Louis, E. J.; MacDiarmid, A. G.; Chiang, C. K.; Heeger, A. J. *J. Chem. Soc., Chem. Commun.* **1977**, 578.

(12) Mihaly, G.; Vansco, G.; Pekker, S.; Janossy, A. *Synth. Met.* **1980**, *1*, 357.

(13) Park, Y. W.; Druy, M. A.; Chiang, C. K.; MacDiarmid, A. G.; Heeger, A. J.; Shirakawa, H.; Ikeda, S. *J. Polym. Sci., Polym. Lett. Ed.* **1979**, *17*, 195.

(14) (a) Wanqun, W.; Mammone, R. J.; MacDiarmid, A. G. *Synth. Met.* **1985**, *10*, 235. (b) Nigrey, P. J.; MacInnes, D.; Nairns, D. P.; MacDiarmid, A. G.; Heeger, A. J. *Synth. Met.* **1984**, *9*, 1.

(15) (a) Tani, T.; Grant, P.; Gill, W.; Street, G.; Clarke, T. *Solid State Commun.* **1980**, *33*, 499. (b) Shirakawa, H.; Ikeda, S.; Aizawa, M.; Yoshitake, J.; Suzuki, S. *Synth. Met.* **1981**, *4*, 43.

(16) Butler, M.; Grinley, D. *Chem. Eng. News* **1987**, *65*(6), 24.

(17) Heeger, A. J.; Blanchet, G.; Chung, T. C.; Fincher, C. R. *Synth. Met.* **1984**, *9*, 173.

(18) Blanchet, G.; Fincher, C. R.; Chung, T. C.; Heeger, A. J. *Phys. Rev. Lett.* **1983**, *50*(24), 1983.

(19) Lauchlan, L.; Etemand, S.; Chung, T. C.; Heeger, A. J.; MacDiarmid, A. G. *Phys. Rev. B* **1981**, *24*(7), 3701.

(20) Vardeny, A.; Orenstein, J.; Baker, G. *Phys. Rev. Lett.* **1983**, *50*(25), 2032.

(21) Deits, W.; Cukor, P.; Rubner, M.; Jopson, H. *Synth. Met.* **1982**, *4*, 199.

(22) Aldissi, M.; Bishop, A. R. *Synth. Met.* **1986**, *14*, 13.

(23) Aldissi, M. *Synth. Met.* **1986**, *13*, 87.

(24) Bates, F.; Baker, G. *Macromolecules* **1983**, *16*, 1013.

(25) Bates, F.; Baker, G. *Macromolecules* **1983**, *16*, 704.

(26) Bolognesi, A.; Catellani, M.; Destri, S.; Porzio, W. *Polymer* **1986**, *27*, 1128.

(27) Chien, J. C. W.; Babu, G. N. *Macromolecules* **1985**, *18*, 622.

(28) Edwards, J. H.; Feast, W. J. *Polymer*, **1980**, *21*, 595.

(29) For publications on the resulting ("Durham") polyacetylene, see (a) Edwards, J.; Feast, W. J.; Bott, D. *Polymer*, **1984**, *25*, 395. (b) Friend, R.; Bradley, D.; Pereira, C.; Townsend, P.; Bott, D.; Williams, K. *Synth. Met.*, **1986**, *13*, 101. (c) Bott, C.; Brown, C.; Chai, C.; Walker, N.; Feast, W. J.; Foot, P.; Calvert, P.; Billingham, N.; Friend, R. *Synth. Met.*

1986, *14*, 245.

(30) Wessling, B.; Volk, H. *Synth. Met.* **1986**, *15*, 183.

(31) Ito, T.; Shirakawa, H.; Ikeda, S. *J. Polym. Sci., Polym. Chem. Ed.* **1975**, *13*, 1943.

(32) Chiang, C. K.; Park, Y. W.; Heeger, A. J.; Shirakawa, H.; Louis, E. J.; MacDiarmid, A. G. *J. Chem. Phys.* **1978**, *69*(11), 5098.

(33) Pochan, J. M.; Pochan, D. F.; Rommelmann, H.; Gibson, H. W. *Macromolecules* **1981**, *14*(1), 110.

(34) Pochan, J. M.; Gibson, H. W.; Harbour, J. *Polymer* **1982**, *23*, 439.

(35) Mueller, H. K.; Höcker, J.; Menke, K.; Ehinger, K.; Roth, S. *Synth. Met.* **1985**, *10*, 273.

(36) Rubner, M. F.; Tripathy, S. K.; Georger, J.; Cholewa, P. *Macromolecules* **1983**, *16*(6), 870.

(37) Aldissi, M. *Synth. Met.* **1986**, *15*, 141.

(38) Masuda, T.; Tang, B.; Higashimura, T. *Macromolecules* **1985**, *18*, 2369.

(39) Druy, M.; Rubner, M.; Walsh, S. *Synth. Met.* **1986**, *13*, 207.

(40) Peierls, R. E. *Quantum Theory of Solids*; Oxford Univ. Press: London, 1955; p 108.

(41) Fincher, C.; Chen, C. E.; Heeger, A. J.; MacDiarmid, A. G.; Hasting, J. B. *Phys. Rev. Lett.* **1982**, *48*, 100.

(42) Clarke, T. C.; Street, G. B. *Synth. Met.* **1980**, *1*, 119.

(43) Su, W.; Schrieffer, J. *Proc. Natl. Acad. Sci.* **1980**, *77*, 5626.

(44) For reviews of ring-opening metathesis, see (a) Ivin, K. J. *Olefin Metathesis*; Academic Press: London, 1983. (b) Grubbs, R. H. In *Comprehensive Organometallic Chemistry*; Wilkinson, G. E., Ed.; Permagon Press: Oxford, 1982; Vol. 8, pp 499-551. (c) Gilliom, L. R.; Grubbs, R. H. *J. Am. Chem. Soc.* **1986**, *108*, 733.

(45) Swager, T. M.; Grubbs, R. H. *J. Am. Chem. Soc.* **1987**, *109*(3), 894.

Chapter 2

Kinetic Control in the Polymerization of a Feast Monomer: A Route into Finite Polyenes

ABSTRACT

The [2 +4] Diels-Alder adduct of 1,3,5,7-cyclooctatetraene and benzyne is polymerized through ring-opening metathesis by titanium methylidene sources to produce a soluble polyacetylene precursor. The polymerization proceeds through first order kinetics and linear increase in polymer molecular weight, providing a route into conjugated polyene segments of various and controllable length. This research represents the first successful polymerization enabling experimental control over the length of polyacetylene chains.

INTRODUCTION

Although polyacetylene is one of the most thoroughly studied materials,[1] many key questions plague researchers in this field. One of the more fundamental questions involves the affect that chain length has upon properties. It is known that chain length for short polyenes is the determining factor for the $\pi-\pi^*$ transition energy,[2] but what is the situation in longer polyenes? To what degree does chain length govern the band gap, and consequently, the electronic populations of the valence and conduction bands? What is the minimum conjugation length necessary to support electronic conduction in polyacetylene? While early studies have suggested that transport properties are not affected by chain length,[3] the high conductivity of polyacetylene prepared by Naarmann and co-workers[4] has been attributed by some researchers as the result of chains with unprecedented conjugation lengths. Polyacetylene researchers are still uncertain as to the correlation between chain length (for polyenes having 15 double bonds or more) and material properties such as atmospheric stability, dopability, carrier mobility, and electrical conductivity.

The vast majority of research is performed on polyacetylene prepared by the Shirakawa method. While this method provides polyacetylene of known high quality, the heterogeneous conditions and instantaneous reaction involved in Ziegler-Natta polymerization of acetylene at a gas-slurry interface allow little flexibility or kinetic control during the synthesis. Of particular interest would be the ability to grow any polymer chain length desired. However, the insolubility of even short chain polyacetylene chains precludes the possibility of homogeneous conditions essential for kinetic control.

Feast and Edwards have recently reported the preparation of polymers which, through extrusion of aromatic molecules by a thermally-allowed electrocyclic process, are transformed into polyacetylene.[6] The strategy is depicted as follows:

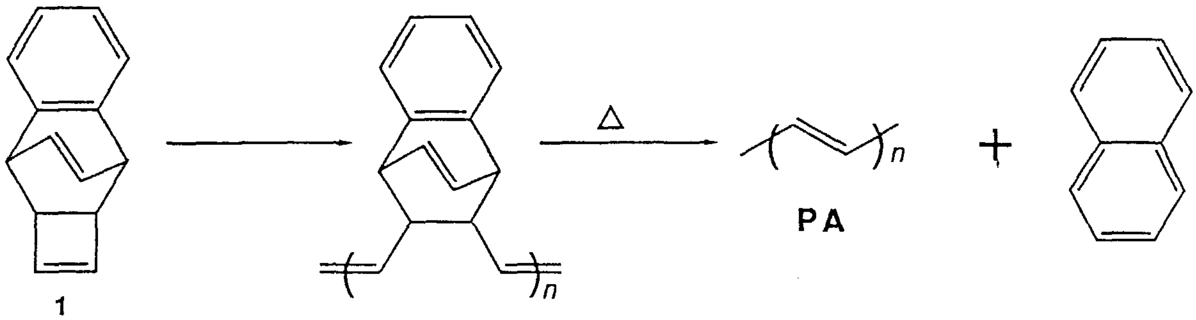

Polyacetylene — intractable by nature of the π-conjugated backbone — can thus be manipulated through these *soluble* precursors. This prospect has subsequently spurred much activity towards the characterization of both the precursor and the resulting polyacetylene.[7]

Currently, the precursor polymers are formed through the metathesis polymerization of monomer by a two-component initiator ($WCl_6/SnMe_4$). The limitations of such a catalyst system are realized in terms of uncontrollable kinetics, broad molecular weight distributions of polymer, and possible undesirable side reactions such as "back-biting" and allylic chlorination.[8,9]

Previous work[10] has focused upon the utilization of the following well-defined *bis*-(η^5-cyclopentadienyl)titanium carbene sources

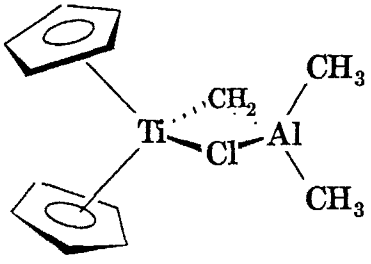

2a

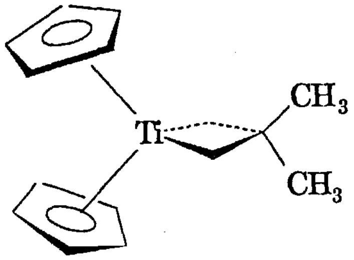

2b

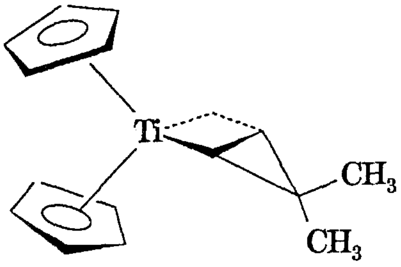

2c

in ring-opening metathesis polymerization (ROMP) to resolve some of the limitations of "classic" metathesis systems such as $WCl_6/SnMe_4$. The metathesis polymerization of norbornene with these titanocene metallacycles provides a living system with well-defined kinetics, no side reactions, and monodisperse polymeric product.[11] This study applies these titanocene carbene sources to the polymerization of cycloolefin **1** enabling a route into polyacetylene of control in the preparation of chain lengths.

Experimental.

General Considerations. All work involving air or moisture sensitive compounds was performed using standard high-vacuum or Schlenk techniques under argon purified by passage through BASF RS-11 (Chemalog) and Linde 4Å moloecular sieves. All gas chromatography was performed on a Shimadzu GC-mini 2 flame ionization instrument equipped with a 0.24 mm x 25 m SE-30 capillary column. Gel permeation chromatography (GPC) studies utilized Shodex KF-803 and KF-804 columns, a Spectroflow 757 absorbance detector with l = 254 nm, and a Knauer differential refractometer. All catalyst and monomer stock solutions (for kinetics) were stored at -40 °C in a nitrogen filled Vacuum Atmospheres drybox equipped with refrigeration unit. NMR spectra were recorded with either a JEOL FX-90Q (89.6 MHz ^1H; 22.53 MHz ^{13}C) or a JEOL GX-400 (399.65 MHz ^1H; 100.40 MHz ^{13}C), each equipped with variable temperature thermostatting.

Materials. Toluene was vacuum distilled from a sodium benzophenone ketyl, as were deuterated benzene and toluene (Cambridge Isotope Laboratories). Deutero-chloroform was dried over 3Å molecular sieves. Titanium metallacycles (**2b**, **2c**) and Tebbe's reagent (**2a**) were prepared as previously described.[10] Monomer **1** was prepared as in literature,[12] and purified by repeated sublimation until free from contamination as determined by GC. Acetone, perdeutero-acetone (Cambridge Isotopes), and methanol (all anhydrous) were handled as such and degassed prior to use. GC internal standard 9,10-dihydroanthracene (Aldrich) was sublimed *in vacuo* and subsequently transferred to the drybox for storage.

Since relatively *low concentrations of catalyst* are employed in the polymerizations, it is emphasized that solvent, monomer, and internal standard (in kinetic studies) must be free from catalyst-poisoning agents (most notably oxygen, acidic/protic functionalities, and ketones or aldehydes).

Polymerization. A 0.617 M standard solution of catalyst **2c** (132 mg dissolved in .83 mL toluene) was prepared and stored under inert atmosphere at -40 °C. Stock solutions of **1** were laced with approximately 5% of purified internal standard.[13] Relative ratio of **1** to internal standard was monitored throughout the polymerization by GC. Response factor of internal standard ($C_{14}H_{12}$) relative to monomer ($C_{14}H_{12}$) was determined to be 1.0 based on 18 injections of standardized solutions. Reproducibility per injection was 5-8%.

Catalyst and monomer solutions were mixed by means of air-tight, calibrated syringes. A 1-ml Kontes glass vial equipped with septum-protected syringe port served as reaction vessel. Efficient magnetic stirring was maintained throughout the polymerization. No effort was made to thermostat the room temperature polymerizations; at 50 °C, a Therm-O-Watch controlled oil bath was used. Kinetics at this temperature revealed $k_1 = 0.015 \pm .002\ \text{sec}^{-1}$.

GPC Analysis of Polymer. All analyses were performed on 0.2% w/v solutions of polymer in THF. Flow rate was 1 mL / minute. Calibration was based upon monodisperse polystyrene samples (Polysciences) of various molecular weight. Polydispersities were calculated by standard procedures[14] from the UV trace and were not corrected for peak broadening.

Low-temperature ^{1}H NMR. Monomer **1** (1.8 mg in 0.10 mL d_8-toluene, 0.5 equivalents) was added *via* syringe to Tebbe's reagent **2a** (5.7 mg in 0.50 mL d_8-toluene) in a septum-capped NMR tube at -40 °C. Upon the addition of excess base (0.05 mL pyridine), **1** was instantly consumed. Cyclopentadienyl protons for the metallacycle $\mathbf{5}^1$ occur at δ 5.20 (s) and 5.06 (s) (80% integration) and for the metallacycles $\mathbf{5}^i$ (= $\mathbf{5}^2$, $\mathbf{5}^3$, $\mathbf{5}^4$, *etc...*) at δ 4.87 (s) and 5.34 (s) (20% integration). Additional resonances for the metallacycle α hydrogens occur at δ 3.99 (broad) and 1.77 (broad).[16] Addition of more **1** (or warming to room temperature) results in the disappearance of metallacycle **5**[1] peaks δ 5.20 and 5.06.

End-capping of Polymer. To 0.5 mL of a 0.00617 M d_8-toluene solution of catalyst **2b**, 28 mg of **1** (50 equivalents) was added and allowed to completely react, as observed by proton NMR. After stirring this solution at room temperature for 24 hours with excess acetone (10 mL), proton NMR revealed the peak for acetone (δ 1.56) as well as two new peaks (δ 1.55 and δ 1.58) for the end-capped polymer.

End-capping with d_6-acetone was as above, except that after 24 hours the solution was poured into 5 mL methanol, and the precipitated polymer washed repeated with pentane and dried under 1mm Hg vacuum for 6 hours. The polymer was dissolved in benzene with a trace of C_6D_6 added as reference. A broad peak in D-NMR at δ 1.4-1.6 results.

Results and Discussion.

This work utilizes the well-researched chemistry of titanium metallacycles (Figure 1) for metathesis polymerization of **1**. Metallocycle **2c** was chosen as the catalyst for the majority of studies due to its thermal stability at ambient temperatures. Polymerization kinetics were determined through monitoring of the monomer concentration by gas chromatography.

Initial experiments confirmed that the amount of napthalene extruded from precursor polymer, plus the amount of monomer yet unpolymerized, is at all times equivalent to the inital monomer concentration (Figure 2). This demonstrates that the precursor polymer is completely soluble, and indeed extrusion of napthalene under such conditions is complete and instantaneous (sharp chromatography peak for napthalene). Quantitative extrusion is necessary if the resultant polyacetylene is to have an uninterruped π-conjugated backbone. Subsequent experiments have shown the reaction to be first order in catalyst, zeroeth order in monomer, with $k_1 = 3.9 \times 10^{-3}$ sec^{-1} at 25 °C (Figure 3).

Figure 1: Titanium Methylidene Chemistry

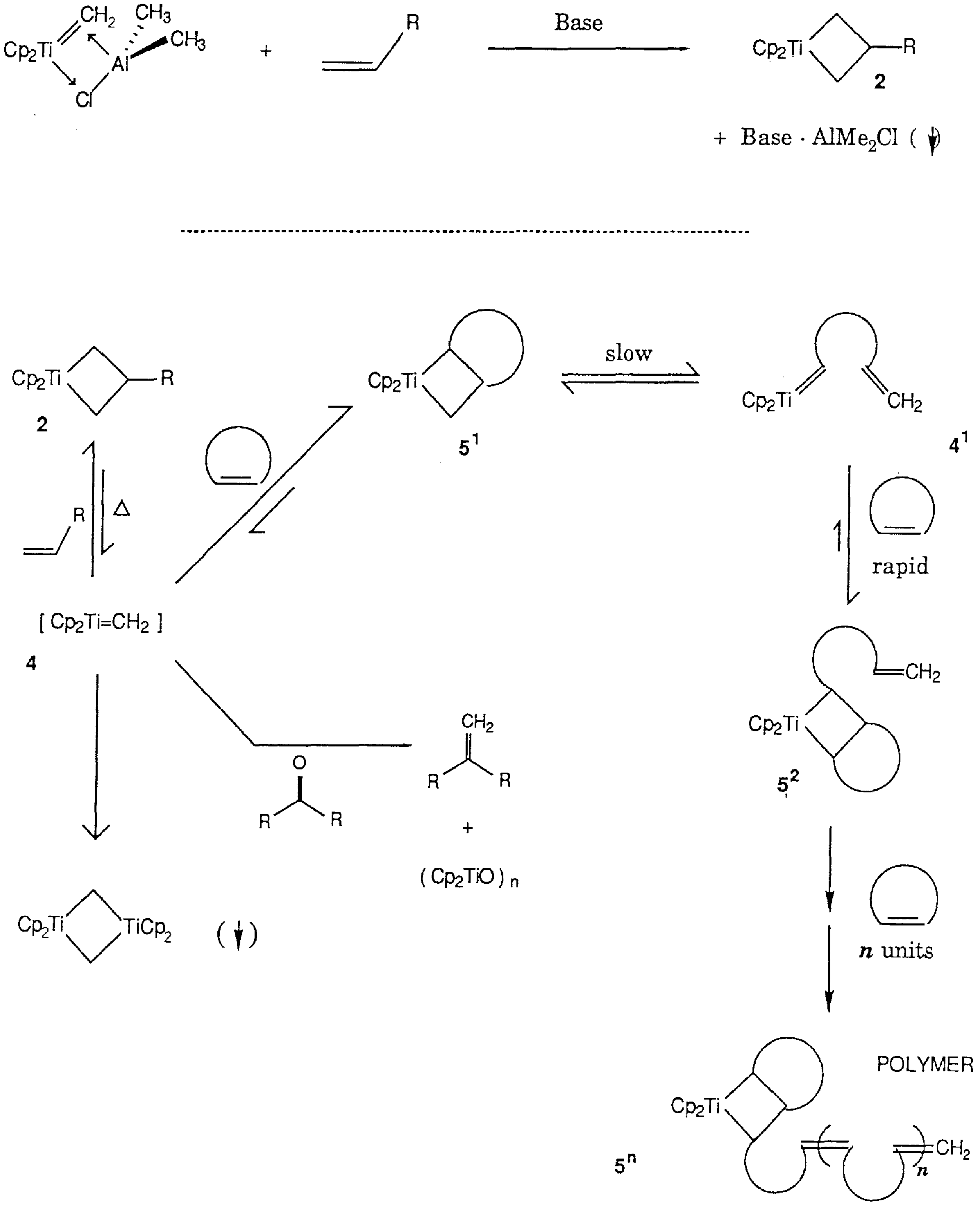

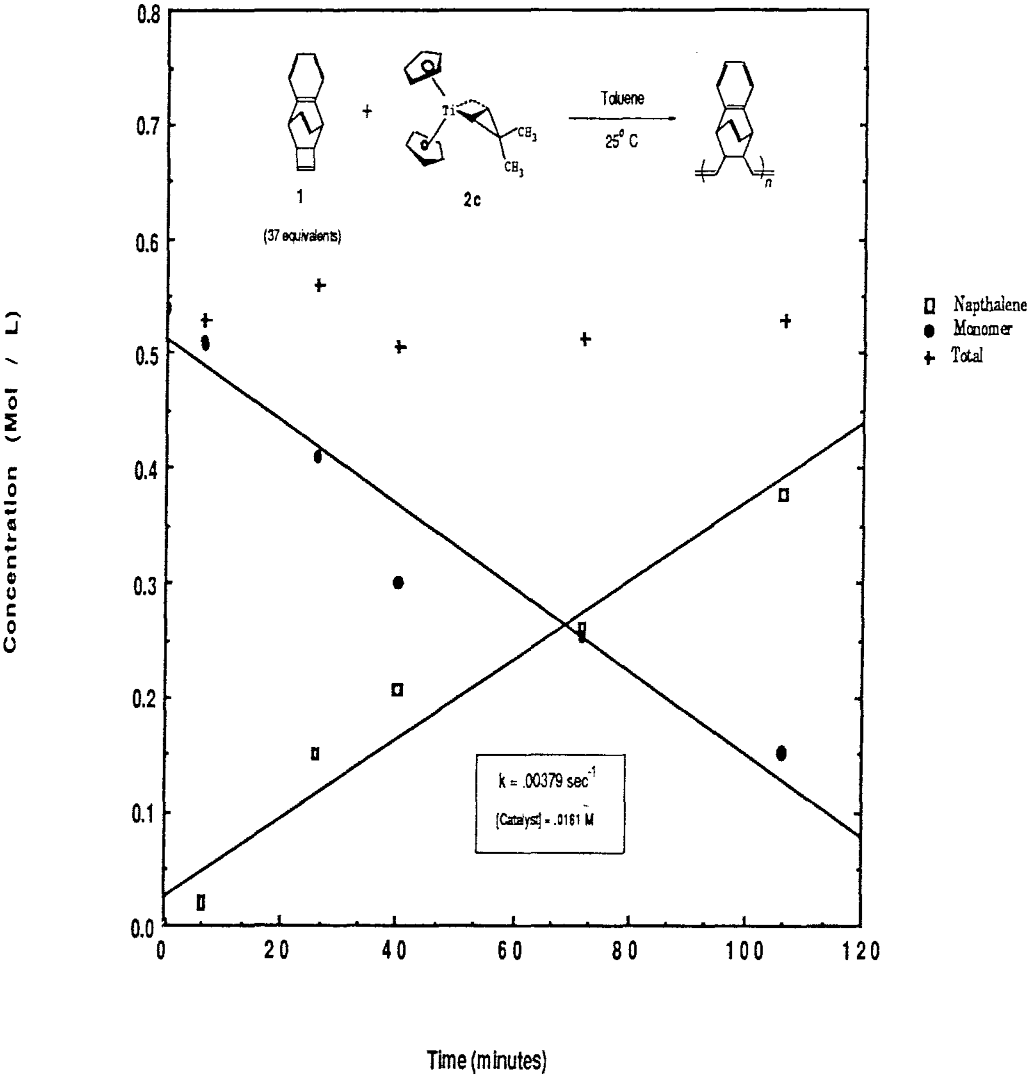

Figure 2. GC analysis of reacton mixture reveals that throughout the reaction, summation of unreacted monomer plus napthalene equals the initial amount of monomer. This indicates that the precursor polymer is quantitatively extruding napthalene.

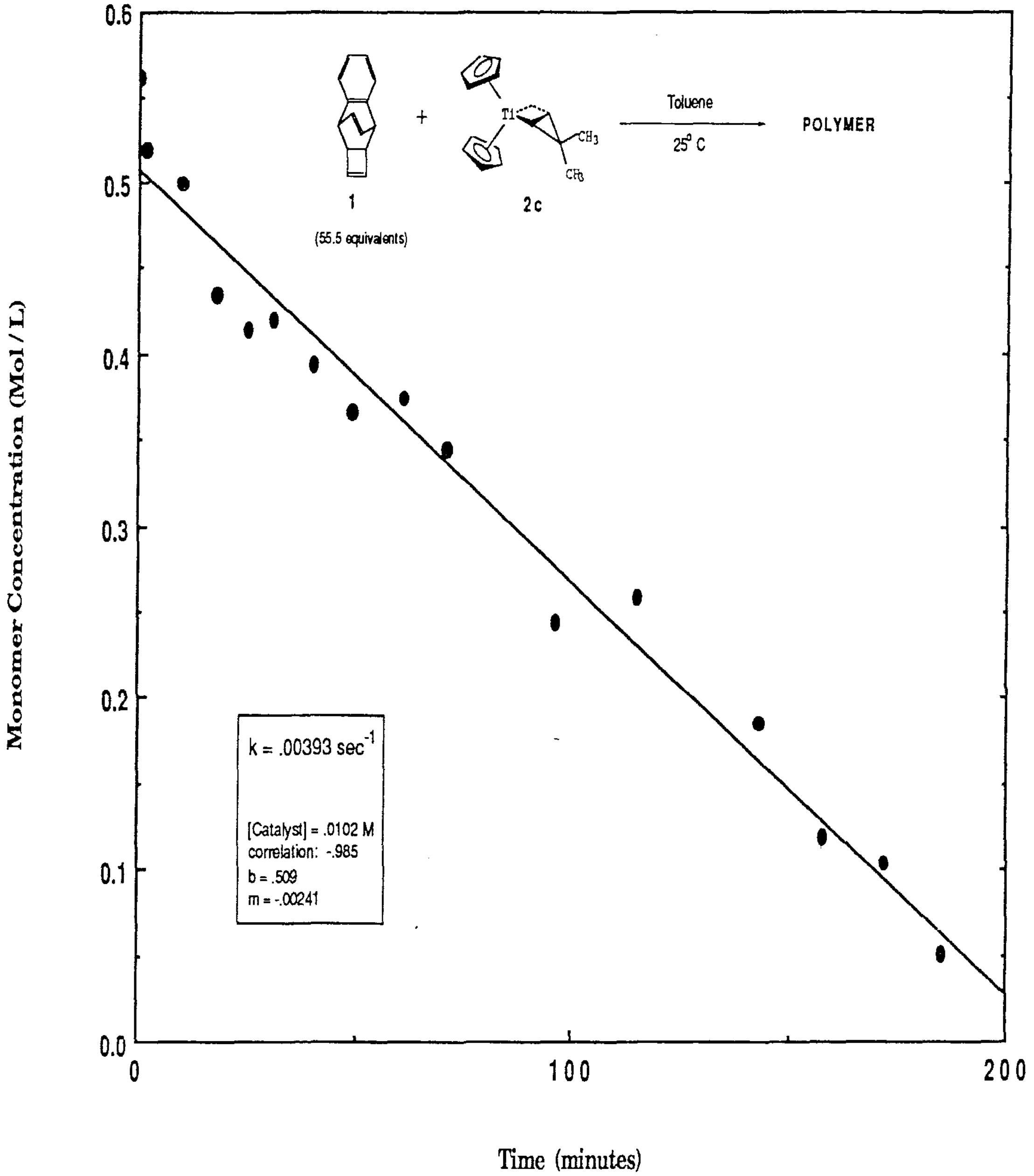

Figure 3. Kinetics reveal the polymerization rate to be zeroeth order with respect to monomer.

That varying the monomer concentration results in no change of rate can be understood from the mechanism (Figure 1). The rate-limiting step of the polymerization is the slow, intramolecular decay of metallacycle to the carbene ($\mathbf{5^i} \rightarrow \mathbf{4^i}$), followed by rapid trapping of the monomer to produce another mettalocycle. Thus, monomer concentration has no role in the rate-determining step. Although each step is indicated as an equilibrium, in actuality the polymerization is driven to completion, probably due to the ring strain in the monomer unit **1**. The process of $\mathbf{5^1} \rightarrow \mathbf{4}$ would result in formation of the strained cyclobutene adduct (monomer), a thermodynamically unfavorable process.

As in the acyclic analogues of titanium methylidene chemistry, the metallacycles ($\mathbf{5^i}$) are more stable than the carbenes ($\mathbf{4^i}$). In the polymerization of a less strained cycloolefin — norbornene — with titanocene carbene sources, the metallacycle has been isolated and defined by X-ray analysis. Attempts to isolate the more reactive metallacycle of **1** have not been successful; however, resonances attributable to this metallacycle have been identified by variable-temperature ^{1}H NMR at -40 °C, in addition to the presence of oligomer resonances. The metallacycle ($\mathbf{5^1}$) peaks, at this temperature, do not decay *as long as no free monomer is present.* Upon addition of several equivalents of **1** however, the metallacycle ($\mathbf{5^1}$) peaks decay and the oligomer/polymer peaks are gradually enhanced until all monomer is consumed. The polymer "hibernates" until more monomer is added, which again is completely consumed. Attempts at ^{1}H NMR kinetics by peak integration are frustrated by broad polymer peaks overlapping the monomer peaks.

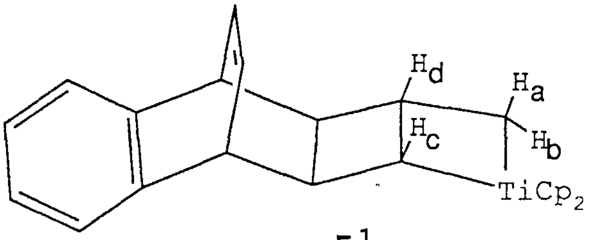

5^1

A *living* polymerization proceeds through islands of stability (in this case, metallacycles) and accordingly demonstrates well-behaved kinetics. If the living polymerization is truly clean (no secondary metathesis involving "back-biting" of double bonds in the polymer chain as depicted below),

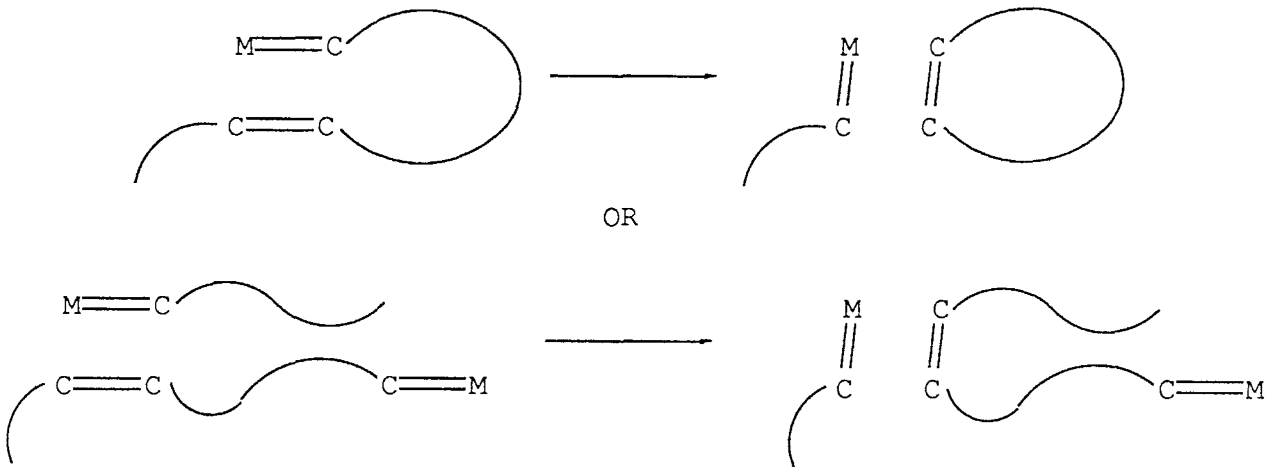

then the length of the polymer chain should increase only at the expense of monomer molecules. Thus, polymer molecular weight *vs*. monomer conversion plots should be linear, and the polydispersity (molecular weight range, or deviation in chain length) of the polymer sample should be low.

Figure 4 shows molecular weight of polymer (by gel permeation chromatography) as a function of conversion of monomer (by gas chromatography). Polydispersity (M_w/M_n, from gel permeation chromatography) values range from 1.6 to 2.1. This compares to a polydispersity of greater than 4 using the W/Sn catalyst system. Efforts are underway to lower polydispersity values further by employing conditions to increase rate of initiation (**2** → **4**) relative to rate of propagation ($\mathbf{5^i} \rightarrow \mathbf{4^i}$).

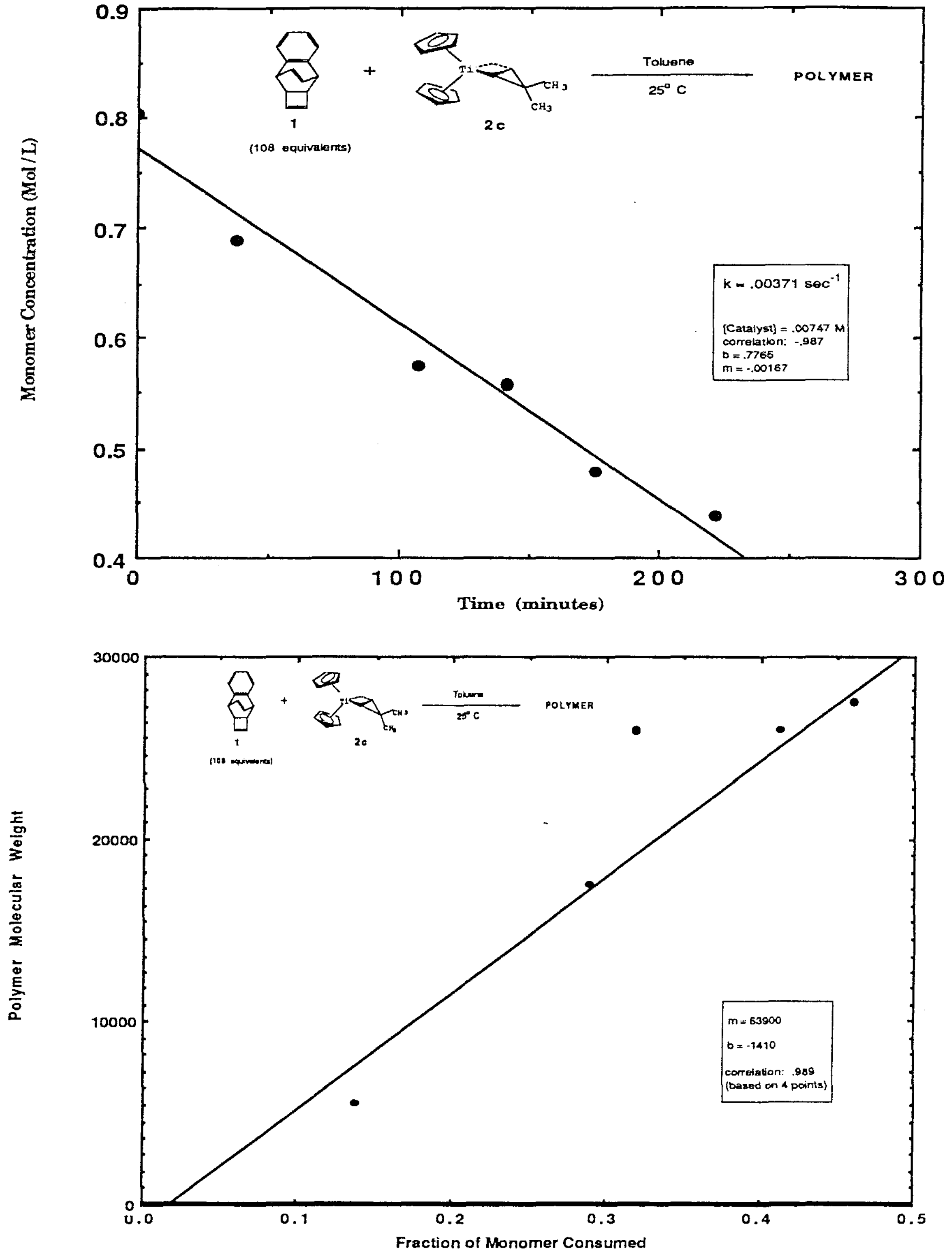

Figure 4. Top graph shows monomer consumption as a function of time. Bottom graph shows increase in polymer molecular weight as a function of monomer consumption for the same experiment.

Finally, it has been demonstrated that the carbene-carrying polymer **4**^{i} is a reactive methylidene-transfer agent, analogous to titanocene carbene **4**. The catalyst **2b** was used to polymerize 50 equivalents of monomer **1**, after which no **2b** or **1** remained (only polymer, by ^{1}H NMR). Excess acetone was then added. As expected, the acetone peak slowly decayed, as new signals (splitting) appeared at resonances nearly identical to the resonance of isobutylene methyl protons.

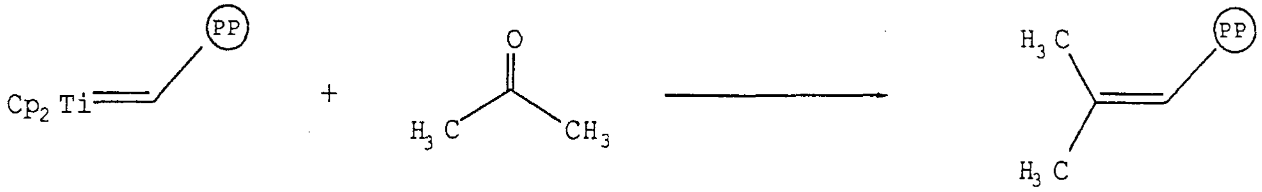

(PP) = Precursor Polymer

6

For verification of the polymer end-capping, the experiment was repeated with perdeutero-acetone. Upon work-up and investigation of polymer (**6**), deuterium NMR confirmed incorporation of the d_6-acetone, showing only a broad resonance, the chemical shift again indicative of isobutylenic hydrogens.

SUMMARY AND OUTLOOK

The ring-opening polymerization of monomer **1** with titanium carbene sources can be conducted over a wide range of temperatures affording first order kinetics and control of polymer molecular weight. The logical continuation of this research would be to prepare various chain lengths of the precursor polymer in large enough quantities to allow for the materials investigation of the polyacetylene formed upon thermal extrusion of napthalene.

The reactive titanocene carbene functionality remains appended to the chain throughout the polymerization. This latter feature is currently being exploited[15] in the preparation of di-block and tri-block copolymers of polynorbornene with the polyacetylene precursor (Figure 5). The impetus for preparing such copolymers stems from the very different properties of the polynorbornene and polyacetylene segments: polyacetylene is a rigid semi-conducting polymer, whereas polynorbornene is a flexible insulating polymer. Copolymers having such "hard" and "soft" segments are likely to undergo microphase separation, thus producing polyacetylene islands of controllable size within this copolymer matrix. The semi-conductor islands can be thought of as quantum wells which, when pheripheral overlap begins to occur, give rise to non-classical electrical and optical properties.

The reactive carbene functionality could also be used in end-capping the polyacetylene precursor with electron donor or acceptor moieties, increasing the hyperpolarizability of the polyacetylene chain. Since the $\chi^{(3)}$ susceptibility of a molecule is directly related to the hyperpolarizability, the incorporation of electron donors or acceptors at chain terminus should increase the already moderately strong non-linear optical response.

Di-block

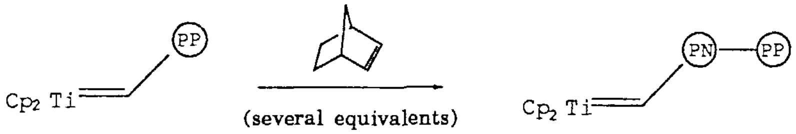

Tri-block

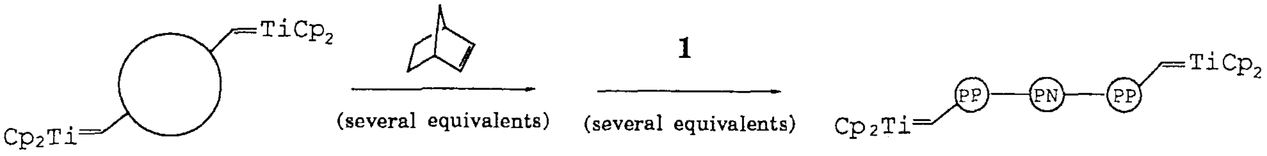

(PN) = Polynorbornene

(PP) = Precursor Polymer

Figure 5. Preparation of di-block and tri-block copolymers.

REFERENCES

(1) (a) Gibson, H. W.; Pochan, J. M. *Encyclopedia of Polymer Science and Engineering*; Wiley-Interscience: New York, 1985; Vol. 1, pp 87-130. (b) Lichtmann, L. S.; Fitchen, D. B. *Synth. Met.* **1979**, *1*, 139. (c) Minoura, Y.; Ikeda, H. *J. Appl. Polym. Sci.* **1971**, *15*, 2219. (d) Brunthaler, J. K.; Stelzer, F.; Leising, G. *J. Mol. Catal.* **1985**, *28*, 393. (e) Okamoto, Y.; Hwang, E.; Wang, M. *J. Polym. Sci., Polym. Lett. Ed.* **1985**, *23*, 285. (f) Gill, W. D.; Clarke, T. C.; Street, G. B. *Appl. Phys. Comm.* **1982**, *2*(4), 211. (g) Feast, W. J. In *Handbook of Conducting Polymers*; Skotheim, T. A., Ed.; Marcel Dekker, Inc.: New York, 1986; Vol. 1, pp 1-43. (h) Chien, J. C. W. *Polyacetylene*; Academic Press: Orlando, FL, 1984.

(2) (a) Rimai, L.; Heyde, M. E.; Gill, D. *J. Am. Chem. Soc.* **1973**, *95*, 4493. (b) Lichtmann, L. S. *Thesis Dissertation, Cornell University*; Univ. Microfilms Int.: Ann Arbor, MI, 1981; pp 94-96.

(3) Chien, J. C. W.; Warakomski, J. M.; Karasz, F. E.; Schen, M. A. *Macromolecules* **1985**, *18*, 2380.

(4) Basescu, N.; Liu, Z.-X.; Moses, D.; Heeger, A. J.; Naarmann, H.; Theophilou, N. *Nature* **1987**, *327*, 403.

(5) Ito, T.; Shirakawa, H.; Ikeda, S. *J. Polym. Sci, Polym. Chem. Ed.* **1974**, *12*, 11.

(6) Edwards, J.H.; Feast, W.J. *Polymer*, **1980**, *21*, 595.

(7) For publications on the resulting ("Durham") polyacetylene, see (a) Edwards, J.; Feast, W.J.; Bott, D. *Polymer*, **1984**, *25*, 395. (b) Friend, R.; Bradley, D.; Pereira, C.; Townsend, P.; Bott, D.; Williams, K. *Synthetic Metals*, **1986**, *13*, 101. (c) Bott, C.; Brown, C.; Chai, C.; Walker, N.; Feast, W.J.; Foot, P.; Calvert, P.; Billingham, N.; Friend, R. *Synthetic Metals*, **1986**, *14*, 245.

(8) Reif, L.; Höcker, H. *Macromolecules*, **1984**, *17*, 952.

(9) Ceausescu, E.; Cornilescu, A.; Nicolescu, E.; Popescu, M.; Coca, S.; Belloiu, C.; Dimonie, M.; Gherorghui, M.; Dragutan, V.; Chipara, M. *J. Molec. Catal.*, **1985**, *28*, 337.

(10) Straus, D.A.; Grubbs, R.H. *J. Molec. Catal.*, **1985**, *28*, 9.

(11) Gilliom, L.R.; Grubbs, R.H. *J. Am. Chem. Soc.*, **1986**, *108*, 733.

(12) Paquette, L.; Kukla, M.; Stowell, J. *J. Am. Chem. Soc.*, **1972**, *94*, 4920.

(13) Dihydroanthracene was confirmed to be inert towards titanocene carbenes by ^{1}H NMR.

(14) Hall, L.D.; Sanders, J.K. *J. Am. Chem. Soc.*, **1980**, *102*, 5703.

(15) Unpublished results, this laboratory.

(16) The β-hydrogen peak for metallacycle **5**^{1} is not detectable, likely due to overlapping peaks. The chlorodimethylaluminum·pyridine adduct which forms upon addition of base to Tebbe has methyl proton shift at δ -0.14. The shift reported for the norbornene metallacycle β-hydrogen is δ 0.14 (Ref. 11).

Chapter 3

Cyclooctatetraene Liquid Polymerization: A Condensed Phase Route to High-Quality Polyacetylene

ABSTRACT

The author presents a versatile and convenient route to polyacetylene — the condensed phase metathesis polymerization of 1,3,5,7-cyclooctatetraene (COT). Dissolution of catalyst in "neat" cyclooctatetraene provides a means of transforming the liquid into a highly lustrous film at ambient temperature and pressure.

Poly-COT films are shown to have physical and spectral properties very similar to polyacetylene prepared by the Shirakawa methodology. Iodine-doped films demonstrate conductivities greater than 300 Ω^{-1}/cm. New processing modes and novel morphologies for polyacetylene have been discovered.

Novel polyacetylene derivatives have been prepared to demonstrate the versatility of this method. Bromo-cyclooctatetraene has been polymerized to a strong, flexible golden film. Both electron-releasing groups and electron-withdrawing groups have been placed off the polyacetylene backbone chain. These derivatives, with their various band structures, hold great promise for the fabrication of solid state devices, as demonstrated through the preparation of a purely organic capacitor.

INTRODUCTION

The morphology of polyacetylene has been demonstrated to have a decided influence upon such properties as density,[1] conductivity,[1,2] electrical and optical anisotropy,[3] and tensile strength.[4] Polyacetylene morphology is likewise an important consideration in the design of solar cells[5] or solid state batteries.[6] Due to the intractable nature of polyacetylene, its morphology is largely fixed during the polymerization process. New modes of preparation which generate novel morphologies and allow facile fabrication are therefore instrumental in understanding and exploiting this conducting polymer.

Initial research efforts in this field, procedures which involved bubbling acetylene through various catalyst solutions, produced polyacetylene only in powder form.[7] A major breakthrough occurred in 1971 when Shirakawa and co-workers succeeded in preparing free-standing films by polymerizing acetylene at the gas/liquid interface of a concentrated catalyst solution.[8] Adaptations of the Shirakawa method have resulted in polyacetylene as a low-density gel,[1] polymerizations in liquid crystalline media,[9] and polymerizations conducted under shear flow conditions to induce chain alignment.[10] Edwards and Feast have produced polyacetylene from a processable precursor polymer.[11] More recently, Naarmann's modification of the Shirakawa method has led to high-density polyacetylene with a conductivity approaching that of copper metal.[12]

Several research groups have targeted the metathesis polymerization of 1,3,5,7-cyclooctatetraene (COT) as a route to polyacetylene (Figure 1). In 1985, Höcker *et. al.* reported the polymerization of COT with the "classic" metathesis catalyst system $WCl_6/AlEt_2Cl$.[13] Dilute solution conditions resulted in very low yields of insoluble powder, and vapor deposition of COT onto a catalyst slurry over a period of days produced films containing chlorination and saturation defects. No conductivities were reported for any of the samples.

The author herein presents a versatile and convenient route to polyacetylene through the condensed-phase metathesis polymerization of 1,3,5,7-cyclooctatetraene. Dissolution of catalyst in "neat" COT provides a means of transforming the liquid into a high-quality film. Properties of these poly-COT

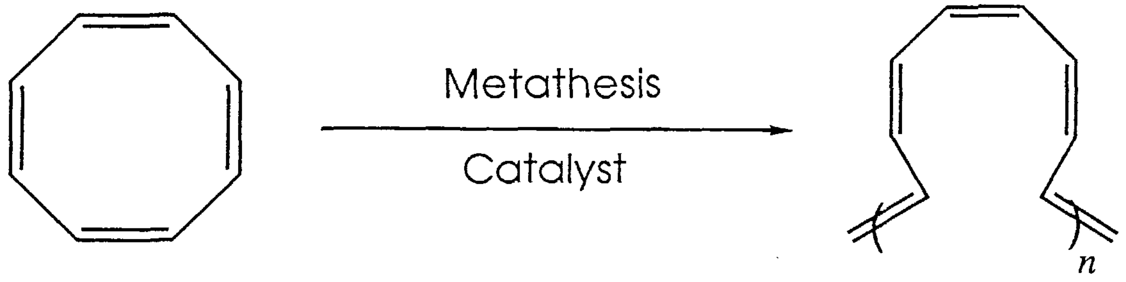

Figure 1. Metathesis polymerization of 1,3,5,7-cyclooctatetraene.

films are nearly identical to those of polyacetylene produced by the Shirakawa method. Linear copolymers of varying conjugation lengths can be prepared by the addition of a second monomer and new derivatives of polyacetylene can be prepared from substituted COT . This previously unpromising approach now appears to be an excellent route to conducting organic materials.

Experimental.

General Considerations. All work involving air or moisture sensitive compounds was performed using standard high-vacuum or Schlenk techniques under Argon purified by passage through BASF RS-11 (Chemalog) and Linde 4Å molecular sieves. Solids manipulation and "neat" polymerizations were conducted in a nitrogen filled Vacuum Atmospheres drybox equipped with refrigeration unit. Solution NMR spectra were recorded on a JEOL FX-90Q (89.60 MHz ^1H) or a JEOL GX-400 (399.65 MHz ^1H). Analytical gas chromatography was performed on a Shimadzu GC-mini 2 flame ionization instrument equipped with a 0.24 mm x 25 m SE-30 capillary column. Low resolution GC-MS analysis was obtained using Hewlett-Packard 5890/5970 instrumentation. Conductivities were measured in an inert atmosphere using a 4-point probe arrangement in order to negate contact resistance. Surface area measurements employed B.E.T. analysis with nitrogen as the chemical sorbate. Scanning electron microscopy of gold-coated samples (10 nm coating, sputtered deposition) was performed using 20-KeV electrons (micrographs taken in the back-scattering mode). X-ray diffraction was measured by wide angle scattering from a Guinier camera employing monochromatic Cu K_α radiation. Differential scanning calorimetry was performed on a Perkin Elmer DSC-7 instrument under nitrogen purge, at a scanning rate of 30 °C per minute. Elemental analysis of pentane/MeOH washed films was performed by Spang Laboratories.

Materials. Cyclooctatetraene was prepared by Reppe cyclotetramerization of acetylene.[14] COT was fractionally distilled (45 °C, 25 mm Hg), filtered through neutral alumina, and vacuum distilled from CaH_2. Purity was confirmed by GC analysis before use (>99.9%). Purified COT was stored under nitrogen, below its melting point, protected from light. Bromo-cyclooctatetraene was synthesized according to literature[15] purified by vacuum distillation from CaH_2. Solvents were vacuum distilled from benzophenone ketyls, except for CCl_4 which was vacuum distilled from P_2O_5. All polymerization substrates were cleaned thoroughly and subjected to vacuum before use. $AlCl_3$ (anhydrous, Aldrich, 99%), I_2 (resublimed, MC/B), $RuCl_3 \cdot H_2O$ (Strem), and $EtAlCl_2$ were used without further purification. WCl_6 (Aldrich, 97%) was sublimed at 50 °C under .1 mm Hg, affording shiny purple needles. $WOCl_4$,[17] $(CO)_5W{=}C(Ph)(OMe)$,[33] and $Cp_2Ti{=}CH_2 \cdot AlMe_2Cl$[34] were prepared according to literature procedures. Catalysts **1**[16] and **2**[17] were synthesized as previously described. D_8-cyclooctatetraene was synthesized by a method similar to that previously reported.[18] Isotopic purity (percent deuterium incorporation) of this COT was determined by mass spectroscopy to be between 90 and 95%.

Polymerization of COT with Various Catalysts:

$AlCl_3$. In the drybox, 100 equivalents of COT were added to aluminum trichloride powder in a small vial. After a few seconds the reaction yielded a dark brown powder (~70%, by mass). The powder was transferred to a Soxhlet apparatus and extracted with degassed MeOH under Argon atmosphere. The insoluble brown powder — never exposed to air or moisture — was loaded in the drybox into rotors for CP-MAS ^{13}C solid state NMR (see Figure 2).

Iodine. On a glass slide, powdered I_2 crystals were added to 100 equivalents COT and immediately stirred. No effort was made to exclude air or moisture. The solution became a very viscous dark brown tar within several seconds, and upon setting for 5 hours formed a solid, slightly sticky film. The conductivity as measured with a 4-point probe apparatus was $\sigma = 10^{-7}\ \Omega^{-1}/\text{cm}$. Extracting this tar-like film with MeOH yielded a light-brown universally-insoluble powder which was not further characterized.

$EtAlCl_2$. Polymerization conducted in the drybox, as with $AlCl_3$, but with no observable reaction.

WCl_6. Same conditions as with $EtAlCl_2$.

$WOCl_4$. Same conditions as with $EtAlCl_2$.

WCl_6 / $EtAlCl_2$. In the drybox, 4 equivalents $EtAlCl_2$ were ground together with 1 equivalent WCl_6 by morter and pestle, and subsequently allowed to "age" for 10 minutes to form a dark brown paste. COT (~100 equivalents) was added, and almost immediately all liquid reacted, leaving only a black powder which was not further characterized.

$WOCl_4$ / $EtAlCl_2$. Same conditions as for WCl_6 / $EtAlCl_2$.

$(CO)_5W{=}C(Ph)(OMe)$ . . . thermal. In a Schlenk tube equipped with a teflon screw valve, the red carbene was dissolved in 100 equivalents COT under nitrogen atmosphere and heated 24 hours at 60 °C. The COT was removed in vacuum to yield colorless platelets. These platelets were transferred to a sublimation chamber and purified by sublimation at 100 °C under 0.1 mm Hg. ^1H NMR in $CDCl_3$ reveals two sharp singlets at δ = 5.30 ppm and δ = 2.16 ppm, with integrated ratios precisely 1:1. A trace (< 5%) of COT with δ = 5.78 ppm was also observed. Proton-decoupled ^{13}C NMR in $CDCl_3$ revealed singlets at δ = 191, δ = 53, and δ = 30 ppm. Infrared spectroscopy of a Nujol mull of this solid yielded only peaks corresponding to the mineral oil (~3000, 1450, 1380 cm^{-1}) and 1 strong, sharp sample peak at 1970 cm^{-1}.

$(CO)_5W{=}C(Ph)(OMe)$ . . . photochemical. A Schlenk tube was loaded as in the thermal reaction, but was evacuated to the vapor pressure of COT at 25 °C and was placed in an ice bath, then irradiated with a Hanovia lamp (broad visible spectral range) over a period of 10 hours. A black powder precipitated and was not further investigated.

[$Cp_2Ti=CH_2$]. In an inert atmosphere, Tebbe reagent ($Cp_2Ti=CH_2 \cdot ClAlMe_2$) was dissolved in 100 equivalents COT and then excess pyridine was added to generate the titanocene carbene. A small amount of precipitate formed (likely the carbene dimer) in the pool of COT liquid.

$RuCl_3 \cdot H_2O$. Same conditions as with $AlCl_3$, forming a black powder precipitated in a pool of unreacted COT. Precipitate was ~20% yield by mass, and not further investigated.

Preparation of poly-COT films. Films are prepared routinely by dissolution of catalyst **1** in 50 to 150 equivalents of COT, and subsequent polymerization on a glass surface at ambient temperature and pressure. As example: 4.2 mg (0.0053 mmol) catalyst **1** is dissolved in 50 mL pentane, dropped by syringe onto a glass slide over an area of approx. 1 cm^2, and the pentane allowed to evaporate to provide a thin film of catalyst. COT (60 mL, 0.53 mmol, 100 equivalents) is added all at once by syringe on top of the catalyst film. Immediately the liquid is stirred with the flat end of a glass rod for several seconds to dissolve the catalyst. The color proceeds from the initial yellow hue of COT through orange, red, and magenta to a highly-reflective silver. Viscosity gradually increase during the polymerization. At room temperature and using the above conditions, the transformation from a liquid to solid film occurs in 5 to 15 seconds. Lower monomer/catalyst ratios produce films exothermically within a few seconds. Much higher monomer/catalyst ratios result in a black powder precipitated in a pool of unreacted COT.

Films are removed from the glass slide and rinsed generously with pentane (~3 mL total), then methanol (~1 ml). Typical film thickness is 150 mm, as measured with a micrometer.

Films prepared by vapor deposition of COT. A 50-cc cylindrical Schlenk tube is loaded with 25 mg catalyst **1** and 0.5 mL toluene. The solution of catalyst is constantly swirled around the inner walls of the tube while being pumped upon at pressure 0.05 mm Hg. As the toluene evaporates, a thin film of catalyst forms. This Schlenk tube is connected by a glass bridge to a reservoir of 2 mL purified COT, and the entire apparatus evacuated to 0.05 mm Hg. After 24 hours, the black film formed on the inner wall of the Schlenk tube is washed with pentane, then methanol, and dried by vacuum. Pieces of the relatively brittle film were removed from the Schlenk tube (in drybox) for SEM analysis.

Polymerization on cellulose. Ordinary postal string (composed of intertwined strands each 4-5 mm thick as determined by SEM) was subjected to 1 micron vacuum for 24 hours and then submersed in a 0.01 M pentane solution of catalyst **1**. The string was removed and pentane allowed to evaporate. The string was then dipped in "neat" COT, upon which polymerization occurred (exothermicity apparent) immediately. Poly-COT on a string, when cut with a razor blade, 'snaps' as would fiberglass. Figure 9 shows the interior of poly-COT on a string after one such cut. If after soaking in a catalyst solution the string was rinsed several times with pentane before dipping in "neat" COT, no polymerization occurred.

Stretch aligning of poly-COT. On a thin, smooth piece of polyethylene terepthalate (0.5 mm thick, stretchable to 600% original length), the polymerization was conducted as described in **Preparation of poly-COT films.** During the liquid stage of polymerization, the substate was slowly stretched pulling with two pairs of tweezers (in drybox). The poly-COT film was left on substrate for subsequent examination by electron microscopy (see Figure 10).

Solid state CP-MAS ^{13}C NMR experiments. Spectra were recorded at 50.36 MHz on a home built spectrometer described elsewhere,[42] using contact time 2 ms and recycle time of 2 s. Samples were subjected to magic angle spinning at 4.0-4.5 KHz in a high pressure stream of pure nitrogen gas, which also served to protect the samples from atmospheric oxidation. Poly-COT film was powdered with dried KBr (mortar/pestle in drybox) and loaded (~20 mg) into a sapphire rotor with polyethylene caps (Doty Sci.). To isomerize the pristine sample, the rotor was removed from the spectrometer, heated to ~150 °C for 15 minutes, and returned to the spectrometer for additional analysis. Spectra shown consist of 1000-1200 averaged scans. Reported shifts (see Table 1) are referenced to TMS.

Raman experiments. Spectra were obtained for excitation wavelength 488 nm from a Argon ion laser source. One to three scans (reflected from film's surface) were taken using a power of 300-330 mWatts; signal-to-background was approx. 40:1. Reproducibility was within 3 cm^{-1}, and each sample was referenced to known absorption frequencies of a CCl_4 sample. Optical filters were placed in front of the target sample so as to limit external dispersion effects. Samples were polymer films enveloped between two thin glass plates (biological cover slips). No attempt was made to cool the sample during analysis. In the range of 600-2200 cm^{-1}, two major peaks with maximums 1113 cm^{-1} and 1491 cm^{-1} are observed. Frequencies of COD/COT copolymer C=C absorption are reported in Table 2.

Infrared experiments. Spectra were obtained between 4000 and 400 cm^{-1} on a Shimadzu IR-435 continuous wave infrared spectrometer. Polymer films (~150 mm) were sandwiched between NaCl plates and placed in the infrared beam path. Some such samples were subsequently heated at ~150 °C for 15 minutes to induce isomerization, and then re-investigated by IR. Major absorption frequencies for poly-COT are reported in Table 1. IR absorptions for films prepared from d_8-COT are (in cm^{-1}): 2230 (w), 960 (s), 905 (s), and 740 (s).

Microprobe analysis and sample preparation. Quantitative analyses were performed with a JEOL 733 electron microprobe equipped with wavelength-dispersive X-ray detectors. The W M_α line was used for measurement relative to a tungsten metal standard. Analyses were performed at 15 KeV. Data were corrected using the ZAF correction procedures of LOVE and SCOTT (1978) and PACKWOOD and BROWN (1981) as modified by ARMSTRONG.[43] Standard deviations for the data are estimated to be within 1% relative to absolute amount.

Films were mounted in epoxy (Colpot, Resins 12A and 12B). After curing, the epoxy was cut with a slow-speed diamond blade rotary saw perpendicular to the film's surface, producing thin epoxy wafers each containing cross sections of the poly-COT film. Samples were prepared from poly-COT film (100 equivalents COT/catalyst **1**) which was not washed with solvent (Figure 4), and from poly-COT film washed with 0.1 M HCl in methanol.

Preparation of a Schottky diode. A 1 mm x 1 mm x 0.1 mm wafer of n-coped silicon was affixed to gold wires which served as contacts to a power supply. The silicon was immersed in a liquid pool of polymerizing COT to form the polyacetylene/Si heterojunction. The diode was doped in an iodine/CCl_4 solution, then embedded in epoxy to inhibit atmospheric degradation during the measurements. Current-voltage curves exhibited rectification ratios of 5000 - 10000.

RESULTS AND DISCUSSION

Polymerization catalysts

Cyclooctatetraene has been known to undergo polymerization catalyzed by radiation, heat, Lewis acids, or free radicals.[32] However, only metathesis polymerization of COT is expected to yield the conducting polymer polyacetylene. The result upon mixing various catalysts with COT is surveyed in Table 1. With the exception of the first three species, all these catalysts are known to be metathesis-active (WCl_6 and $WOCl_4$ often are used with Lewis acid cocatalysts). The products range from light brown powder, to soluble colorless crystals in which COT has actually complexed to the transition metal complex, to highly lustrous films.

Table 1: COT Polymerization Catalysts

Catalyst	Product
$AlCl_3$	Brown powder
I_2	Yellow-brown powder
$EtAlCl_2$	No reaction
WCl_6	No reaction
$WOCl_4$	No reaction
$WCl_6/EtAlCl_2$	Black powder
$WOCl_4/EtAlCl_2$	Black powder
$(CO)_5W{=}C(Ph)(OMe)$ (thermal)	$(CO)_nW.COT$ complex
$(CO)_5W{=}C(Ph)(OMe)$ (photochemical)	Black powder
$[Cp_2Ti{=}CH_2]$	No polymer
$RuCl_3$	Black powder
$W(OR)_2(=NAr)(=CH\text{-}t\text{-}Bu)$	Powder or film
$W(OR)_2Br_2(=CHR).\ GaBr_3$	Powder or film

Insoluble products are not readily characterized; however, solid state cross-polarization magic-angle-spinning ^{13}C NMR reveals valuable information concerning the structure of the polymer backbone. Metathesis polymerization by a metal carbene formally involves ring cleavage of the COT, preserving the sp^2 nature of all carbon atoms. On the other hand, cationic polymerization by a Lewis acid catalyst preserves the ring structure by addition across double bonds, transforming sp^2 carbon atoms into sp^3 centers, thus interrupting conjugation. Figure 2 shows that metathesis polymerization of COT does indeed result in polyacetylene, while cationic polymerization of COT produces a highly-crosslinked network in which almost seventy percent of the carbon atoms (^{13}C integration) have become sp^3 hybridized.

The well-defined metathesis catalysts **1** and **2** were found to be effective in the polymerization of COT into films:

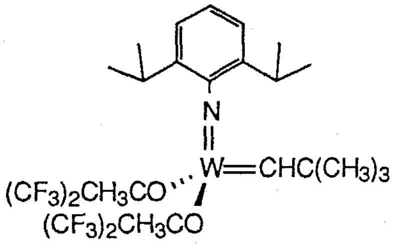

1

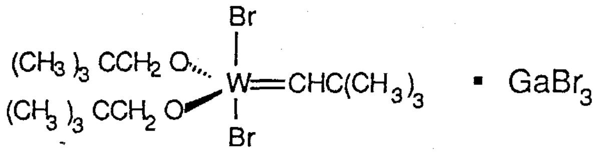

2

Our experience is that catalyst **1**, readily soluble in hydrocarbon solvents such as COT, produces the highest quality poly-COT films. In Table 2, properties of these poly-COT films are compared with those of polyacetylene prepared by the widely used Shirakawa method. All films were prepared using 100 equivalents COT to catalyst **1**, as described in the **Experimental** section.

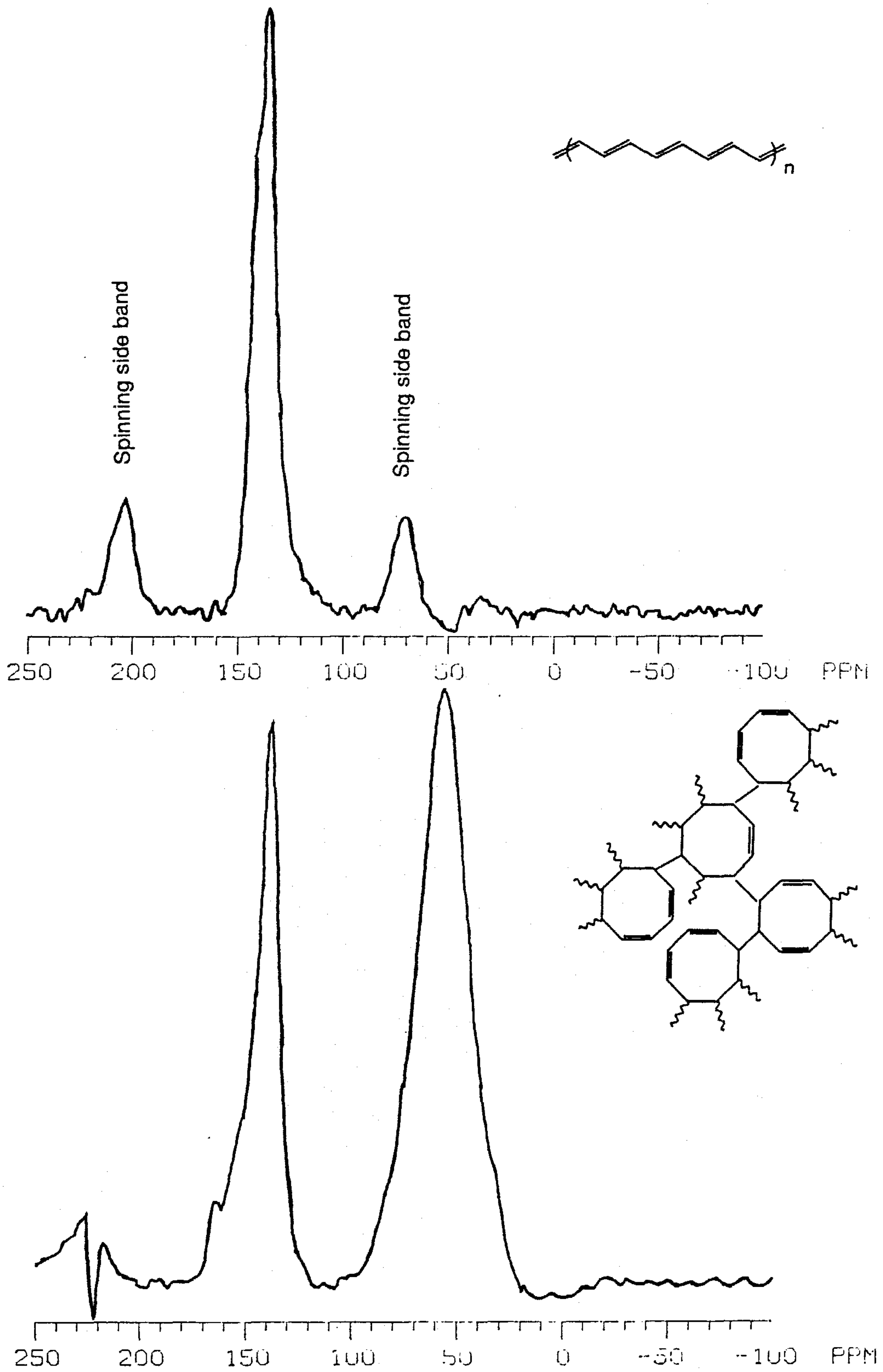

Figure 2: Solid state CP-MAS ^{13}C NMR of polymerized COT. In the top spectrum, COT polymerized by the tungsten carbene catalyst **1** produces polyacetylene. In the lower spectrum, COT polymerized cationically with $AlCl_3$ is largely saturated.

Physical Properties of Films.

Whereas polyacetylene films prepared by the standard Shirakawa technique have fibrillar or globular morphology,[26] scanning electron microscopy (SEM) of poly-COT films reveals a smooth surface morphology (Figures 3a,b). Surface area measurements imply a more compact structure for poly-COT, in accord with SEM observations. However, the bulk density (determined by M/V) of poly-COT film is similar to that of Shirakawa polyacetylene. A more compact structure would be expected to have a higher density. The results are rationalized by examining the cross section of a thin poly-COT film. As shown in Figure 4, the interior of the film is considerably more fibrillar than is the surface. Thus, what begins as a homogeneous polymerization solution develops into a heterogeneous material, in the absence of external perturbations.

Table 2: Properties of Poly-COT Film

Property	Poly-COT	Shirakawa PA	Ref.
Appearance	shiny, silver; smooth surface	shiny, silver; fibrillar surface	19
Surface Area (m^2/g)	31 ± 3	66	20
Density, bulk (g/cc)	.40 ± .04	0.4-0.5	21
Density, flotation (g/cc)	1.12 ± .01	1.13	21
X-ray spacing (d, in Å)	3.90 ± .05	3.80-3.85 (cis)	8
Conductivity, undoped (ohm^{-1}/cm)	$< 10^{-8}$	10^{-5} (trans) 10^{-9} (cis)	22
Conductivity, iodine-doped (ohm^{-1}/cm)	50-350	160 (trans) 550 (cis)	22
Solid state CP-MAS ^{13}C NMR (ppm)	126.4 132.2	126-129 (cis)	23
Thermally isomerized	135.9	136-139 (trans)	
Infrared major peaks (cm^{-1})	930, 980 765	1015 (trans) 740 (cis)	8
Thermally isomerized	1015	1015 (trans)	
DSC exotherm (temp., °C)	150	150	24
Elemental Analysis: Carbon	91.95 (92.26)	C + H > 99%	25
Found (Expected) Hydrogen	7.66 (7.74)		

Figure 3a. Poly-COT film: smooth side of film, in contact with polymerization surface (magnification x 18,000).

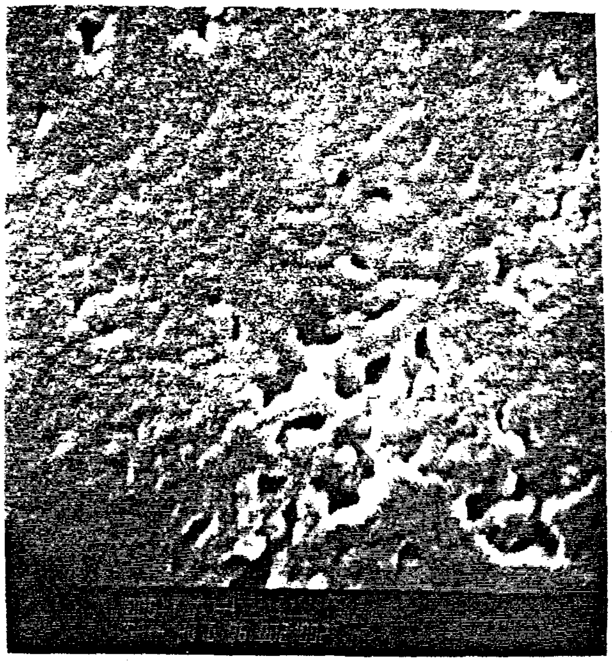

Figure 3b. Poly-COT film: rougher side of film, away from polymerization surface (magnification x 20,000).

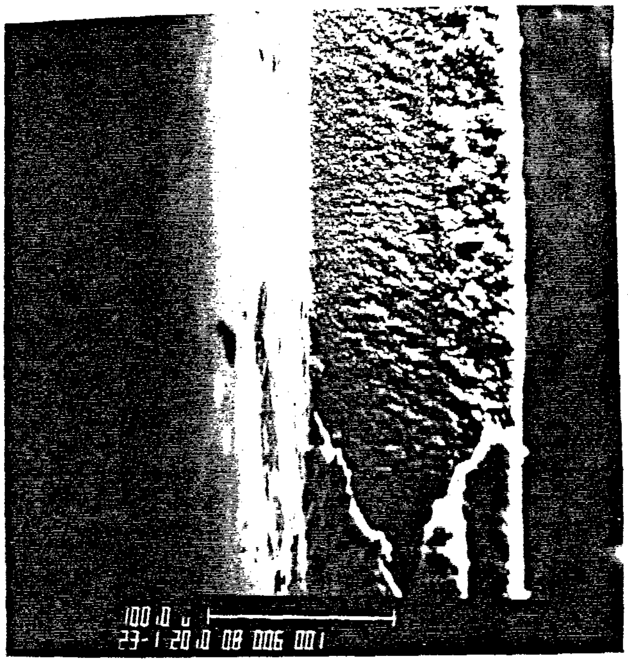

Figure 4. Poly-COT cross section, film standing on edge tilted to right (magnification x 230).

Figure 5. Surface of poly-COT film as prepared by vapor deposition of COT onto a film of catalyst (magnification x 30,000).

Smoothness of morphology is largely dependent upon compactness of polymer chains, which in turn depends upon local catalyst concentration. The smooth surface morphology of poly-COT is understood to be the result of a *uniform* concentration of active catalyst species at the surface. By adopting the polymerization conditions of the Shirakawa technique (vapor deposition of monomer onto a layer of catalyst **1**), the same globular texture present in Shirakawa PA develops in poly-COT (Figure 5).

Electron microprobe analysis of residual catalyst in unwashed poly-COT film is shown in Figure 6a. Depicted is a profile of tungsten concentration throughout the cross section of a thin poly-COT film. The analysis indicates that during polymerization the catalyst is indeed getting dispersed throughout the COT liquid, from 'top to bottom.' In poly-COT film which has been rinsed with methanolic HCl, electron microprobe analysis reveals no residual tungsten (Figure 6b).

The crystallinity of poly-COT films has been investigated by wide-angle X-ray scattering. The only major reflection in poly-COT corresponds to d=3.90 Å, whereas the only major reflection of Shirakawa *cis*-polyacetylene has a spacing of 3.80 Å.[8] Width at peak's half-height of this reflection in both PA and poly-COT is approximately 1.1° in θ, indicating similar degrees of crystallinity.

Poly-COT films are oxidatively doped by exposure to iodine vapor or submersion in saturated solutions of I_2 in CCl_4[12] to conductivities greater than 10^2 ohm^{-1}/cm. Final composition of the film determined by weight uptake of iodine is $(CHI_{.17-.20})$, the mole fraction of iodine varying slightly from sample to sample. This corresponds to saturative doping, based on the model of one I_3^- dopant molecule for every 15-16 carbon atoms as seen in Shirakawa polyacetylene.[12]

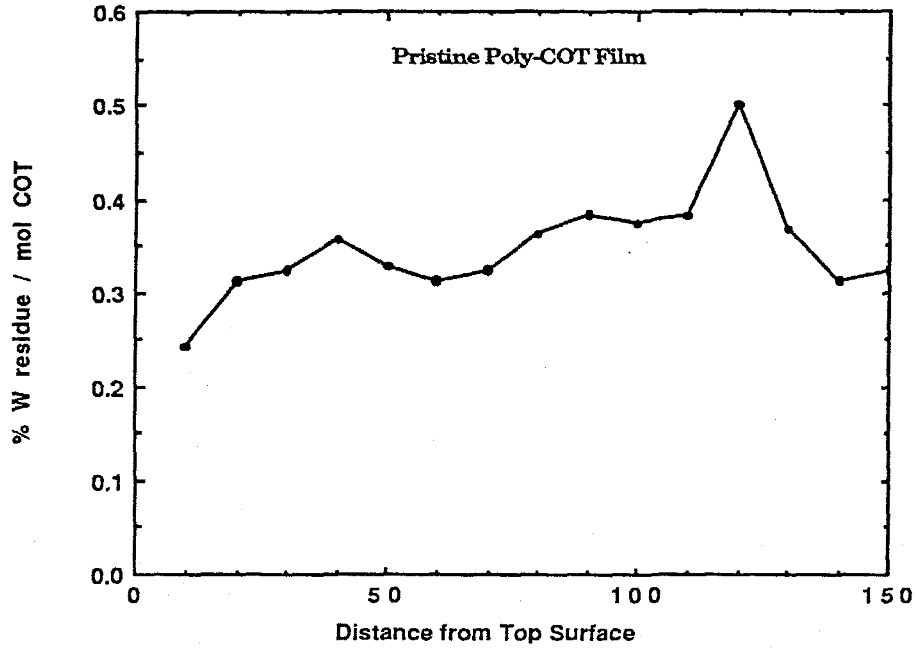

Figure 6a. Cross-sectional microprobe analysis of pristine poly-COT film. A profile of tungsten from the top (surface away from polymerization substrate) to the bottom (surface in contact with polymerization substrate) of 180 μm poly-COT film.

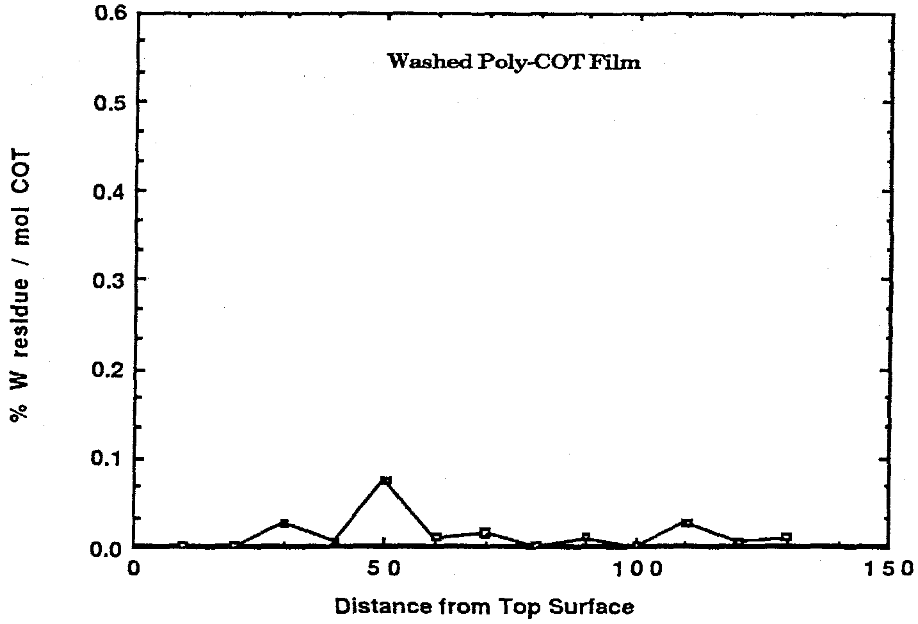

Figure 6b. Cross-sectional microprobe analysis of methanolic HCl washed poly-COT film.

Structure of Films.

There are four pure isomeric structures available for polyacetylenes (Figure 7). Acetylene polymerization at low temperatures (Shirakawa method) results in isomer **II**. Heating **II** produces the thermodynamically-favored isomer **IV**. Even though the *cis-cisoid* helical structure **I** prevents extended planarity, there is X-ray evidence for its existence in soluble di-block copolymers.[27]

Figure 7. Polyacetylene isomers.

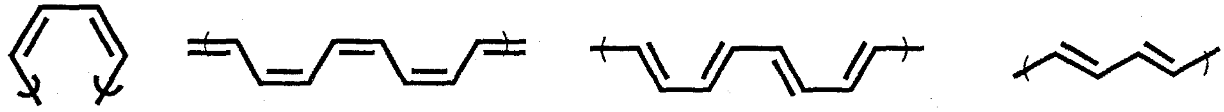

cis-cisoid **I**

cis-transoid **II**

trans-cisoid **III**

trans-transoid **IV**

The structure of poly-COT film as prepared contains two distinct sp^2 carbon types as shown by solid state CP-MAS ^{13}C NMR (Figure 8a). The low field peak at 126.4 ppm can be attributed to carbons situated in *cis* double bonds. The high field peak at 132.2 ppm is assigned to *trans* double bond carbons. The ^{13}C NMR shifts of structures **II** and **IV** have previously been reported as ~126 ppm and ~136 ppm, respectively. Whereas the NMR shift of carbons in conjugated *cis* double bonds are largely insensitive to the surrounding *cis-trans* sequencing, carbons in conjugated *trans* double bonds are known to shift up to 5-6 ppm depending upon the configuration of surrounding double bonds.[28] Upon heating the sample, one peak with shift 135.9 ppm is observed (Figure 8b). As expected, heating induces thermal isomerization to produce long segments of *trans-transoid* structure (**IV**) within the polymer chains. The low field shoulder reveals that the sample was not completely isomerized.

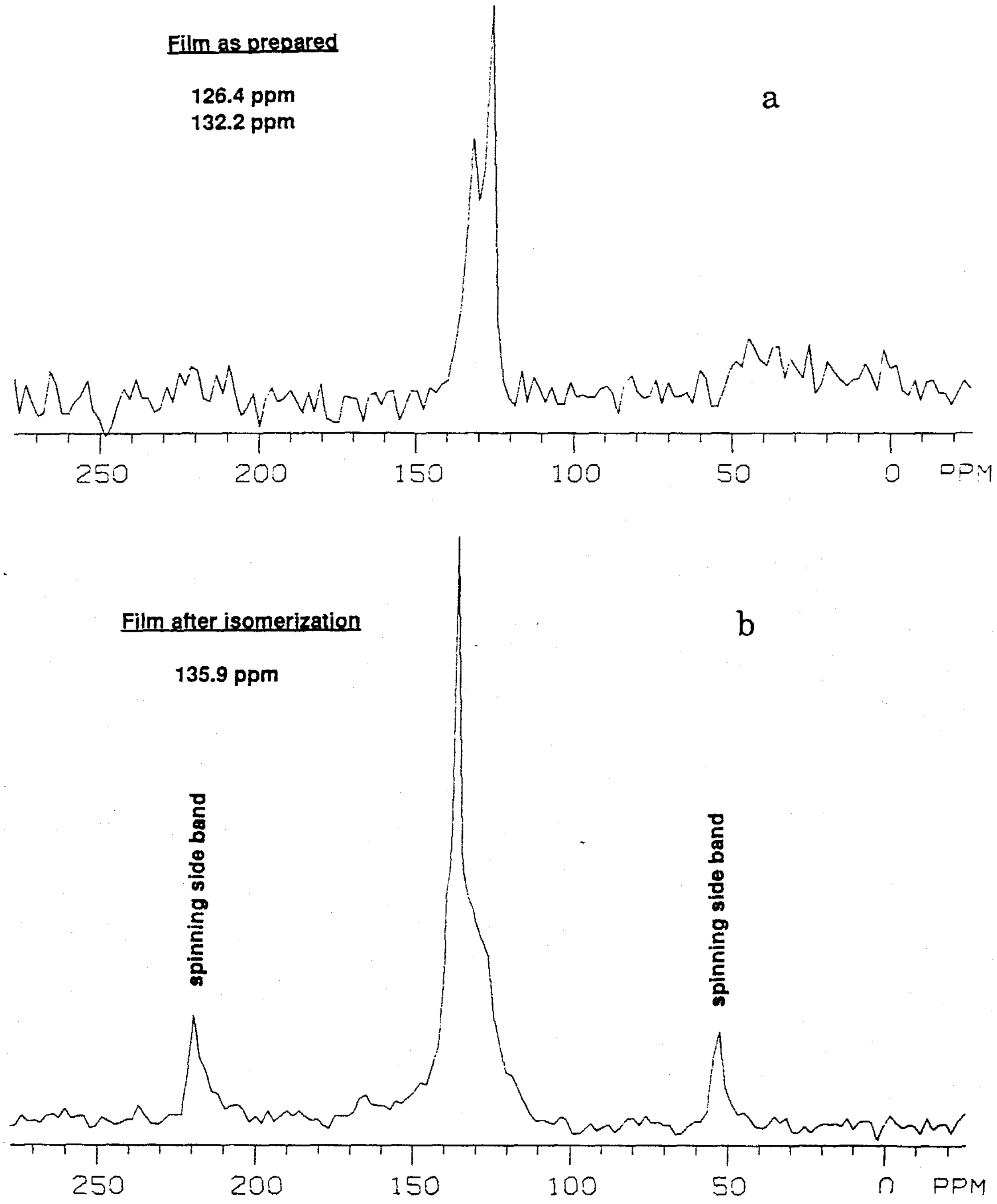

Figure 8. Solid state CP-MAS ^{13}C NMR of poly-COT film. The top spectrum (8**a**) is of pristine poly-COT film. Shown in the bottom spectrum (8**b**) is the same film, after being thermally isomerized.

Infrared spectra also indicate the presence of *cis* (745 cm^{-1}) and *trans* (915, 985 cm^{-1}) conjugated double bonds. Heating the film produces the new peak (1005 cm^{-1}) in the *trans* region at the expense of the *cis* peak. The C=C Raman vibronic peak for poly-COT extends down to the low $\pi-\pi^*$ energy regime of 1460 cm^{-1}, indicative of extensive conjugation.

Finally, an exotherm centered at 150 ^0C is observed for poly-COT by differential scanning calorimetry (DSC). Integration of the exotherm indicates enthalpy change for poly-COT is -50 ± 1 cal/g. Tober and Ferraris have found that the heat evolved during isomerization (h) is linear with respect to *cis* content:[29]

$$\% \, cis = (1.3 \text{ g/cal}) \, h + 1$$

The observed isomerization energy of -50 cal/g for poly-COT corresponds to a *cis* content of 66% for the pristine[30] film, consistent with FT-IR and solid state ^{13}C results.

Processability

Whereas the Ziegler-Natta polymerization of acetylene gas at a heterogeneous interface allows very little flexibility in the preparation of polyacetylene, the bulk polymerization of COT is well suited for processability. Catalyst is simply dissolved in the liquid monomer and allowed to react. Once the polymerization solution has "cured," the material is largely intractable as is the case with all preparative routes to polyacetylene. But during the polymerization, while the solution still retains its fluidity, the material is very conducive to being processed.

Interchain meshing seems to be important for the formation of films with good mechanical properties. In dilute solution polymerizations of COT (also at high monomer/catalyst ratios) where the tungsten centers are far apart, the rigid chains being formed become insoluble and precipitate as a powder before the chain-chain meshing necessary for film formation can occur. However, it has been found that too low monomer/catalyst ratios are also deleterious to film formation, presumably due to the preponderance of low molecular weight chains which crystallize rather than entangle. Conditions for high-quality film formation at room temperature involve a 100:1 monomer/catalyst ratio, with polymerization time (fluid → film) of approximately 10 seconds.

Methods for extending the polymerization reaction, to allow more time for processing, were explored. The fact that the monomer COT freezes at slightly above 0 °C precludes low temperature bulk polymerization, and dissolving catalyst in COT just above its melting point seems to have little effect upon reaction time. An alternative means for moderating the reaction has been developed through catalyst modification, adding a reversibly-binding ligand such as the common solvent tetrahydrofuran (THF). By incorporating 1-10% THF into the COT before catalyst is added, the reaction time can be extended by several seconds to several minutes (mechanistic details are discussed in **Mechanism** section of this manuscript). This procedure has been very valuable in fabricating the film into certain shapes and in fact, during the liquid stage of this modified "neat" polymerization, the polymer can literally be painted onto substrates. A photograph demonstrating the success of this stratgey is shown in Figure 9.

The extended polymerization times has been used in attempts to stretch align the polyacetylene as it is transformed from liquid to solid. Polyethylene terepthalate (PET) served as substrate for the COT polymerization, during which the PET was gradually stretched. Although SEM reveals that the morphology of the polyacetylene has been affected by this procedure (Figure 10), such films showed no increase of doped conductivities as compared to poly-COT films prepared by the conventional method.

The condensed-phase polymerization of COT offers additional possibilities. A preliminary survey of COT polymerizations conducted within various host materials reveals (by SEM analysis) some intriguing results. Shown in Figure 11a is an electron micrograph of ordinary twine, and shown in Figures 11b,c,d are micrographs of polyacetylene polymerized within the twine. Although the "polyacetylene-on-a-string" was confirmed to be conductive upon iodine doping, no further investigation was made into the properties.

Figure 9. Photograph of poly-COT painted on a glass slide.

Figure 10. Stretch-aligned poly-COT film (magnification x 1,900).

Figure 11a. Ordinary string (postal twine, magnification x 400).

Figure 11b. Poly-COT polymerized in string (magnification x 1,500).

Figure 11c. Same view as Figure 11b (magnification x 15,000).

Figure 11d. Same string as 11b - c, different view (magnification x 2,000).

Derivatives.

Bromocyclooctatetraene has been polymerized to a strong, flexible golden film (Figure 12). The film is swollen in THF to a blue-black material. Upon removal of THF, the polymer shrinks and the gold luster returns. Raman spectroscopy reveals a low-energy C=C vibronic absorption (peak extending down in energy to ~1460 cm^{-1}), indicating extensive conjugation. Though the pristine film is an insulator, exposure to iodine increases the conductivity to 0.5 ohm^{-1}/cm. The final composition of the film as determined through weight uptake of iodine is $(C_8H_7BrI_{.34})_n$, or $(CH_{.88}X_{.17})_n$. Again, this corresponds to saturative doping, having the same carbon/halogen ratio as does iodine-doped polyacetylene.

Demonstrating that substituted cyclooctatetraenes such as bromocyclooctatetraene can be polymerized is a major advance in the field of polyacetylene. The ready accessability of various substituted cyclooctatetraenes synthesized from bromocycloctatetraene, combined with the versatility in processing afforded by this process of condensed-phase polymerization, now paves the way for the facile preparation and fabrication of numerous polyacetylene derviatives which havee been previously inaccessible. Table 3 lists members of the cyclooctatetraene family which have been polymerized by catalyst **1** into films.[31]

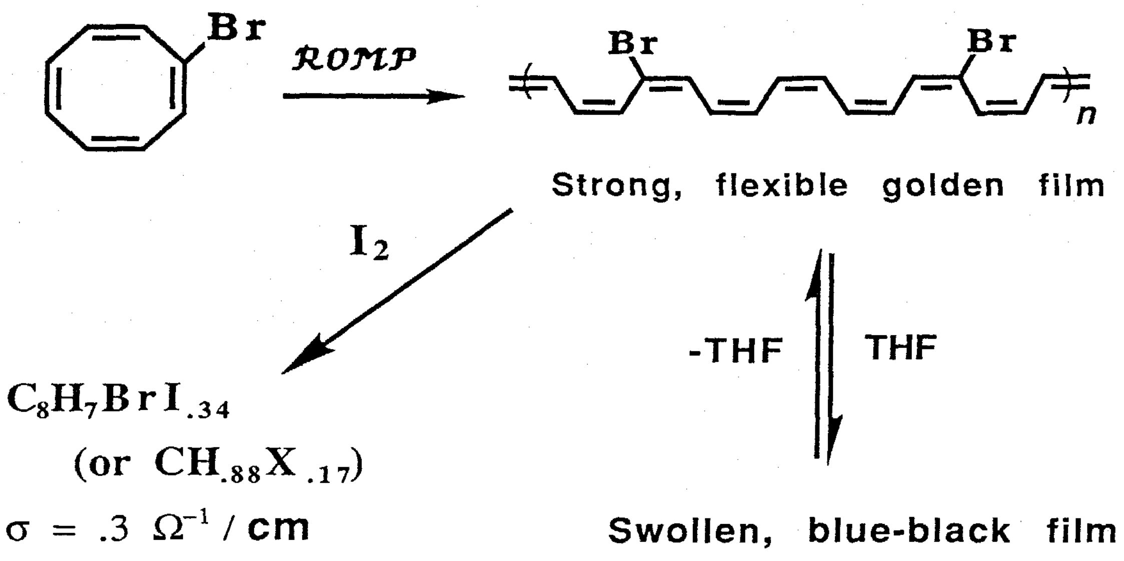

Figure 12: Ring-opening metathesis polymerization of *neat* Br-COT.

Table 3. Metathesis Polymerization of COT Derivatives

Polymerizable

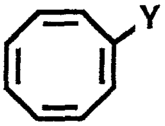

Y = Br
F
CH_3
$(CH_2)_3CH_3$
$(CH_2)_7CH_3$
$Si(CH_3)_3$
$Sn(CH_3)_3$
$Ge(CH_3)_3$
Ph
OR

Non-polymerizable

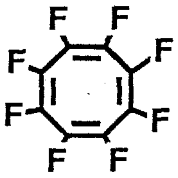

Also of major significance in the polymerization of bromocyclooctatetraene is that it represents the first polyacetylene derivative containing electron-withdrawing groups off the conjugated backbone. The intent was that, if the backbone were partially oxidized by the electron-withdrawing effects of the bromine substituents, perhaps the conjugated backbone would be less susceptible to atmospheric oxidation. Perhaps the backbone would be sufficiently oxidized that no external dopant would be required — that is, polyacetylene might be rendered intrinsically conducting through this bromine substitution. Although the latter postulate was not realized, the atmospheric stability of the films does seem to be improved with the bromine-substituted derivative. No quantitative studies have yet been performed, but poly-BrCOT films retain their shiny appearance in air for two to three weeks, whereas unsubstituted poly-COT films begin to lose their luster in a matter of two to three days.

It will be important to explore the electron-withdrawing and electron-releasing effects of various substituents upon the band structure of these novel polyacetylene derivatives. Electron-withdrawing groups would be expected to raise the ionization energy of the valence band electrons, whereas electron-releasing groups should lower the ionization energy (Figure 13). Band gaps between polyacetylene derivatives in contact with one another will be subject to experimental control, depending upon the amount of electron-withdrawing or electron-releasing groups in each derivative. The author strongly believes that this condensed-phase route to polyacetylene, coupled with the flexibility in substitution, suggests the possibility for unprecedented experimental control for band-gap engineering in the field of synthetic metals.

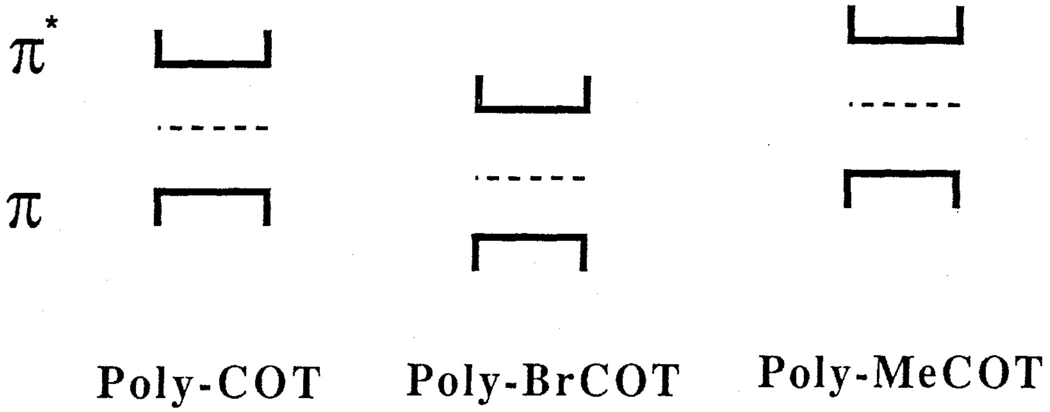

Figure 13. Substituent effects upon the relative energy for the valence and conduction bands is illustrated. Bromine substitution should lower the electronic energy, whereas electron-releasing methyl groups would be expected to raise the energy. Dotted lines represent the various Fermi energy levels.

Solid State Contacts

Polyacetylene has a unique advantage as a conductive material in that the conductivity ranges over 15 orders of magnitude, allowing polyacetylene to act as either a semiconductor or a metal, dependent upon dopant concentration. Researchers have prepared polyacetylene/Si Schottky barriers in which polyacetylene acts as the metal, and have also prepared heterojunction diodes of lightly p-doped polyacetylene with n-doped ZnS in which the polyacetylene acts as a semiconductor.[36] The effective use of polyacetylene in more sophisticated devices has been limited by the lack of a "cleaner" polymerization route, as evidenced by the recent fabrication of an MIS field effect transistor based upon "Durham" polyacetylene.[37]

The condensed phase metathesis polymerization of COT allows a processable, clean, room temperature route into the fabrication of solid-state electronic devices. Shown in Figure 14 is a schematic diagram of a polyacetylene/n-Si diode prepared by this route, in which the silicon semiconductor conveniently serves as polymerization substrate. The device exhibits strong diodic behavior, with a rectification ratio of ~10,000. Shown in Figure 15a is an electron micrograph cross section of an iodine-doped poly-COT/poly-COD/poly-COT film. The poly-COT layers are highly conducting, whereas the poly-COD layer is insulating (Figure 15b illustrates dopant distribution). This device represents, to the best of the author's knowledge, the first working example of a purely organic capacitor.

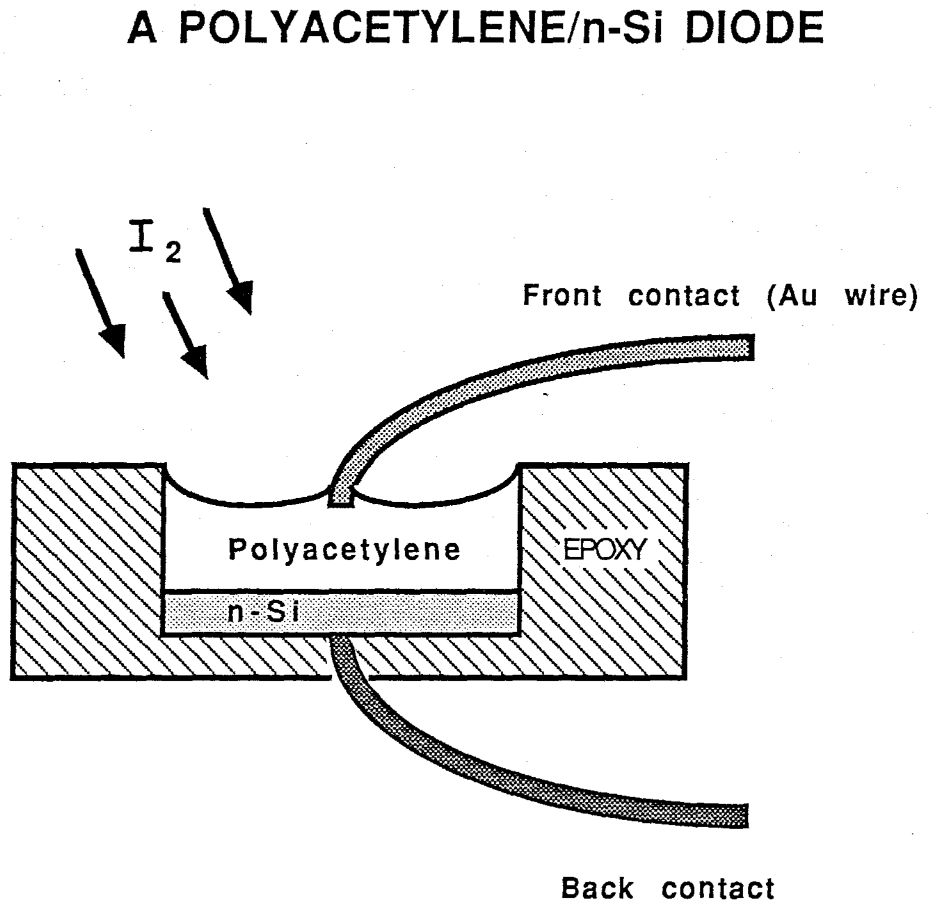

Figure 14. Polymerization of COT on a silicon surface.

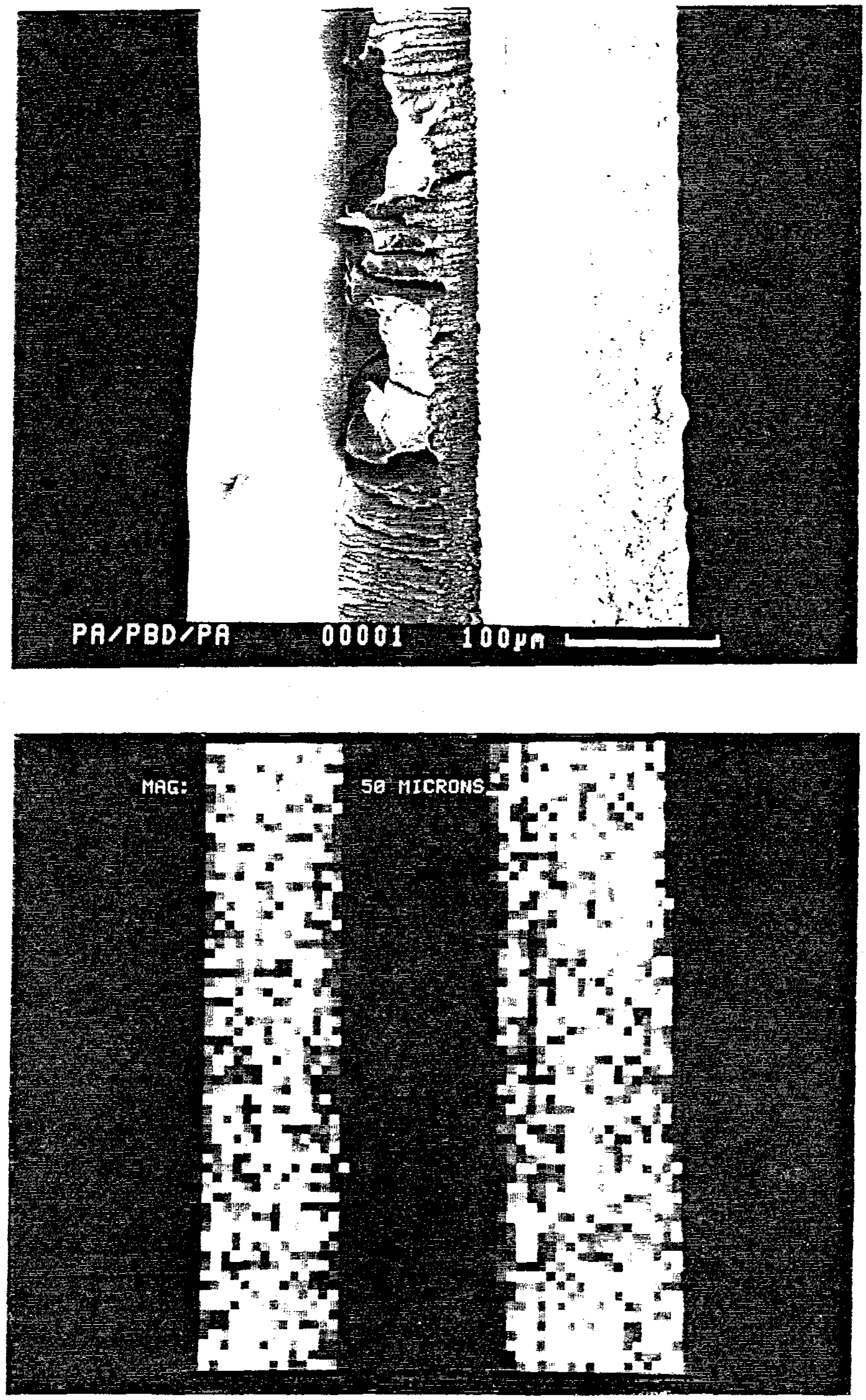

Figure 15. Iodine-doped poly-COT/poly-COD/poly-COT film. Electron micrograph of film (15a, top) shows the considerable contrast between poly-COT and poly-COD layers. Microprobe analysis of the iodine distribution (15b, bottom) shows that the iodine is clearly concentrated in the poly-COT layers.

SUMMARY

Cyclooctatetraene can now be polymerized to give high-quality films with iodine-doped conductivities in the metallic regime. Physical and spectral characteristics indicate that poly-cyclooctatetraene *is* polyacetylene. The one outstanding feature of poly-COT films is an extremely smooth surface, understood to be a consequence of polymerization conditions.

During the liquid stage of "neat" polymerizations, the polymer can be painted onto substrates, a significant advance in the processability of polyacetylene. The processability of a polymerizing liquid, and the versatility of substates on which and in which this polymerization can be conducted, unleashes numerous options for the fabrication of solid-state devices.

Much of the ingenious morphology research dedicated to improving the properties of polyacetylene--including shear flow polymerization conditions, polymerizations in liquid crystalline media, and film stretching to align chains--should be applicable to the polymerization of "neat" COT. During the liquid stage of the "neat" polymerization, it should be possible to induce the morphology of pre-formed substrates onto poly-COT. The ultimate goal in controlling morphology of organic conductors would be to grow single crystalline material in sheets or in bulk, so as to maximize the electrical/optical properties and allow for the possible fabrication of superlattices.

Unlike Ziegler-Natta catalyst polymerization of acetylene, this route employs a catalyst which tolerates several functionalities, including halogens. As evidenced by the example of bromocyclooctatetraene, metathesis polymerization of the readily available mono- and poly-substituted derivatives are expected to yield a series of polyacetylene derivatives previously unavailable. The derivatives of COT are varied and plentiful, and the means for their transformation into polyacetylene analogues has been developed by this research on this novel condensed-phase route to polyacetylene.

REFERENCES

(1) Wnek, G. E.; Chien, J. C. W.; Karasz, F. E.; Druy, M. A.; Park, Y. W.; MacDiarmid, A. G.; Heeger, A. J. *J. Polym. Lett. Ed.* **1979**, *17*, 779.

(2) For instance, see Woerner, T.; MacDiarmid, A. G.; Heeger, A. J. *J. Polym. Sci. Polym. Lett. Ed.* **1982**, *20*, 305.

(3) Fincher, Jr., C. R.; Peebles, D. S.; Heeger, A. J.; Druy, M. A.; Matasumura, Y.; MacDiarmid, A. G.; Shirakawa, H.; Ikeda, S. *Solid State Comm.* **1978**, *27*, 489.

(4) Druy, M.; Tsang, C.; Brown, N.; Heeger, A.; MacDiarmid, A. *J. Polym. Sci. Polym. Phys. Ed.* **1980**, *18*, 429.

(5) Chen, S. N.; Heeger, A. J.; Ziss, Z.; MacDiarmid, A. G.; Gau, S. C.: Peebles, D. L. *Appli. Physc. Lett.* **1980**, *36*, 96-98.

(6) Etemad, S.; Heeger, A. J.; MacDiarmid, A. G. *Ann. Rev. Phys. Chem.* **1982**, *33*, 443-69.

(7) Natta, G.; Mazzanti, G. P.; Corrandi, P. *Atti. Naz. Lincei. Cl. Sci. Fis. Mat. Nat. Rend.* **1958**, *25(8)*, 3.

(8) Shirakawa, H.; Ikeda, S. *Polym. J.* **1971**, *2*, 231.

(9) Akagi, K.; Katayama, S.; Shirakawa, H.; Araya, K.; Mukoh, A.; Narahara, T. *Synth. Met.* **1987**, *17*, 241.

(10) Meyer, H. *Synth. Met.* **1981**, *4*, 81.

(11) (a) Edwards, J. H.; Feast, W. J. *Polymer* **1980**, *21*, 595. (b) Edwards, J. H.; Feast, W. J.; Bott, D. C. *Polymer* **1984**, *25*, 395. (c) Bott, D. C.; Brown, C. S.; Chai, C. K.; Walker, N. S.; Feast, W. J.; Foot, P. J. S.; Calvert, P. D.; Billingham, N. C.; Friend, R. H. *Synth. Met.* **1986**, *14*, 245.

(12) Basescu, N.; Liu, Z.-X.; Moses, D.; Heeger, A. J.; Naarmann, H.; Theophilou, N. *Nature* **1987**, *327*, 403.

(13) Korshak, Y. V.; Korshak, V.; Kansichka, G.; Höcker, H. *Makromol. Chem. Rapid Commun.* **1985**, *6*, 685.

(14) Reppe, W.; Schichting, O.; Klager, K.; Toepel, T. *Ann.* **1948**, *560*, 1.

(15) Gasteiger, J.; Gream, G.; Huisgen, R.; Konz, W.; Schnegg, U. *Chem. Ber.* **1971**, *104*, 2412.

(16) Schaverien, C.; Dewan, J.; Schrock, R .R. *J. Am. Chem. Soc.* **1986**, *108*, 2771.

(17) Kress, J.; Wesolak, M.; Osborn, J. A. *J. Chem. Soc., Chem. Sommun.* **1982**, 514.

(18) Lippincott, E. R.; Lord, R. C.; McDonald, R. S. *J. Am. Chem. Soc.* **1951**, *73*, 3370.

(19) Ito, T.; Shirakawa, H.; Ikeda, S. *J. Polym. Sci.* **1974**, *12*, 11.

(20) Chien, J. C. W. in *Polyacetylene*, Academic Press: Orlando, p. 150 (1984).

(21) Gibson, H. W.; Pochan, J. M. *Encyclopedia of Polymer Science and Engineering*: Wiley-Interscience: New York, 1985; Vol. 1, pp 87-130.

(22) See MacDiarmid, A.; Heeger, A. *Synth. Met.* **1980**, *1*, 101.

(23) Reference 20, p. 249.

(24) Ito, T.; Shirakawa, H.; Ikeda, S. *J. Polym. Sci.* **1975**, *13*, 1943.

(25) Reference 20, p.37.

(26) Reference 20, p. 121.

(27) Bates, F. S.; Baker, G. L. *Macromolecules* **1983**, *16*, 1013.

(28) Gibson, H. W.; Kaplan, S.; Mosher, R. A.; Prest, Jr., W. M.; Weagley, R. J. *J. Am. Chem. Soc.* **1986**, *108*, 6843.

(29) Tober, R. L.; Ferraris, J. P. *Polymer Comm.* **1987**, *28*(12), 342.

(30) Upon cooling the sample and re-heating through 200 °C no exotherm is observed, as the sample has already undergone *cis-trans* thermal isomerization during the first scan.

(31) Unpublished results, this laboratory.

(32) Fray, G. I.; Saxton, R. G. *The Chemistry of Cyclooctatetraene and Its Derviatives*; Cambridge Univ. Press: Cambridge, 1978.

(33) Casey, C. P.; Burkhardt, T. J. *J. Am. Chem. Soc.* **1974**, *96*, 7808.

(34) Straus, D. A.; Grubbs, R. H. *J. Mol. Catal.* **1985**, *28*, 9.

(35) Eckert, H.; Yesinowski, J. P.; Sandman, D. J.; Velazquez, C. S. *J. Am. Chem. Soc.* **1987**, *109*, 761.

(36) Ozaki, M.; Peebles, D. L.; Weinberger, B. R.; Chiang, C. K.; Gau, S. C.; Heeger, A. J.; MacDiarmid, A. G. *Appl. Phys. Lett.* **1979**, *35*, 83.

(37) Burroughs, J. H.; Jones, C. A.; Friend, R. H. *Nature* **1988**, *335*, 137.

Chapter 4

Mechanistic Aspects of Metathesis Polymerization with a Well-Defined Tungsten Carbene

ABSTRACT

The mechanism of 1,3,5,7-cyclooctatetraene (COT) metathesis polymerization with a tungsten carbene catalyst is discussed, demonstrating and rationalizing concentration dependence upon product formation, and explaining mechanistic influence upon the observed *cis-trans* stereochemistry. A novel mechanism has been elucidated for the formation of benzene during dilute solution COT metathesis, and the statistics of this cycloextrusion reaction are explored for various COT derviatives.

Thermodynamic and kinetic data of a reversibly binding ligand are obtained for the well-defined tungsten carbene. The rate of 1,5-cyclooctadiene (COD) polymerization spans orders of magnitude, depending upon choice of solvent. Kinetics obtained in benzene-tetrahydrofuran (THF) solutions have shown that the rate of polymerization can be effectively controlled through choice of solvent composition. Rather than dismissing the various rates obtained as "due to solvent effects" and merely reporting as such, a mechanistic scheme for metathesis polymerization with the carbene catalyst has been evince to rationalize and quantitatively predict reaction rate as a function of the amount of THF present. Currently, this knowledge is being applied to improve the processability during the "neat" polymerization of COT. Addition of THF to COT (~10%) lengthens the liquid stage of polymerization to several minutes, thus allowing more time for the fabrication of this highly conducting polymer.

INTRODUCTION

The result of ring-opening metathesis polymerization (ROMP)[1] is cleavage of a cycloolefin carbon-carbon double bond, and intermolecular recombination of the sp^2 centers to form an unsaturated polymer as follows:

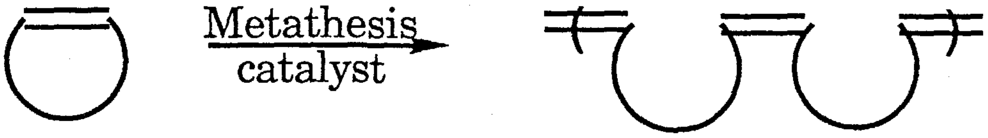

The active species in metathesis polymerization catalysts are transition metal carbenes ($L_nM{=}CHR$, metal doubly-bonded to carbon), either generated *in situ.*, or present by nature of the synthetic preparation of the catalyst. The *in situ.* generation of active species for the "classical" metathesis system $WCl_6/SnMe_4$ requires an aging time, during which a variety of reactions occur:[2]

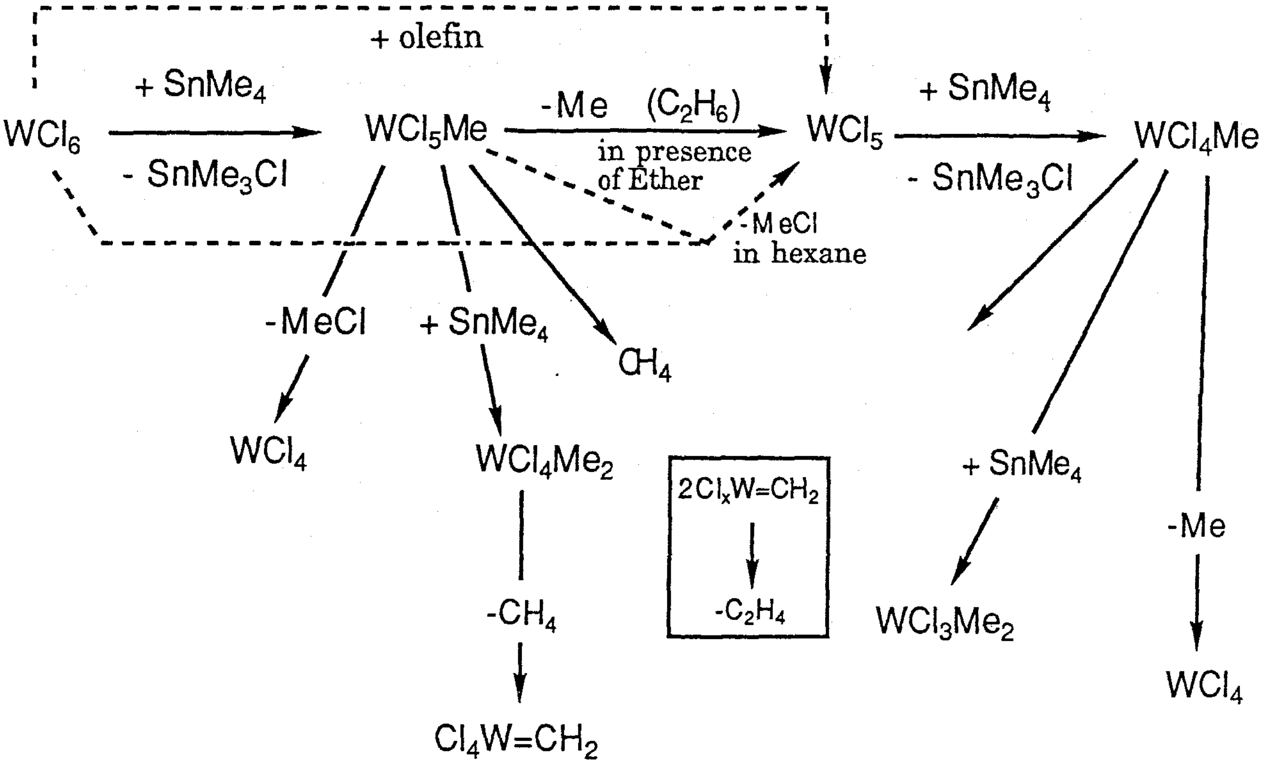

Many of these species are merely inferred from products. Solvent (aromatic molecules are alkylated) and olefin (allylic chlorination and coupling occur) complicate the reaction scheme. Unlike well-defined metathesis catalysts, the inclusion of trace amounts of moisture or air actually *accelerates* the metathesis reaction with WCl_6 (by forming $WOCl_4$).[2,3] More than this ill-defined amount of moisture, though, may inhibit the metathesis activity entirely. The mechanism is concentration dependent, and is different in diethyl ether than in chlorobenzene.[2] Two active methylidene species are known to be present (even under strictest exclusion of air/moisture),[4] though neither species has been isolated nor positively identified. Recent ESR studies have correlated rapidity of the metathesis reaction to a W(III) species when cyclopentene is the reagent; however, cyclooctene undergoes metathesis with the same conditions, and no W(III) is observed.[5] The termination step for the catalytic cycle has been proposed to be a bimolecular coupling of the tungsten carbenes,[6] but is yet to be proven.

An alternative, more useful approach in the investigation and understanding of metathesis polymerization has utilized well-defined, isolated carbenes or carbene•olefin adducts (metallacycles). The mechanism in the polymerization of norbornene with titanium metallacycles has been intensively researched by Gilliom and Grubbs (Figure 1).[7] The initial metal carbene is generated cleanly by thermal decomposition of the carbene•olefin adduct, followed by rapid trapping of cycloolefin to form a new metallacycle. This cycloaddition reaction is reversible, in that cleavage can occur across the four-membered ring non-productively to regenerate starting materials, or . . . cleavage can occur in the opposite sense to produce a new metal carbene. The newly formed carbene once again adds cycloolefin, then undergoes ring opening, forming the growing polymer chain. Although each step is indicated as reversible, the polymerization is driven to completion because the relief of monomer ring strain involved in each ring-opening step provides an overwhelming thermodynamic driving force.

Figure 1: Norbornene Metathesis Polymerization with Titanocene Metallacycles

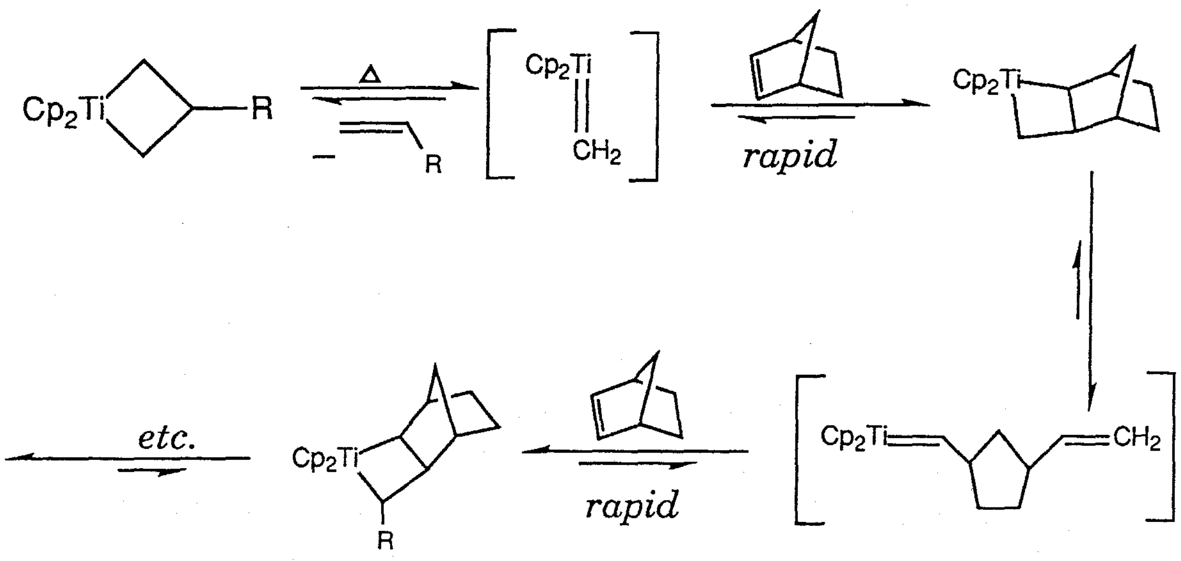

For cyclooctatetraene, the lower monomer ring-strain energy dictates the use of more-reactive catalytic species — the aryl-amido tungsten carbene **1**, designed and first synthesize by R. Schrock and co-workers — where the polymerization mechanism is less clearly defined. The impetus for this mechanistic investigation of catalyst **1** stems from the development of a convenient and versatile route into a family of polyacetylene analogues through the metathesis polymerization of cyclooctatetraenes.[8]

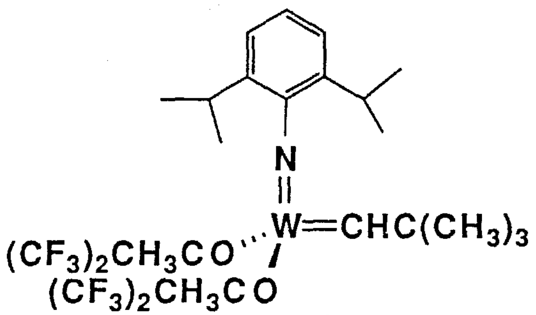

1

EXPERIMENTAL

General considerations. Materials were stored and handled in a nitrogen filled Vacuum Atmospheres drybox outfitted with a refrigeration unit. Solution NMR spectra were recorded on a JEOL FX-90Q (89.60 MHz ^1H) or a JEOL GX-400 (399.65 MHz ^1H) instrument equipped with variable temperature thermostatting (±0.2 °C). Analytical gas chromatography was performed on a Shimadzu GC-mini 2 flame ionization instrument equipped with a 0.24 mm x 25 m SE-30 capillary column, and gas chromatograpy-mass spectroscopy (GC-MS) analyses were performed on a Hewlett-Packard 5890/5970 instrument (10 m SE-30 capillary column). Gel permeation chromatography (GPC) studies utilized Shodex KF-803 and KF-804 columns, a Spectroflow 757 absorbance detector with l = 254 nm, and a Knauer differential refractometer.

Materials. Cyclooctatetraene was prepared by Reppe cyclotetramerization of acetylene.[9] COT was fractionally distilled (45 °C, 25 mm Hg), filtered through neutral alumina, and vacuum distilled from CaH_2. Purity was confirmed by GC analysis before use (>99.9%). Purified COT was stored under nitrogen, below its melting point, protected from light. Norbornene (Aldrich, 99%), 1,5-cyclooctadiene (Aldrich, 99%), 1,3-cyclooctadiene (Aldrich, 98%), 1,3,5-cyclooctatriene (Organometallics, 97%), bromo-cyclooctatetraene[10] were purified by vacuum distillation from CaH_2. Solvents were vacuum distilled from benzophenone ketyls, except for methylene chloride which was vacuum distilled from P_2O_5. Benzaldehyde was fractionally distilled from sodium carbonate and degassed prior to use. Tetrahydrofuran (THF), pentane, benzene, d_6-benzene and d_8-THF (Cambridge Isotopes) were vacuum distilled from benzophenone ketyls. Catalyst **1** was synthesized as previously reported.[11]

Dilute solution polymerization of COT and Br-COT. Catalyst **1** (2.1 mg, 2.7 μmol) was dissolved in d_8-toluene (0.50 mL) in an NMR tube before capping with septum. ^1H NMR shifts vs. residual solvent: δ 8.84 (s, 1H, carbene), 7.06 (s, 1H, *p*-aromatic), 6.95 (s, 2H, *m*-aromatic), 3.52 (septet, 2H, C$\underline{H}$Me$_2$), 1.35 (s, 6H, alkoxide) 1.23 (s, 6H, CH$\underline{Me_2}$), 1.15 (s, 6H, CH$\underline{Me_2}$), 1.06 (s, 9H, t-Bu). COT (3.0 mL, 26.5 mmol) was injected from a septum-capped vial *via* syringe into the NMR tube, and after brief vigorous shaking a spectrum was promptly recorded (~30 seconds) to obtain initial COT integration ratio. COT peak (δ 5.61, s) diminished (absent after 30 minutes) and a new peak (δ 7.13, s), assigned to benzene, grew in. Sharp singlets in the aliphatic region appeared, δ 1.63 and 0.96, tentatively assigned to the alkoxide and t-butyl protons of activated catalyst, respectively. Activated/unactivated catalyst determined by integration δ 1.63/ δ 1.35. COT and benzene integrations were referenced to residual proton concentration of toluene.

For the bromo-cyclooctatetraene kinetics, 0.50 mL of a stock solution--10.0 mg **1** in 2.50 mL CD_2Cl_2--was placed in a septum-capped NMR tube. Approximately 3 mL Br-COT was injected, and after brief shaking a spectrum was taken immediately for initial Br-COT/ catalyst ratio. All integrations were referenced to residual proton concentration of methylene chloride.

Binding studies. In the drybox, a stock solution of catalyst (26.8 mg, 0.033 mmol) in 2.0 mL d_6-benzene was prepared and stored under nitrogen in a capped vial below its freezing point (at -40 °C). For each binding experiment, 500 mL of the catalyst solution (.017 M) was syringed into a 5-mm NMR tube capped with an air-tight septum. Pure THF was placed in a separate septum-capped tube. The proton chemical shift of the catalyst in d_6-benzene was recorded and used as the value of δ_{free} before 1 equivalent of THF (0.67 mL) was transferred into the catalyst solution by syringe. The shift of the carbene proton was recorded at five different temperatures before each subsequent addition of THF. This titration process was repeated for 3 such samples of the catalyst solution, giving a reproducibility within 5% of the binding constants. Values for $\mathbf{K_f}$ are reported in Figure 4.

Kinetic studies. Measured quantities of catalyst, d_8-THF, and d_6-benzene were loaded into a 5-mm NMR tube capped with septum. Pure COD was placed in a seperate septum-capped tube. After the catalyst-ligand solution was in the NMR cavity, COD monomer (10.0 ± .4 equivalents) was added. Reaction of COD was monitored readily by integration of the sp^3 protons (relative to TMS: $\delta = 2.31$ ppm for unreacted monomer, $\delta = 2.09$ ppm for ring-opened species) until no monomer remained.

For the polymerization kinetics in "neat" ligand, a 0.016 M stock solution of catalyst in d_8-THF was prepared. For temperatures 25, 40, and 60 °C, the kinetics of COD polymerization were followed as described above. The rates -d[COD]/dt for the linear portion of the curves are as follow: 0.00037 $M{\cdot}min^{-1}$ for 25 °C, 0.0015 $M{\cdot}min^{-1}$ for 40 °C, and 0.0058 $M{\cdot}min^{-1}$ for 60 °C.

GC-MS analysis of end-capping. In the drybox a stock solution of catalyst in THF (0.016 M) was prepared, and 500 mL aliquots were placed in each of two vials. To only one of the vials, 10.0 equivalents COD were added. Both vials were capped and stirred 4 hours at 23-25 °C, then excess benzaldehyde (10.2 mL; 0.10 mmol) was added to each vial. Both solutions were eluted through a short column of neutral alumina (~50 mg alumina in a glass pipette) with 2 mL pentane.[12] Each solution was diluted 100-fold with pentane and analyzed by GC-MS. The column oven temperature was ramped from 30 °C to 280 °C at a rate of 10 °C / minute.

For the solution to which no COD was added, the sole peaks observed (after pentane/THF fractions) were identified as corresponding to benzaldehyde (parent peak m = 108, retention time t = 4.6 min.), β-t-butylstyrene (m = 160, t = 7.9 min.), β-t-butylstyrene (m = 160, t = 9.3 min.), $2,6\text{-}(i\text{-}Pr)_2\text{-}PhNH_2$ (m = 177, t =12.0 min.) and $2,6\text{-}(i\text{-}Pr)_2\text{-}PhN{=}CHPh$ (m = 265, t = 18.0 min.). The two peaks for the β-t-butylstyrene at 7.9 and 9.3 minutes (ratio 3.1 : 1) most likely correspond to the *trans* and *cis* isomers. The final two peaks represent a hydrolized catalyst fragment, and its shift base condensation with benzaldehyde. The ratio of the peak integration β−t-butylstyrene / benzaldeyhde = 0.32. The retention times for the five components using capillary GC analysis (oven temperature constant at

200 °C) are (in minutes) 4.2, 4.7, 4.9, 6.2, and 18.8.

For the catalyst solution to which COD was added, again a ratio of 3.1 : 1 was observed for the *trans* and *cis* β-t-butylstyrene peaks. The ratio of the peak integrations β-t-butylstyrene / benzaldeyhde = 0.20. Also present are 2 new peaks (t = 10.0 min. and t = 10.4 min.) each with a parent peak at m = 162, likely corresponding to isomers of cyclododecatriene ($C_{12}H_{18}$).

GPC of polymers. All analyses were performed on 0.2% w/v solutions of polymer in THF. Flow rate was 1 mL / minute. Calibration was based upon monodisperse polystyrene samples (Polysciences) of various molecular weights, and molecular weights reported for poly-COD and poly-NBE have not been corrected with respect to the hydrodynamic volume of polystyrene. Polydispersities were calculated by standard procedures[13] from the UV trace and were not corrected for peak broadening.

RESULTS

Role of Cycloextrusion

Dilute Solution Polymerization. In a dilute solution of catalyst **1**, COT is completely consumed affording a 75% yield of benzene,[14] as observed by ^{1}H NMR. Benzene is confirmed by ^{13}C NMR and also by gas chromatography. During the disappearance of monomer and simultaneous appearance of benzene, the solution changes from its initial color of yellow to orange, red, magenta, and finally to a fine suspension of black particles. In an NMR tube where spinning tends to compact the particles against the inner wall, a highly reflective silvery sheen develops. A 0.005 M concentration of catalyst **1** in benzene consumes 10 equivalents COT in about 20 minutes. Only 30-40% of **1** is active in the polymerization, as revealed by ^{1}H NMR. The polymerization has been conducted in toluene, benzene, methylene chloride, tetrahydrofuran, diethyl ether, and pentane.

The rate of polymerization varies by magnitudes of order dependent upon solvent. In pentane, a 0.03 M concentration of catalyst **1**, upon addition of 25 equivalents COT, forms an insoluble black powder within seconds. Similar conditions with toluene extends the reaction time to 2-3 minutes. In THF at these concentrations the polymerization occurs over 1-2 hours. No attempt was made to determine kinetic rate constants for COT polymerization in the various solvents.

Based on the accepted mechanisms of other carbene metathesis reactions,[1,7] the mechanism of Scheme I is proposed for ring-opening metathesis polymerization (ROMP) of COT in dilute solution. The cyclooctatetraene molecule first enters into a 2 + 2 cycloaddition reaction with the tungsten carbene (W=C-R) to form a metallacyclobutane, then undergoes ring-opening cleavage to produce a new tungsten carbene. After rearrangement, the carbene proceeds to back-bite the chain , and then extrudes benzene. If the proposed mechanism is correct, then analogous results should be obtained with structures similar to COT.

Scheme I. Dilute Solution Polymerization of COT

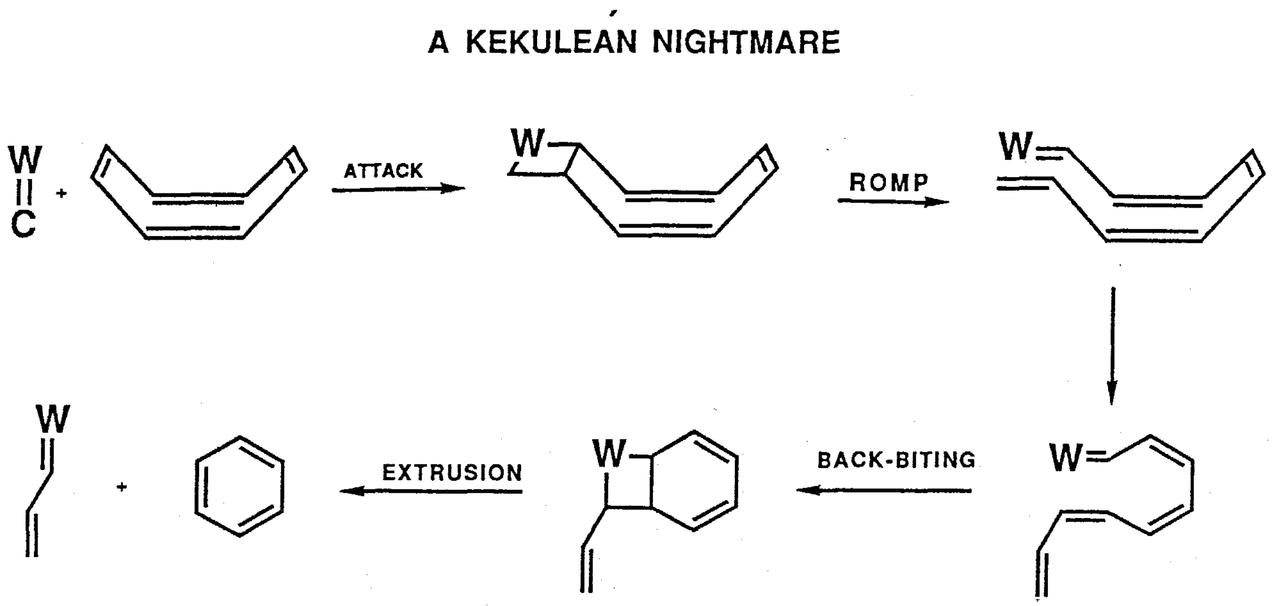

Consistent with the proposed mechanism, 1,3-cyclohexadiene is produced in 55-60% yield during polymerization of 1,3,5-cyclooctatriene, and polymerization of 1,3-cyclooctadiene yields ~40% cyclohexene. Neither cyclooctene nor 1,5-cyclooctadiene give cycloextrusion products when reacted with catalyst **1** in dilute solution. Bromobenzene, but not benzene, is formed during the polymerization of bromocyclooctatetraene (Figure 2). The dilute solution polymerization of all these cycloolefins involves orange, then red, transparent solutions before finally evolving into an opaque brown suspension of particles.

Undiluted Polymerization. It has previously been determined[8] that cycloextrusion plays no major role in the polymerization of *neat* cyclooctatetraene, in which the resulting poly-COT film gives a yield > 95% by mass. The same result should be expected for the polymerization of *neat* 1,3,5-cyclooctatriene. Employing the same conditions used for polymerization of *neat* cycloctatetraene, solid films from liquid cyclooctatriene are produced. Films are red-orange, and soluble to a limited extent in chloroform. Shown in Figure 3 is the ^{1}H NMR spectrum. For reference, the proton shift of grafted polyacetylene[15] occurs at ~7.1

ppm. Thus, by varying experimental conditions, the metathesis polymerization of these cycloolefins can give rise to very different, yet explicable, products.

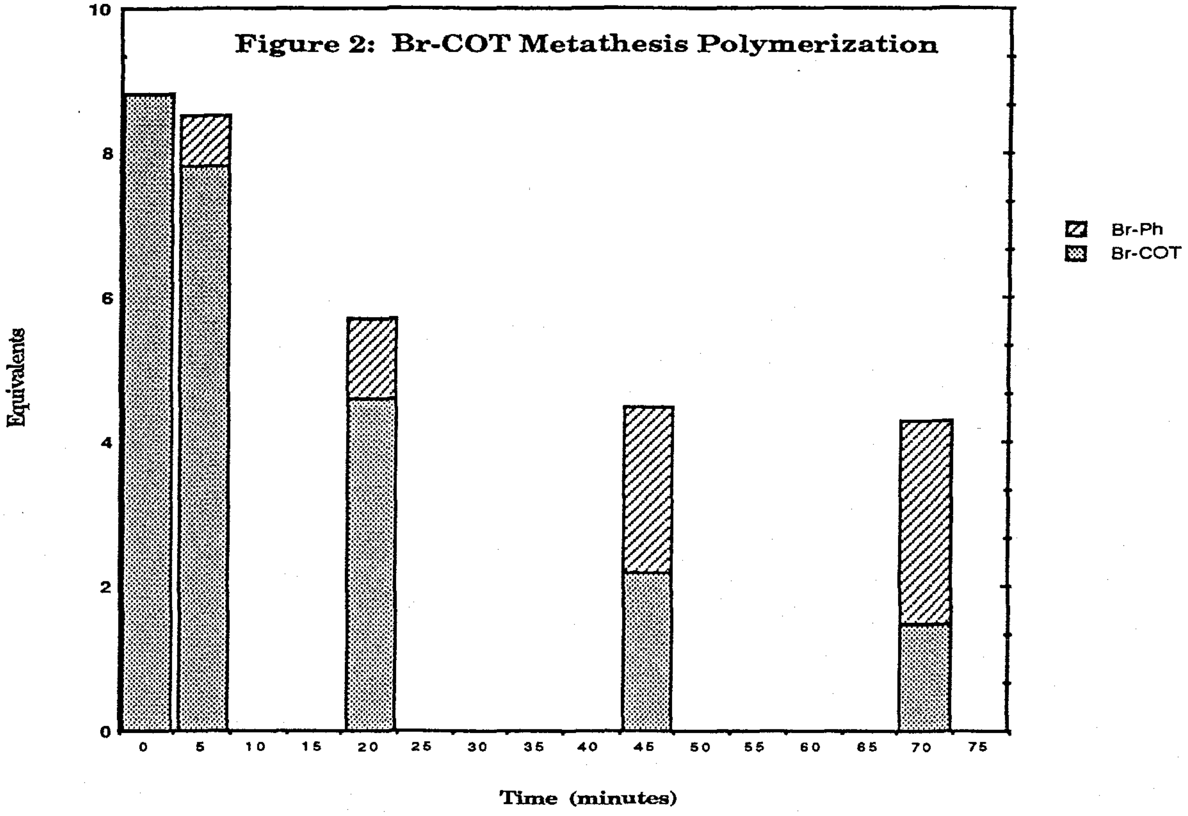
Figure 2: Br-COT Metathesis Polymerization

Role of a Reversibly Binding Ligand

Formation. In order to gain a better understanding of the tungsten carbene catalyst **1**, one would profit from considering its synthetic preparation (Scheme II). Although both tungsten carbynes and tungsten carbenes functionalities have previously demonstrated metathesis activity, the only organometallic complex with metathesis activity in Scheme II is that of the final product — catalyst **1**. Particularly interesting is the fact that while the final product is extremely reactive, its precursor demonstrates no metathesis activity whatsoever, yet they differ only by virtue of a dimethoxyethane ligand. Why this vast difference in activity?

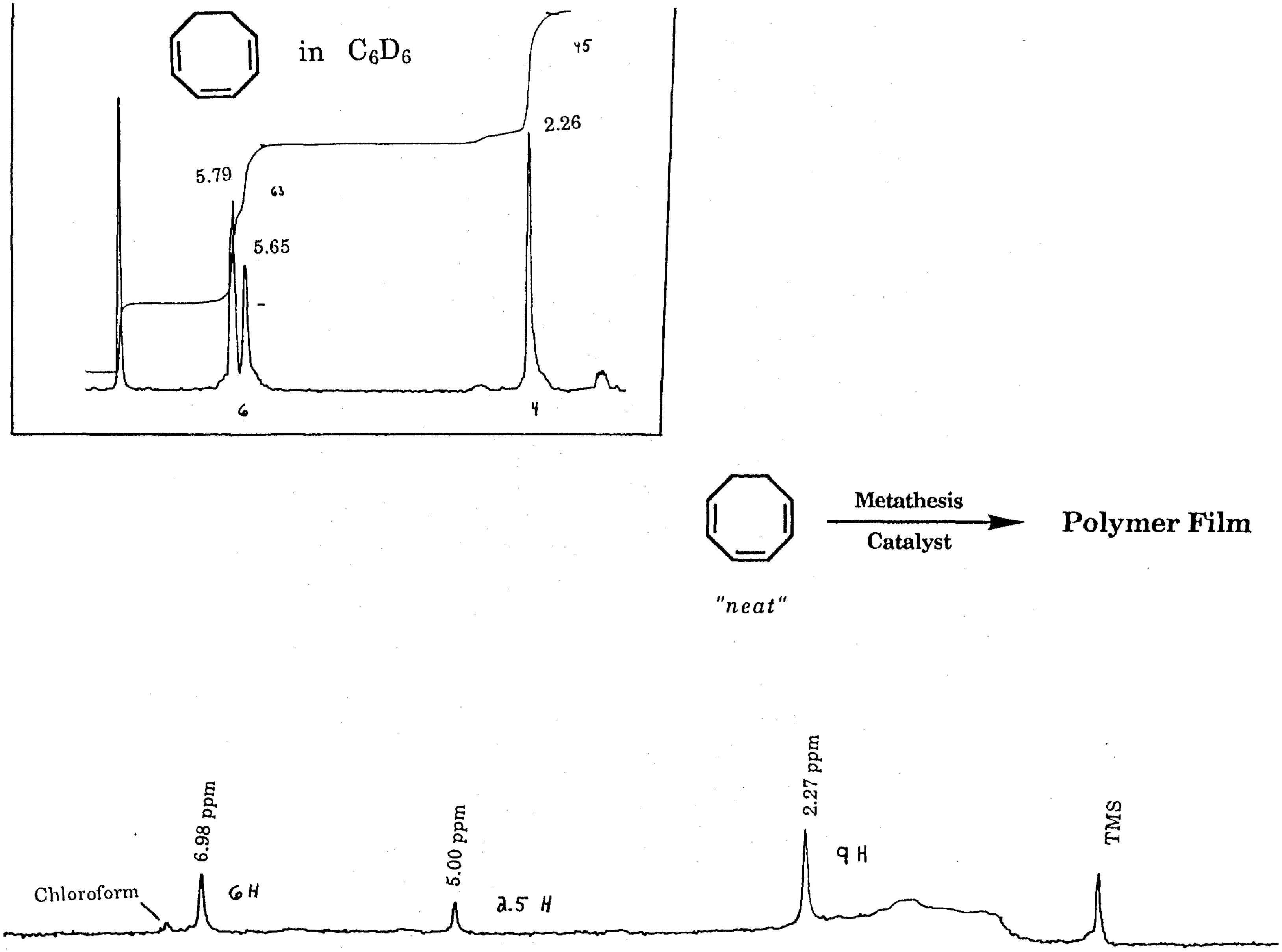

Figure 3. ^{1}H NMR of poly-1,3,5-cyclooctatriene.

Scheme II. Synthesis of Arylamido Tungsten Carbenes

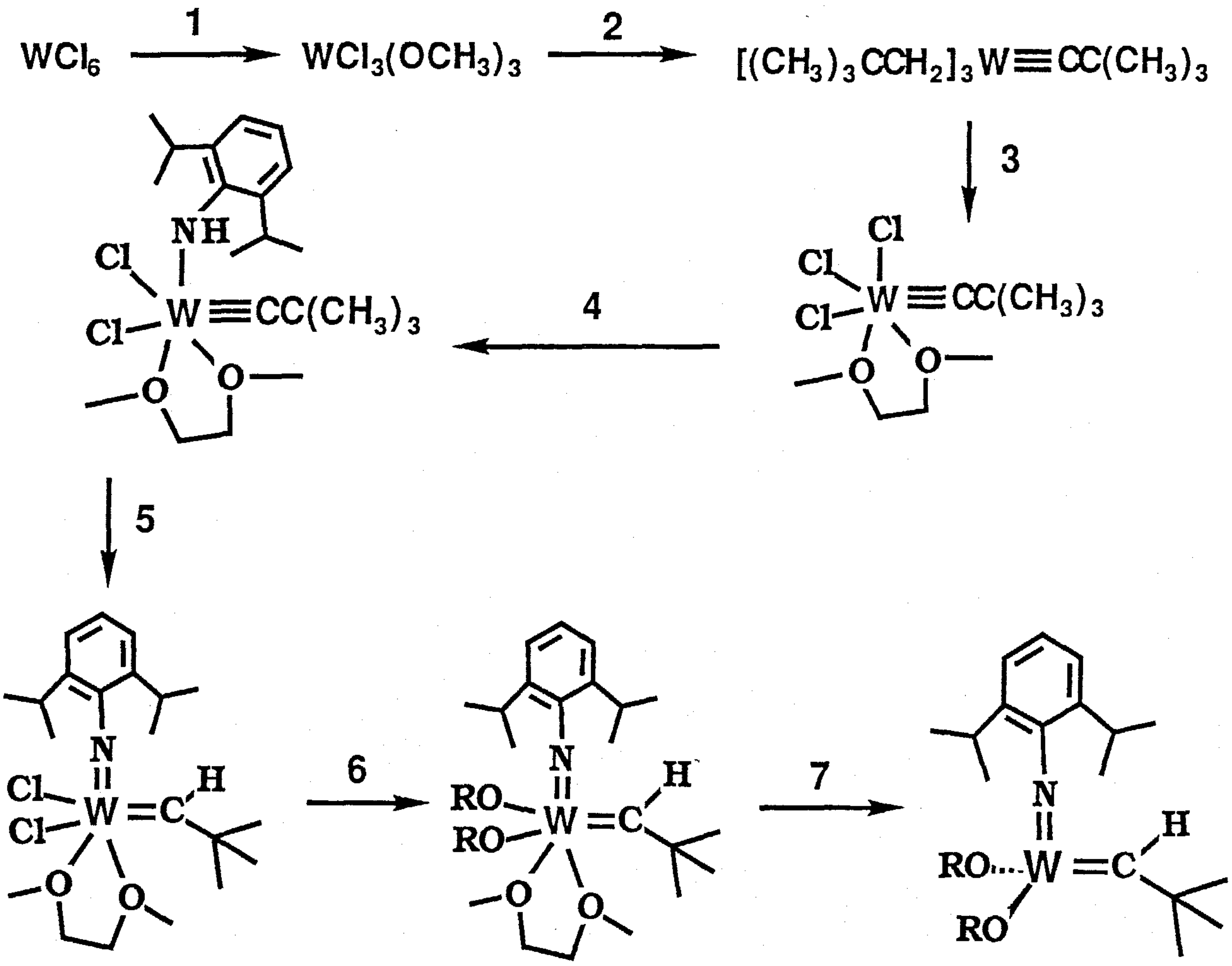

1) CH_3OTMS; ether
2) ${}^tBuCH_2MgCl$; ether
3) HCl + DME; pentane
4) ArNHTMS; ether
5) NEt_3 (trace)
6) LiOR; ether
7) <1 micron, - DME

The metathesis catalyst **1** is 14 electron species with an open site for ligand coordination. The tungsten center is highly oxidized and is expected to readily bind to Lewis basic species such as olefins, phosphines, amines, and ethers. The binding of electron-donating ligands to tungsten not only crowds the coordination sphere, but also reduces the electronegative character of the carbene, making it less reactive towards cycloolefins on both accounts.

Dimethoxyethane is a strongly binding ether due to its having two oxygen atoms. A less strongly bound ether might be expected to have reactivity somewhere between that of the extremely reactive catalyst **1** and its non-reactive dimethoxyethane adduct. Tetrahydrofuran (THF) seemed a logical candidate. It is an ether with only 1 binding site. The perdeutero derivative is readily available for use in NMR studies, and it serves as an excellent solvent for many types of polymers.

Thermodynamic studies. Unbound (**1**) and bound (**2**) catalyst species would be expected not only to have differing chemical reactivities, but also the catalyst protons for the two

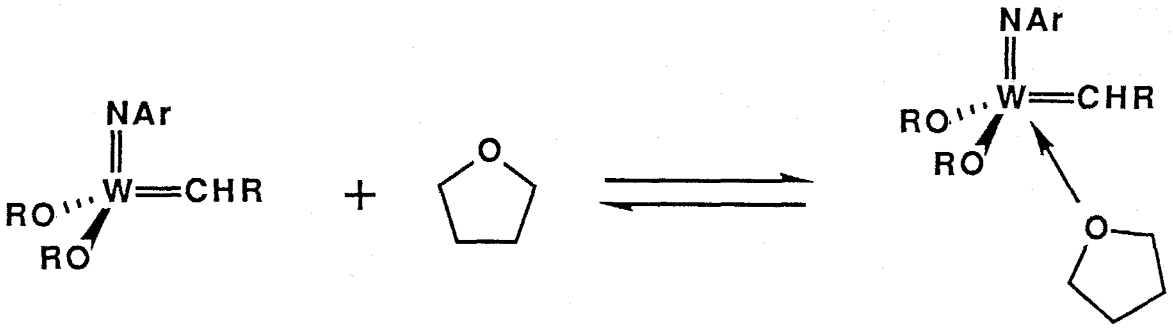

1

2

species should exhibit different chemical shifts in ^{1}H NMR. The carbene (alpha) protons, due to their proximity, are particularly sensitive to the electronic environment of the tungsten center. If both **1** and **2** are present, then two peaks should be observed in proton NMR. If the binding-dissociation equilibrium of the ligand is sufficiently rapid on the NMR time scale, then the shifts of the bound and unbound species coalesce into a single peak whose shift is governed by the relationship:

$$\delta_{obs} = \delta_{free} + (\%\ \text{bound}) * (\Delta\delta) \qquad \textbf{\textit{Eq. 1}}$$

where δ_{obs} = observed chemical shift
δ_{free} = chemical shift of unbound catalyst
% bound = fraction of catalyst bound
$\Delta\delta$ = difference in chemical shift of bound vs. unbound catalyst.

The position of the observed chemical shift is a colligative property of the bound and unbound species.

The "percent bound" parameter is determined by considering the equilibrium

$$\mathbf{K_f} = [\text{CL}] / ([\text{L}]*[\text{C}])$$

where $\mathbf{K_f}$ = formation constant
[CL] = concentration of bound catalyst
[L] = concentration of ligand
[C] = concentration of unbound catalyst.

Using the expressions $[\text{L}] = \mathbf{L_o} - [\text{CL}]$ and $[\text{C}] = \mathbf{C_o} - [\text{CL}]$, where $\mathbf{L_o}$ and $\mathbf{C_o}$ represent the formal concentrations of ligand and catalyst respectively,

$$\%\ \text{Bound} = [\text{CL}]/\mathbf{C_o} = [\text{b} - (\text{b}^2 - 4*\mathbf{L_o}*\mathbf{C_o})^{.5}] / (2*\mathbf{C_o})$$

where $\text{b} = \mathbf{L_o} + \mathbf{C_o} + 1/\mathbf{K_f}$.

Known values in ***Eq. 1*** for any given experiment include δ_{obs} and δ_{free}. Unknown in the expressions "% bound" and "$\Delta\delta$" are the values of K_f and the chemical shift of the bound carbene. Choosing a set of experiments in which the concentrations of ligand and/or catalyst are varied, these two unknown parameters can be determined. A computer program was utilized to best fit the formation constant to observed parameters, giving $K_f = 15.4 \pm 0.5$ M^{-1} for THF binding to the tungsten carbene **1** at 25 °C (see Table 1).

Table 1. Catalyst-THF Binding @ 25 °C

Co	THFo	Obs'd Shift	Calc'd Shift	% C Bound	% THF Bound
0.017	0.017	803.2	803.1	17.72	17.72
0.017	0.17	828.9	828.5	70.86	7.09
0.015	1.50	837.7	840.4	95.81	1.09
0.017	12.2	844.5	842.2	99.47	0.14

Obs'd: Chemical shift of unbound catalyst = 794.6 Hz
Calc'd: Binding constant $K_f = 15.4$ M^{-1}

Calc'd: δ of bound carbene = 842.4 Hz

Calc'd: δ RMS deviation = 1.81 Hz

The binding constant was similarly determined for several temperatures. The $\ln K_f$ *vs.* T^{-1} plot for THF-catalyst binding yields a positive linear slope with excellent correlation (Figure 4). The enthalpy of binding is -8.9 Kcal·mol^{-1}, and the entropy is -24 cal·K^{-1}·mol^{-1}. At 0 °C the free energy of reaction ($\Delta G = \Delta H - T\Delta S$) is calculated as -2.3 Kcal mol^{-1}; at 100 °C the binding becomes thermodynamically unfavorable (positive ΔG).

Figure 4. van't Hoff Plot (Natural Log of Binding Constant vs. 1/T) for THF Binding to Catalyst **1**.

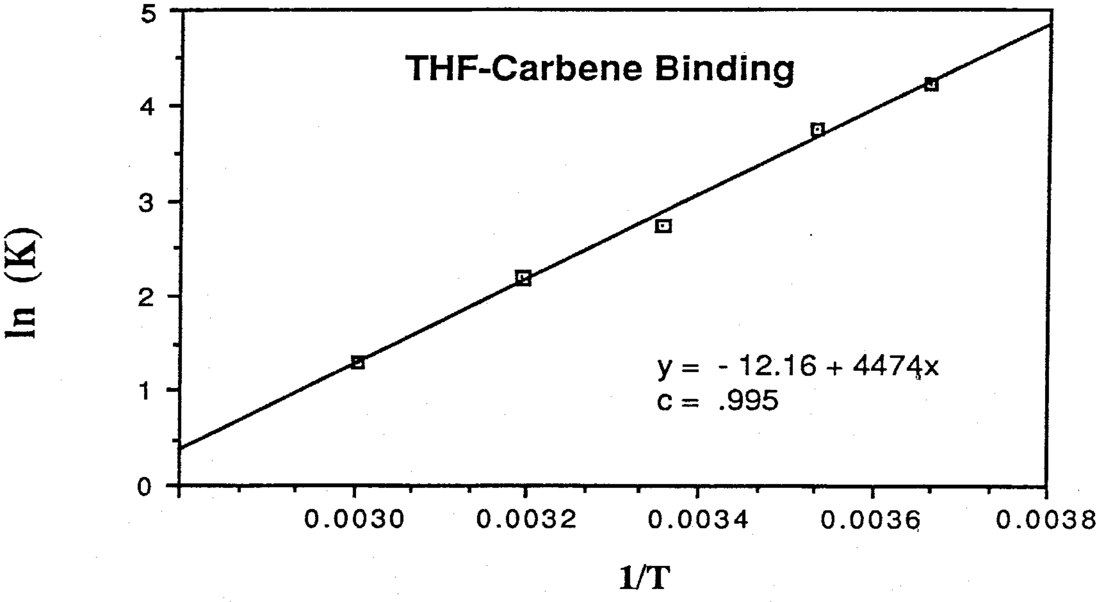

Temp. (^oC)	K_f (M^{-1})	$\Delta G = -RT\ln K_f$ (kcal/mol)
0	67.5	-2.28
10	42.3	-2.10
25	15.4	-1.62
40	8.97	-1.36
60	3.56	-0.84

ΔH = -8.9 kcal/mol
ΔS = -24 cal/mol•K

Propagation Kinetics of Metathesis Polymerization. In a 0.01 M solution of catalyst **1** in pentane, addition of 10 equivalents 1,5-cyclooctadiene (COD) at room temperature results in immediate polymerization. In benzene or toluene the polymerization is concluded within 30 seconds. In THF the metathesis polymerization reaction proceeds at a rate sufficiently moderate so as to allow good kinetic data to be obtained.

For this kinetics study, COD was the monomer of choice. Most importantly, the polymer resulting from metathesis polymerization of COD is very soluble allowing for homogeneous conditions throughout the reaction. Also, COD is not susceptible to the cycloextrusion reaction as is COT, simplifying the kinetics. Finally, COD has a similar ring structure, similar ring strain energy, to that of COT (~2.3 kcal/mol for both), so that both should undergo metathesis polymerization at very similar rates. In fact, this latter hypothesis has been confirmed, and is the basis for the formation of random COD/COT copolymers (as discussed in the **Copolymers** section of this thesis, Chapter 5).

For catalyst concentration $\mathbf{C_o}$ = 0.016 M in THF, and added monomer (COD) concentration $\mathbf{M_o}$ = 0.16 M, monomer concentration as a function of time is depicted in Figure 5 for 25, 40, and 60 °C. In each instance the linear dependence of [COD] vs. time throughout the initial stage of the reaction indicates zeroeth order dependence of rate upon monomer concentration. Near the end of the reaction [COD] vs. time deviates significantly from linearity.

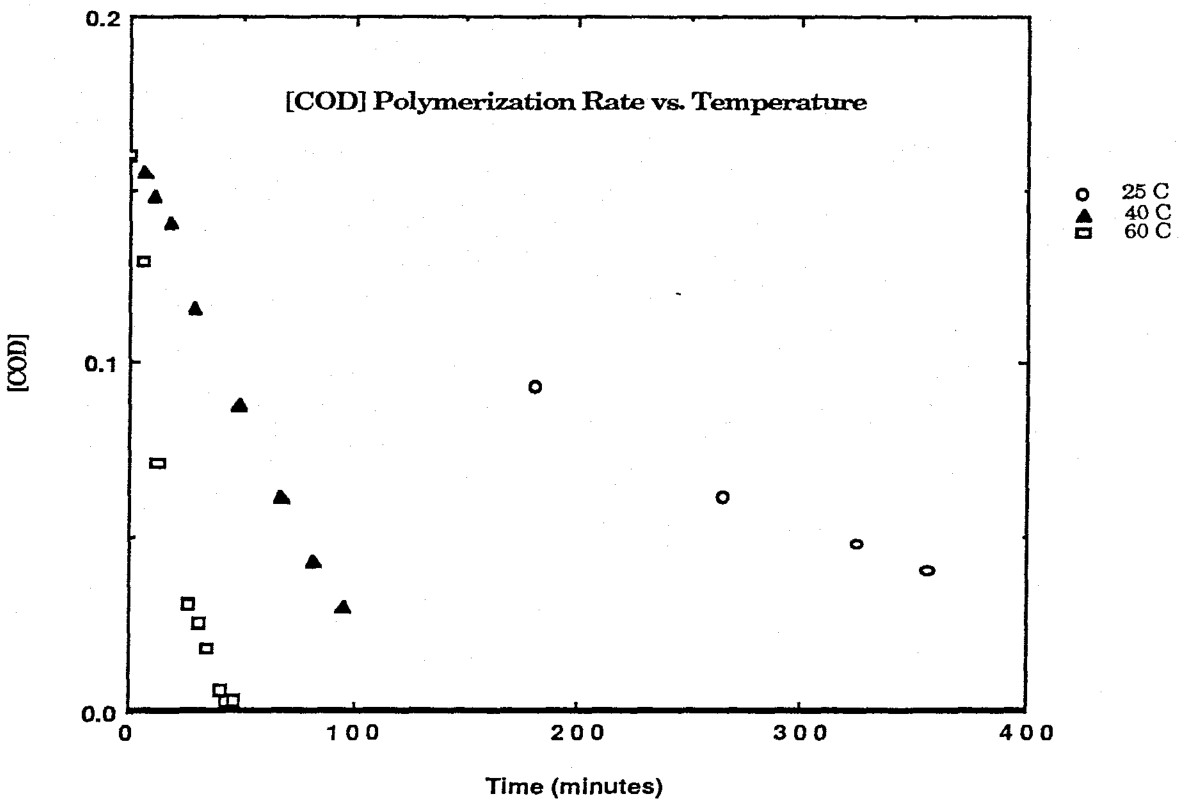

Figure 5. COD polymerization rate with catalyst 1 for 25, 40, and 60 °C.

It has already been determined that THF enters into a rapid equilibrium binding with the tungsten carbene. This suggests that a cycloolefin might also enter into a rapid pre-equilibrium binding with the catalyst to form a substrate-catalyst complex, which then undergoes the metathesis reaction (1) converting bound monomer into an acyclic "polymer tail" attatched to the carbene and (2) regenerating the tungsten carbene catalytic species. This description fits the kinetic model for 'enzyme' kinetics. And since the reaction is being investigated in THF where the THF molecules compete for the reactive site on the catalyst, the description for enzyme kinetics with a competitive inhibitor serves as a relevant model for this metathesis reaction system (Scheme III). In this description

$$-d[M]/dt = k_1 k_2 C_0[M] \,/\, \{(K_f[L] + 1)*(k_2 + k_{-1}) + k_1[M]\} \qquad \textit{Eq. 2}$$

$$\text{or} \quad 1 / \text{Rate} = (K_f[L] + 1)*(k_2 + k_{-1}) / (k_1 k_2 C_0[M]) \; + \; 1 / (k_2 C_0)$$

so that the inverse rate should be linear with respect to $(K_f[L]+1)/(C_0M)$. The rate of metathesis polymerization was monitored by ^1H NMR for various THF concentrations in d_6-benzene (Figure 6a). Figure 6b shows that, in accordance with Equation 2, the inverse rate is a linear function of $(K_f[L]+1)/(C_0M)$.

Scheme III: Metathesis Kinetics with a Reversibly Binding Ligand Present

$$\mathrm{C} + \mathrm{L} \rightleftharpoons \mathrm{C{\bullet}L}$$

$$\mathrm{C} + \mathrm{M} \rightleftharpoons \mathrm{C{\bullet}M}$$

$$\mathrm{C{\bullet}M} \longrightarrow \mathrm{C}$$

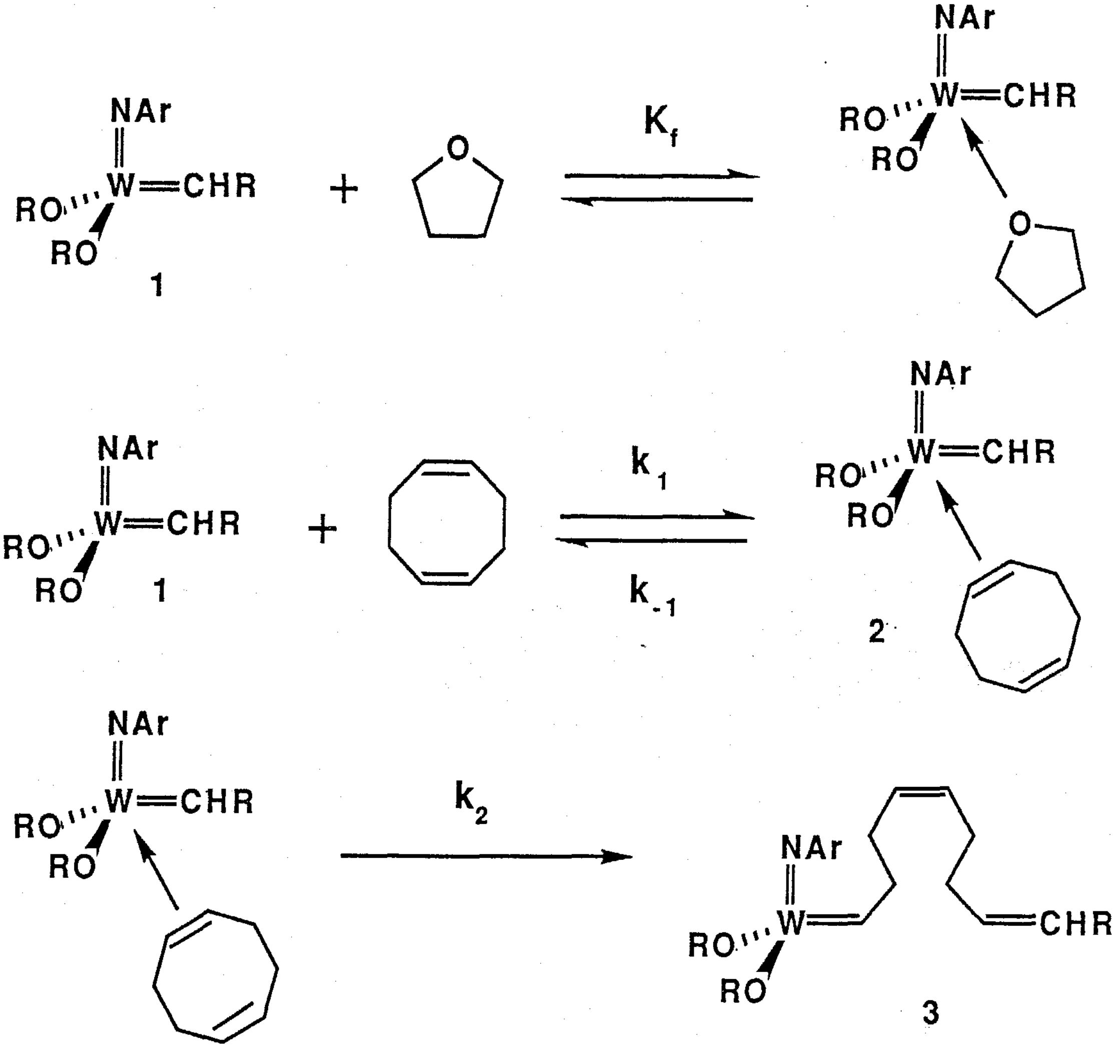

Figure 6a. COD Metathesis Polymerization Kinetics at Various THF Concentrations.

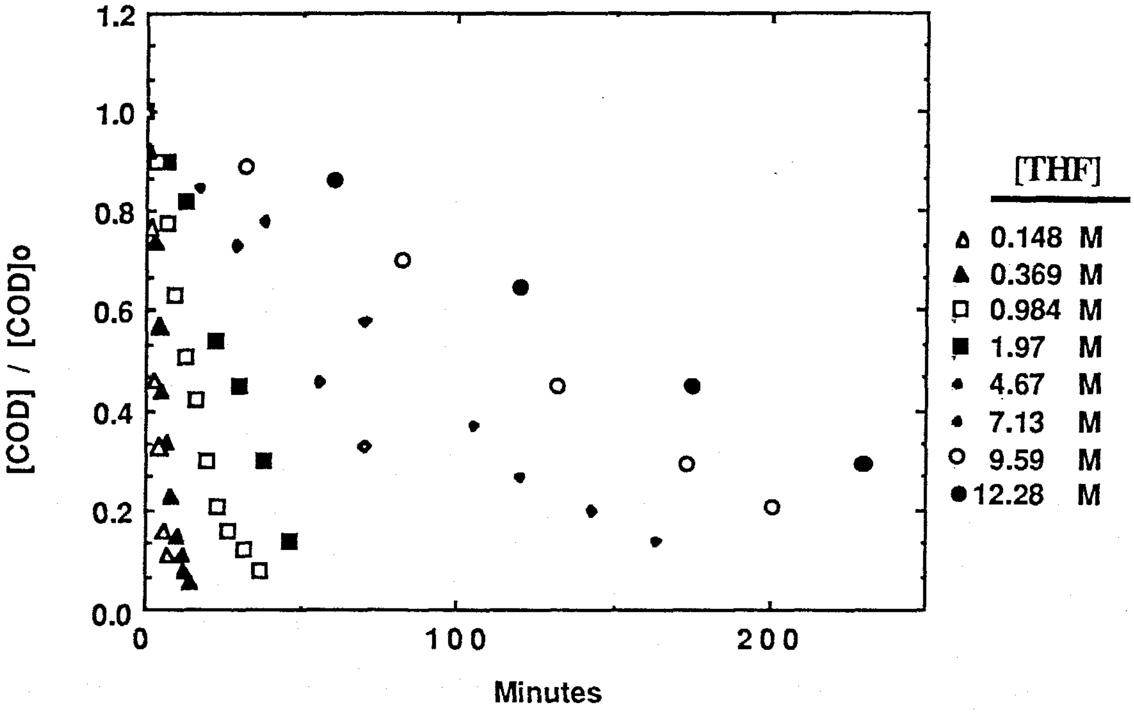

Figure 6b. COD Polymerization Rate Dependence upon THF Concentration Term

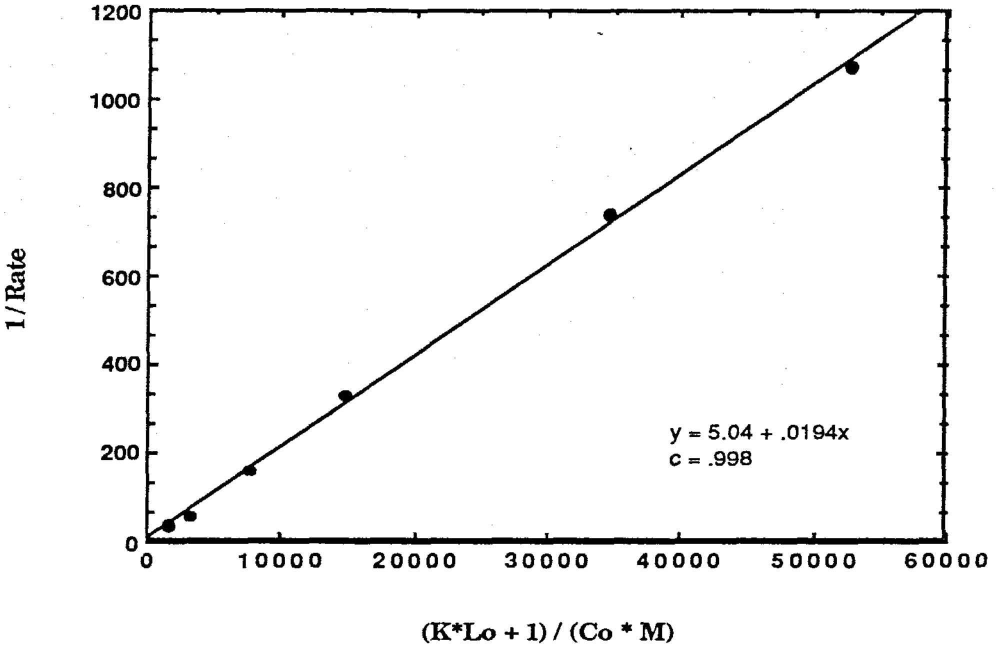

Initiation. Excluded from this kinetic scheme are the initiation step (t-butyl substituted carbene **1** reacting with monomer to yield carbene **3**) and the catalyst binding of the product (acyclic double bonds in oligomeric tail). If initiation of all catalyst were rapid and no chain-transfer occurred during the reaction, then the molecular weight of the growing polymer should increase linearly with respect to monomer conversion. That is, the degree of polymerization (number of monomer units per chain) should at near quantitative conversion be defined by $\mathbf{M_O} / \mathbf{C_O}$, with a narrow distribution of polymer chain lengths.

The degree of catalyst initiation during COD polymerization can be investigated by the addition of some ketone or aldehyde, such as benzaldehyde. Uninititiated catalyst **1** reacts with benzaldehyde yielding β-t-butlystyrene, while the initiated catalyst species **3** yields end-capped oligomers (Figure 7).

Figure 7: Carbene End-capping.

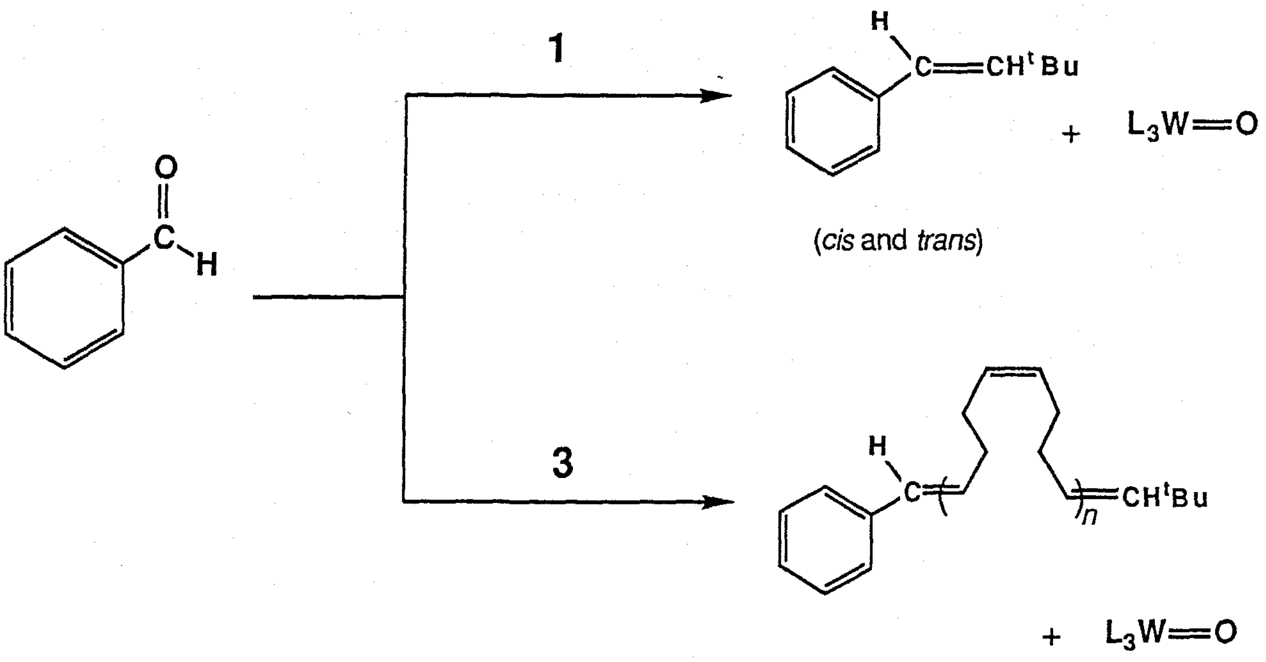

Gas chromatography-mass spectral analysis of the products indicates that after approximately 85% conversion of 10 equivalents COD, only 40% of the catalyst has been activated. This is consistent with previous observations involving a wide variety of cycloolefins that the tungsten carbene **1** has an initiation step much slower than the propagation step. The initial slow reaction of catalyst with cycloolefin is likely due to the stearically hindering t-butyl group present on the a-carbon. Once the catalyst **1** initiates, the stearically unhindered carbene **3** allows for rapid propagation. GC-MS also reveals the minor presence of short cyclic oligomers, produced from catalyst "back-biting."

Gel permeation chromatography (GPC) analysis of the polymer formed from the above reaction indicates a number average molecular weight $M_n = 11400$ (hydrodynamic volume relative to polystyrene; uncorrected) with a polydispersity index PDI = 1.81.

It was reasoned that the role of THF in the metathesis polymerization of COD was to slow down the propagation step relative to initiation, so that the two signatures of a "living" polymerization, 1) well-defined kinetics and, 2) linear increase of molecular weight with monomer conversion could be realized. Determination that a major fraction of the catalyst is not active in polymerization, and the finding of a rather wide distribution of chain lengths, show that a "living" polymerization is not the case. The reason for a majority of the catalyst remaining inactive towards polymerization, even though it is active in binding THF, is not fully understood at this time.

Stability of THF-Bound Catalyst. It is often the desired role of a catalyst to provide as much selectivity, and as rapid conversion, as possible. The family of carbenes represented by **1**[17] perform metathesis polymerization selectively (that is, at the exclusion of cationic addition, free radical, Ziegler-Natta processes) at rapid turnover rates, *in the absence of air*. In air, tungsten carbenes decompose and quickly lose their metathesis activity. The tungsten carbene functionality seems to be very sensitive to the presence of moisture and/or oxygen.

THF acts as a competitive inhibitor to the catalyst — not only competitive with monomer, but also with those atmospheric agents which poison the catalyst. By placing the tungsten carbene in an environ of reversibly binding ligands (a THF solution) greater than 99.9% of the catalyst is saturatively bound (**2**), and should be inert to the atmosphere while in this bound state.

Pentane and benzene solutions of catalyst **1** are quickly discolored brown when exposed to air and lose their metathesis activity. However, even after sitting for 1 hour in air at ambient conditions, a 0.016 M solution of the catalyst in THF retains its yellow color and its metathesis activity. Addition of 10 equivalents of norbornene (NBE) at this time results in instantaneous polymerization, the reaction being sufficiently exothermic to cause boiling of the THF solution.

Proton NMR and ^{13}C NMR of the product obtained from this reaction confirm the material to be polynorbornene with greater than 90% of the double bonds in the *cis* configuration (see Figure 8), as compared with chemical shifts previously reported for ring-opened polynorbornene.[7] The number average molecular weight $M_n = 9700$ obtained by GPC (hydrodynamic response relative to polystyrene; uncorrected), with a PDI = 2.58.

Although to date this application of THF as an inhibitive agent for catalyst poisoning has been demonstrated only for the tungsten carbene **1**, this phenomonon is expected to occur for other tungsten carbenes as well, including the widely used classical metathesis system $WCl_6/SnMe_4$. Lengthening the existence of metathesis activity in all these systems would likewise facilitate the investigation into the active species in the metathesis system, and which components of the atmosphere most readily contribute to their decomposition.

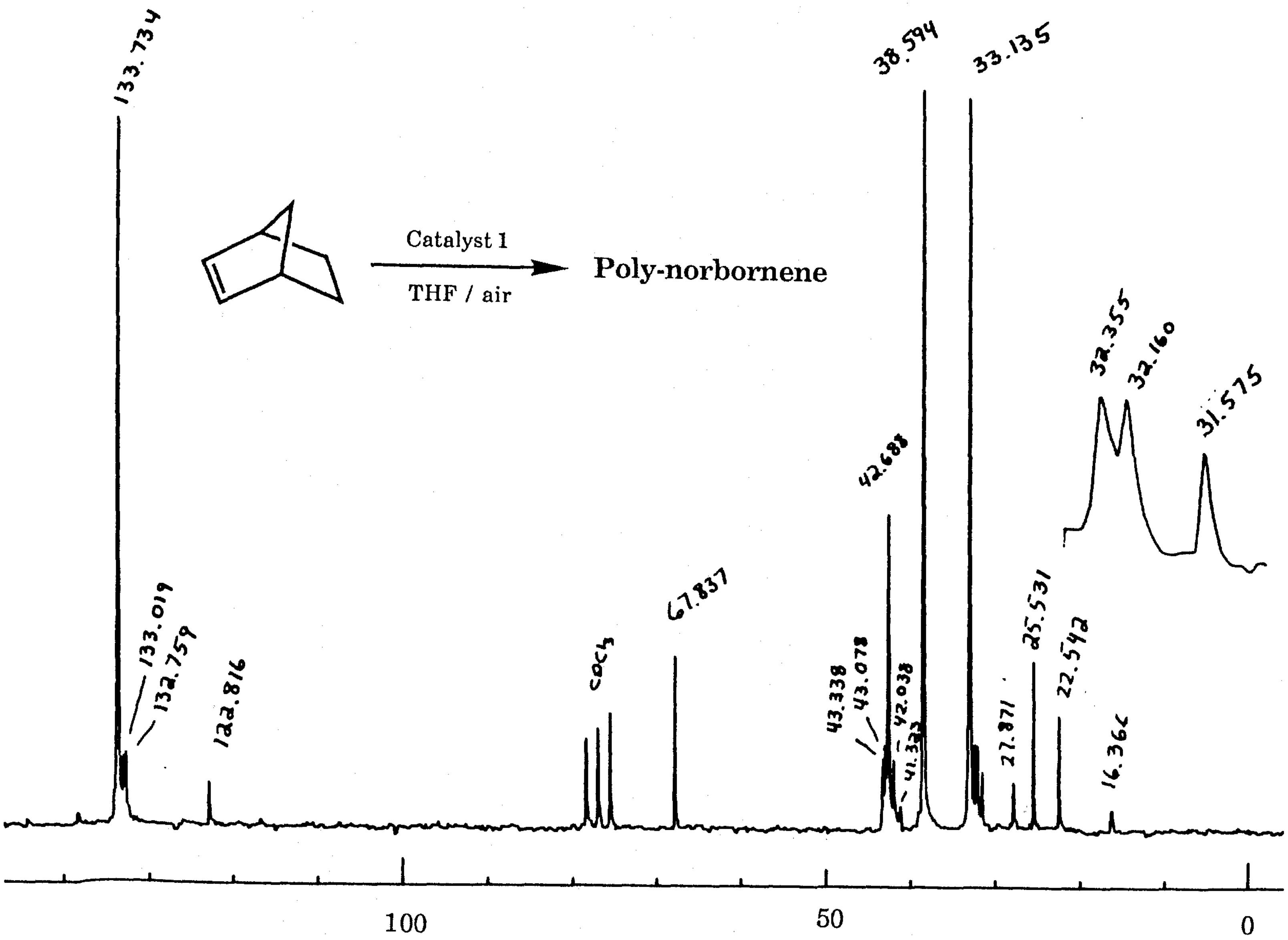

Figure 8. ^{13}C NMR of poly-norbornene, from the polymerization of norbornene in air with a THF solution of catalyst **1**.

DISCUSSION

Cycloextrusion.

In the dilute solution polymerization of COT the cycloextrusion of benzene dominates the reaction. CPK models reveal that the 127° C-C-C bond angles of COT[18] readily assume 120° bond angles once the ring is opened. "Driving forces" are the relief of strain, as well as increased pπ-pπ overlap. Once this rearrangement has occurred, the tungsten carbene is in position to add to the γ-double bond, and then extrude benzene. As benzene is inert to the metathesis catalyst,[19] the cycloextrusion reaction is irreversible.

Cycloextrusion is a phenomenon governed by concentration effects. In dilute solution, the rearrangement process necessary for cycloextrusion has time to occur. However, in the "neat" polymerization of COT the tungsten carbene is surrounded by a pool of reactive sites (double bonds) at all times. The addition of COT to the catalyst reaction site is rapid, and consequently chain growth (polymerization) is favored over the slower cycloextrusion.

The yield of cycloextrusion products can also be dictated by statistics. Cyclooctatetraene is a symmetrical molecule, where attack by the tungsten center of catalyst **1** at any of the eight carbons atoms will allow for the possibility of cycloextrusion. However, such is not necessarily the case with less symmetrical cycloolefins. A consideration of reaction mechanism reveals two possibilities during the polymerization of 1,3-cyclooctadiene (Scheme IV). Pathway **A** involves the addition of one double bond (-CH=CH-) to the chain, whereas pathway B adds three double bonds <u>and</u> a site of saturation (-CH=CH-CH=CH-CH_2-CH_2-CH=CH-). The random addition of the saturation serves to interrupt conjugation. If the tungsten carbene attacks all six sites with equal probability (probably a reasonable approximation), then cyclohexadiene will be produced in 67% yield, assuming no extraneous metathesis. Total consumption of cyclooctatriene results in a 57% experimental yield of cyclohexadiene, which suggests that the carbene does attack the sp^2 sites with deferred preferentiality. The formation of an insoluble brown powder during these polymerizations is consistent with the more unsaturated polymer produced through Pathway **A**.

It was deemed likely that 1,3-cyclooctadiene should provide even more sites of unsaturation in the backbone, and in accord with Scheme IV should produce cyclohexene in 50% yield. The 40% conversion of cyclooctadiene to cyclohexene again indicates a marked randomness in the site of carbene attack.

In the dilute solution polymerization of bromo-cyclooctatetraene it is interesting to note that no benzene is formed, as would be possible if the tungsten carbene were to attack the double bond containing bromine. Steric hindrance of the bromine towards the bulky catalyst is probably sufficient reason that attack does not occur on this double bond (*see* Figure 9). It would prove interesting to study further the dependence of cycloextrusion statistics upon concentration, solvent, and 8-membered ring undergoing metathesis.

Scheme IV. Cyclohexadiene from 1,3,5-Cyclooctatriene

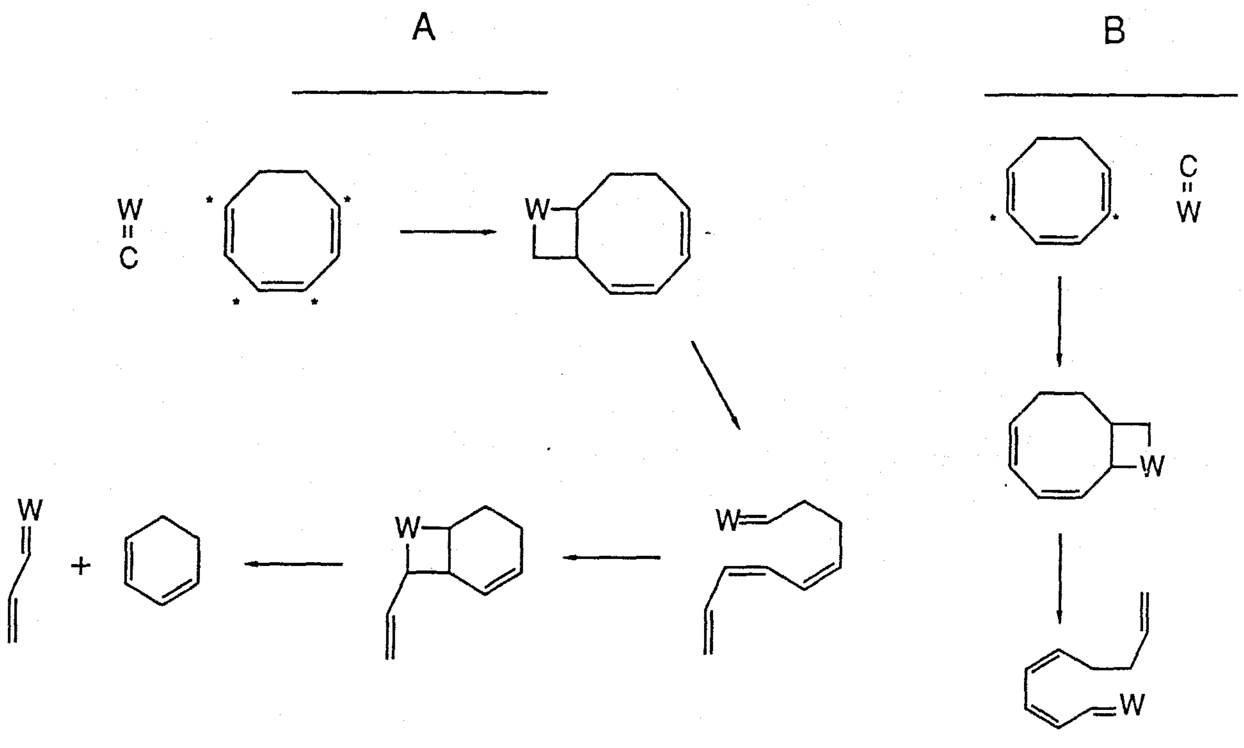

* *Pathway in operation when tungsten attacks these sites.*

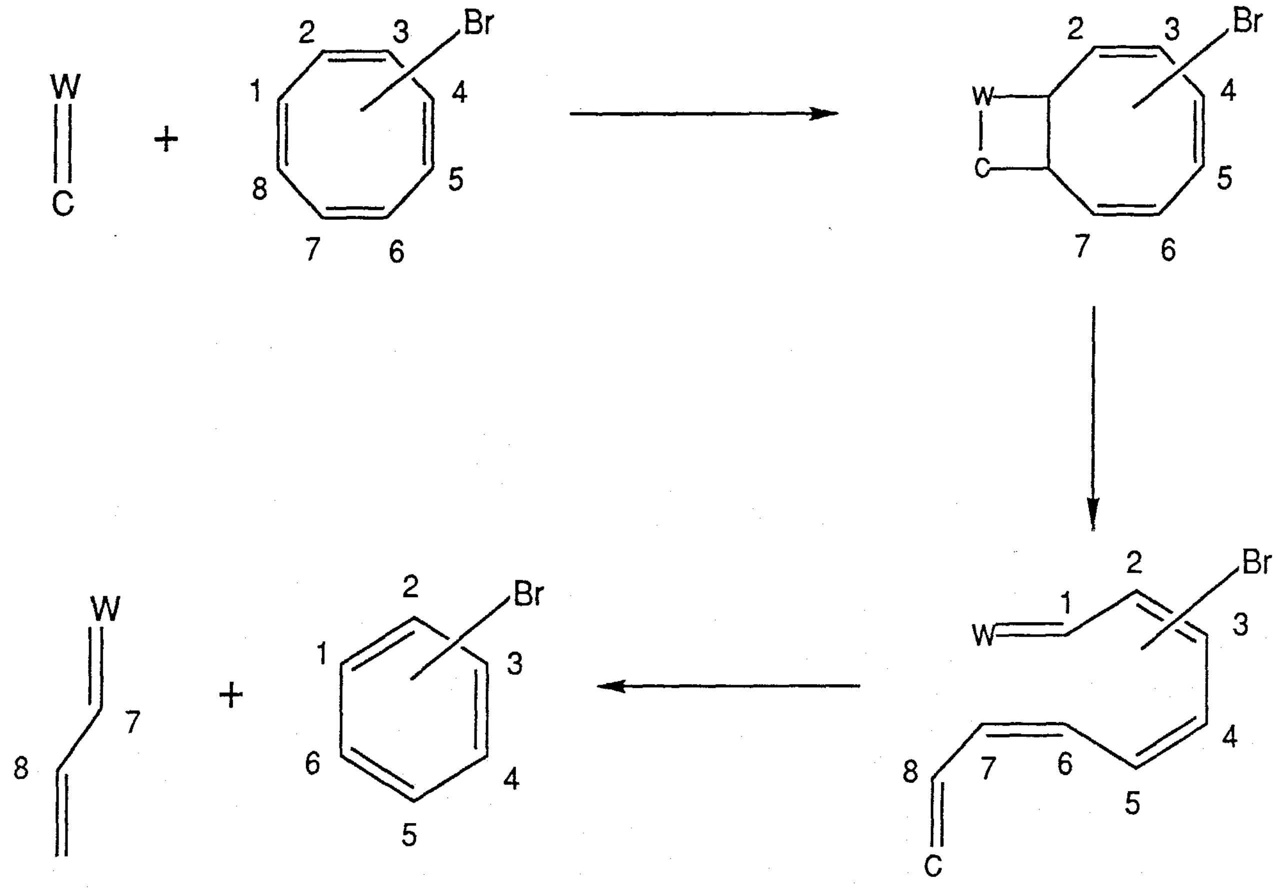

Figure 9: Cycloextrusion of Bromobenzene. The above mechanism illustrates the cycloextrusion reaction resulting from metathesis of bromo-cyclooctatetraene. The single bromine atom per cycloolefin can initially be at any of the carbon atoms labelled 1-8. If the bromine is bonded to C_7 or C_8, however, bromine would occur in the growing polymer tail and benzene would be cycloextruded. Since no benzene is detected, it can be concluded that if bromine is bonded to C_7 or C_8, then no cycloextrusion occurs. If it is the case that the tungsten carbene will attack no double bond having a bromine atom (perhaps due to steric hindrance), then cycloextrusion will occur only if the bromine is situated on C_2, C_3, C_4, or C_5. If the bromine is located on C_1 or C_8, then the bromo-cyclooctatetraene will not be in position to undergo metathesis. If the bromine is on C_6 or C_7, then the cycloolefin will undergo metathesis and be ring-opened, but the subsequent attack of newly formed carbene on the double bond containing C_6 and C_7 will not occur.

Mechanistic influence upon chain structure. During the polymerization of "neat" COT, one of the double bonds undergoes metathesis reaction to form a new double bond having either *cis* or *trans* stereochemistry. If it is assumed that no isomerization occurs during polymerization,[20] 3 of the 4 *cis* double bonds originally present in COT remain *cis*, so that the final polymer should contain no less that 75% *cis* stereochemistry. Scheme V illustrates the formation of isolated *trans* double bonds during the polymerization.[21] The *cis-trans* structure which develops in these chains is consistent with previously reported ^{13}C NMR, IR, and DSC data. Not shown in Scheme V is the relaxation process which allows extended pπ-pπ planarity in poly-COT, as is evidenced by Raman spectroscopy. A study of *cis-trans* content *vs.* degree of cycloextrusion (controlled by dilution factor) will help to delineate mechanistic influence upon observed stereochemistry,[22] since extrusion of benzene eliminates the three "uninvolved" *cis* double bonds. Large rings resulting from *macrocyclic* extrusion may be present in the films, possibly accounting for the incomplete isomerization observed by NMR and IR.

At the terminus of each polymer chain should be a t-butyl group, originally part of the carbene catalyst. Assuming that each catalyst molecule is active in the polymerization with an initial monomer/catalyst ratio 100:1, chains should be ~100 monomer units (800 carbon atoms) in length. Since not all the catalyst initiates as seen in dilute solution studies, chain lengths should be even greater. This large number of sp^2 carbons per t-butyl group ($sp^2/sp^3 > 200$) explains why the appended t-butyl group (neohexene-like) has not been detected in solid state ^{13}C NMR, IR, or elemental analysis. It is emphasized that while sp^3 carbons are expected to be present due to these t-butyl groups, they are the residual functionality of catalyst **1** and do not interrupt backbone conjugation.

Scheme V. Mechanistic Influence upon Stereochemistry in COT Polymerization.

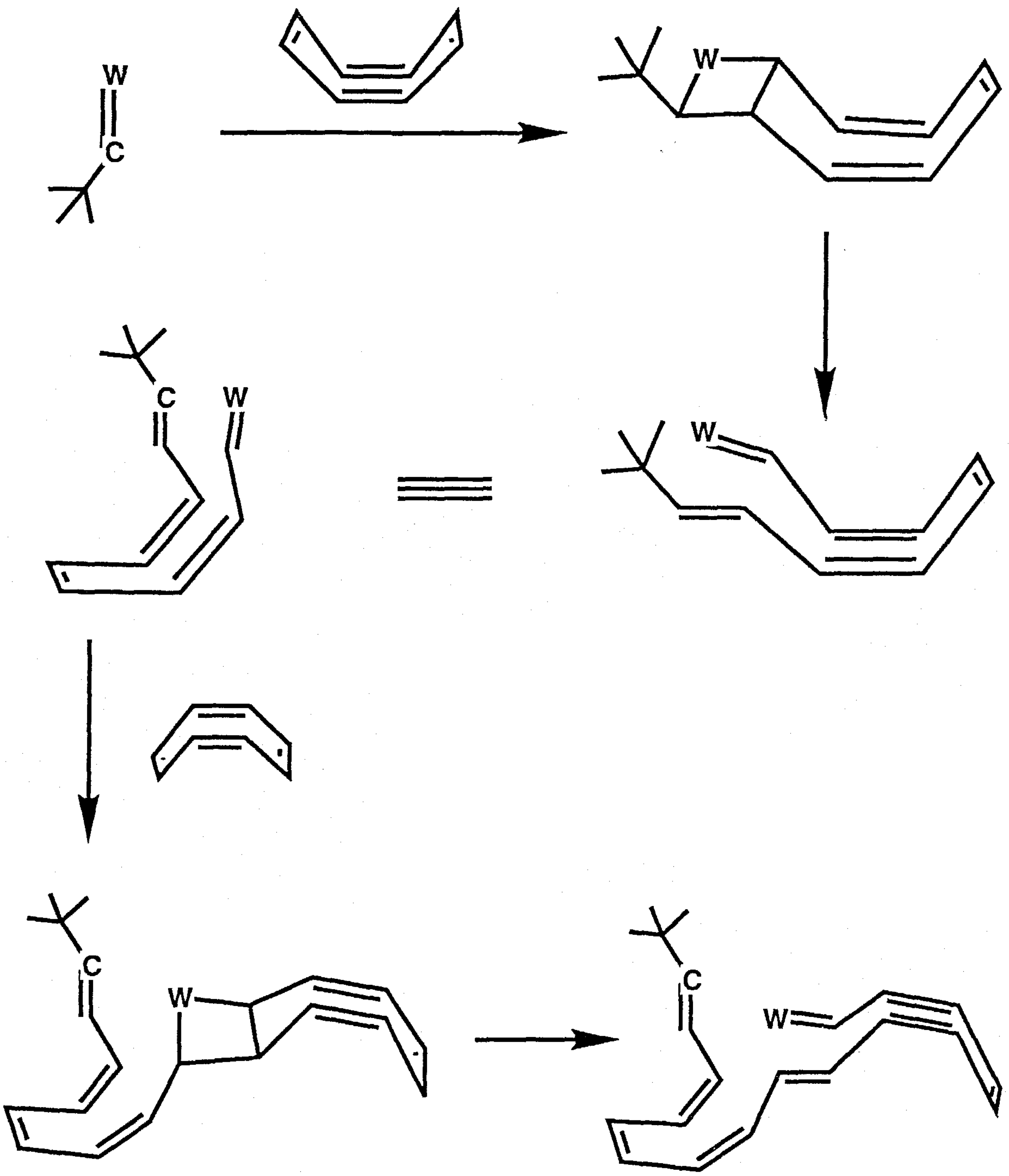

Reversible Binding of THF.

Thermodynamics. The chemical shift for the carbene proton of catalyst **1** ($L_3W{=}CHR$) can be accounted for — and now accurately predicted — for any concentration of catalyst, concentration of THF, and temperature. With the presence of a single concentration-sensitive NMR peak, a lower limit for the exchange constant K_{ex} is determined through the formula $K_{ex} \geq 2.2\ \Delta\delta$.[23] At 25 °C, the minimum value of K_{ex} is 490 sec^{-1}, setting minimum values of 490 sec^{-1} for k_{-1} and 7500 $M^{-1}\cdot sec^{-1}$ for k_1. These values suggest that the free energy of activation $\Delta G^{\dagger}$ is no more than 13 Kcal/mol.[24] As shown in Figure 4, the free energy differnce between bound and unbound carbenes at all temperatures studied is only on the order of 1-2 Kcal/mol.

Despite the low values of ΔG, the binding of THF to catalyst **1** brings about drastic changes, not only in the chemical reactivity, but also in the enthalpic and entropic characteristics. As expected, the binding is exothermic with a substantial negative entropy. Although the electron deficient tungsten center enjoys the coordinate bond with the Lewis basic THF, the interaction severely restricts motional freedom. At 100 °C, the energy gain from bonding is exactly offset by the "energy loss" from decreased entropy.

Kinetics. The polymerization rate of COD with catalyst **1** is neither cleanly zeroeth order nor first order with respect to monomer concentration, but rather some combination of the two, reminiscent of the kinetics associated with enzyme reactions. The equation used to model the kinetics for Scheme III (Equation 2), applicable whether pre-equilibrium (k_1) or ring opening (k_2) is the rate determining step, employs the following assumptions:

(1) Binding-dissociation of ligand is rapid compared to rate of reaction; $\mathbf{K_f}$ is used.

(2) Concentration of monomer•catalyst complex remains nearly constant throughout propagation; d[CM]/dt = 0.

(3) As with all polymerization kinetics, it is assumed that the

propagation rates are the same for all chain lengths.

The first assumption is known to be valid; the reversible binding of ligand is extremely rapid (NMR time scale) while the polymerization rates are slow enough to be measured. The second assumption is valid in the case where $k_1 >> k_2$, so that in the initial stages of the polymerization where the rate $R= k_2[CM]$ is nearly constant, $d[CM]/dt = d[Rate/ k_2]/dt$ is approximately zero.

Kinetics do not allow for the precise determination of k_1 or the relation between k_{-1} and k_2; however, the results do impose a lower limit on the value k_1/k_2. The slope for the plot of Equation 2 (from Figure 6b) is 0.019 M·min = $(k_2+k_{-1})/k_1 \cdot k_2$, or $k_2/k_1 + k_{-1}/k_1 = 0.228$ M. The value of $k_2/k_1 = 12\ \text{min}^{-1}/k_1$ cannot exceed 0.228 M, so that $k_1 \geq 52\ M^{-1} \cdot \text{min}^{-1}$. The large exchange rate found in the binding of THF (450,000 $M^{-1} \cdot \text{min}^{-1}$) suggests that the monomer binding rates might be substantially larger than this minimum value, giving $k_{-1}/k_1 = 0.228$ M. This notion is consistent with chemical intuition. The formation of a reversibly-bound coordinated covalent complex generally is rapid, whereas the stricter geometry requirements for covalent bond formation are rate determining. In this reaction, the slow step is believed to involve slippage of the bound cycloolefin to a tungsten metallacycle, followed by rapid ring opening to regenerate the carbene catalyst.

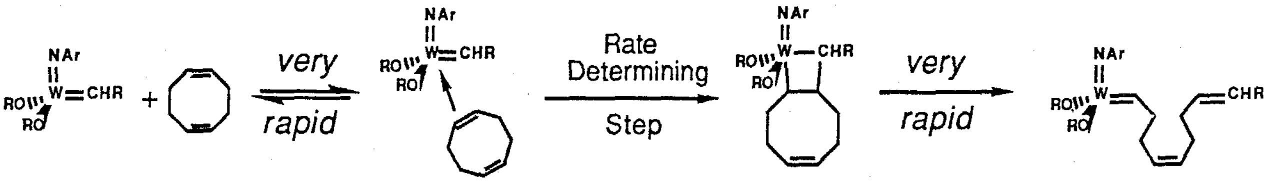

The ring opening step must be very rapid to account for the fact that there is insufficient concentration of tungsten metallacycle during the polymerization to detect by NMR.

Note that in the unimolecular decay of bound complex **2** → **3**, the rate constant

k_2 is actually believed to involve at least two distinct steps: the rate determining formation of metallacycle whose rate constant is k_2, followed by cleavage which is so rapid that it does not affect the kinetics. The distinct intermediacy of a tungsten metallacycle during polymerization is probable, based upon the isolation or proven existence of metallacycles in similar olefin metathesis reactions. The formation of a carbene·cycloolefin bound complex is implied by the analogous carbene·THF complex, and both theoretical and experimental evidence for such carbene·olefin complexes exists. Whether the ring-opening reaction **2** → **3** involves only one step or a combination of several steps is kinetically indistinguishable, providing that the reverse reaction **3** → **2** plays no significant role (see Appendix D for rate dependence on monomer concentration for various mechanistic schemes).

The polymerization mechanism for this tungsten carbene differs from that of the previously well-studied metathesis polymerization using titanium catalysts. With titanium catalysts, the metallacycles are the stable species with the titanium carbene being too reactive to isolate. The rate-determining step is the unimolecular ring opening of the metallacycle, so that rate is for all practical purposes independent of monomer concentration. With this tungsten catalyst, however, the carbene is the stable species and the metallacycle is the reactive intermediate. The rate-determining step is the formation of metallacycle, so that the rate is indeed dependent upon monomer concentration. The major difference between the titanium metathesis catalysts previously studied and this tungsten catalyst is the stability of the metallacycle species. Recently, a well-defined tungsten metathesis catalyst developed by Osborn and co-workers has been detected in both carbene and metallacycle forms during olefin metathesis.[25]

Excluded from the kinetics (Scheme III) is the back reaction **3** → **2**. It is felt that the reverse of the ring opening reaction is negligible in comparison with the forward reaction, as it re-forms the ring-strained cycloolefin — a thermodynamically unfavorable prospect. Probably more significant is the exclusion of carbene binding to the acyclic double bonds in its polymer tail. In the presence of THF which binds to the catalyst strongly, this double bond binding may be considerably less prevalent. The formation of macrocyclic olefins through back-biting (carbene undergoes **3** → **2** reaction with a distant double bond in the polymer tail) is known to dominate the reaction of COD with more "classic" tungsten catalysts, yielding random polymer chain length distributions with very large polydispersities, but in this polymerization resulting in a polydispersity of 1.8, back-biting evidently is not a major side reaction.

Error Analysis of Thermodynamic and Kinetic Constants Determined

The experimental variables involved in the determination of the THF•carbene binding constant are (1) concentration of catalyst, (2) concentration of ligand, and (3) NMR shifts. The procedure used to prepare catalyst/ligand solutions is believed to involve no more than 3% error. The NMR shifts were reproducible to 0.2 Hz over the range of interest $\Delta\delta = 50$ Hz, the error involved being insignificant. For any determination of binding constant, the temperature varied ± 1 K which also represents negligible error. Since there exist only two unknowns (δ for bound carbene and $\mathbf{K}_f$) in the collection of 4-6 data points, the binding constant at each temperature is well over-determined, with an standard deviation less than 3%. The accuracy in the values of the individual binding constants is reflected in the linearity of the $\ln\mathbf{K}_f$ *vs.* $1/T$ plot, which likewise over-determines the values of ΔS and ΔH (van't Hoff plot assumes both of these values are only weakly dependent upon temperature). The values determined for ΔH and ΔS are felt to be accurate to within a couple percent.

There is inherently more inaccuracy present in the kinetics data, but there are also more points to define the equations. Sources of error include the following:

(1) Preparation of solutions: COD, catalyst, THF. Involves ~5% error.

(2) Integration of unreacted COD/reacted COD. Peaks are separated only by 0.1-0.2 ppm (dependent upon [THF]), and *slightly* overlap at low concentrations of THF. Involves up to 10% error.

(3) Determination of time. NMR accumulation of 24 seconds was averaged for each data point, so that accumulation for "t = 2 minutes" was actually begun at 1 minute 48 seconds. Error is negligible for most data points collected in these experiments.

(4) Assumption of constant ligand concentration. The plot for the determination of the kinetic constants involves the term (K_f[L] + 1). Ligand concentration is not canstant with respect to time, but decreases *very slightly* as monomer reacts. Actually, $[L] = L_0 - [CL]$ so that $L_0 - C_0 < [L] < L_0$. Since for most concentrations of THF used $L_0 >> [CL]$, the term (K_fL_0 +1) was used. Even for the lowest concentration of THF = 0.148 M, this approximation involves no more than 10% error and probably substantially less.

(5) In plotting 1/Rate *vs.* $(K_fL_0 + 1)/C_0 \cdot [M]$, since rate and [M] are actually changing, instantaneous values must be used. The determination of an instantaneous rate for any given plot of [M] *vs,* time may involve significant error, since even one errant point in the range of interest could skew the determination of rate. Generally, [COD] polymerization rates were reproducible from trial to trial within 20%.

Despite the various sources of significant errors, the plot of 1/R *vs.* $(K_fL_0+1)/C_0 \cdot M_0$ is linear and yields values for kinetic constants as follows:

$$k_2 = 12 \text{ min}^{-1}$$
$$k_1 / (k_2 + k_{-1}) = 4.3 \text{ M}^{-1}$$

The intercept is sensitive to relatively minor variations in the data; nevertheless, the observed rate constants are on the correct order of magnitude and do provide useful predictive power for this metathesis polymerization reaction. Using the above kinetic constants with $[M]_0 = 0.163$ M and $[C]_0 = 0.0184$ M, theoretical curves are generated for [M] *vs.* time at $[L]_0 = 0.148$ M, 0.369 M, 0.984 M (see Figure 10). The experimental data points are shown for these conditions, demonstrating that the kinetic parameters are consistent with the observed data.

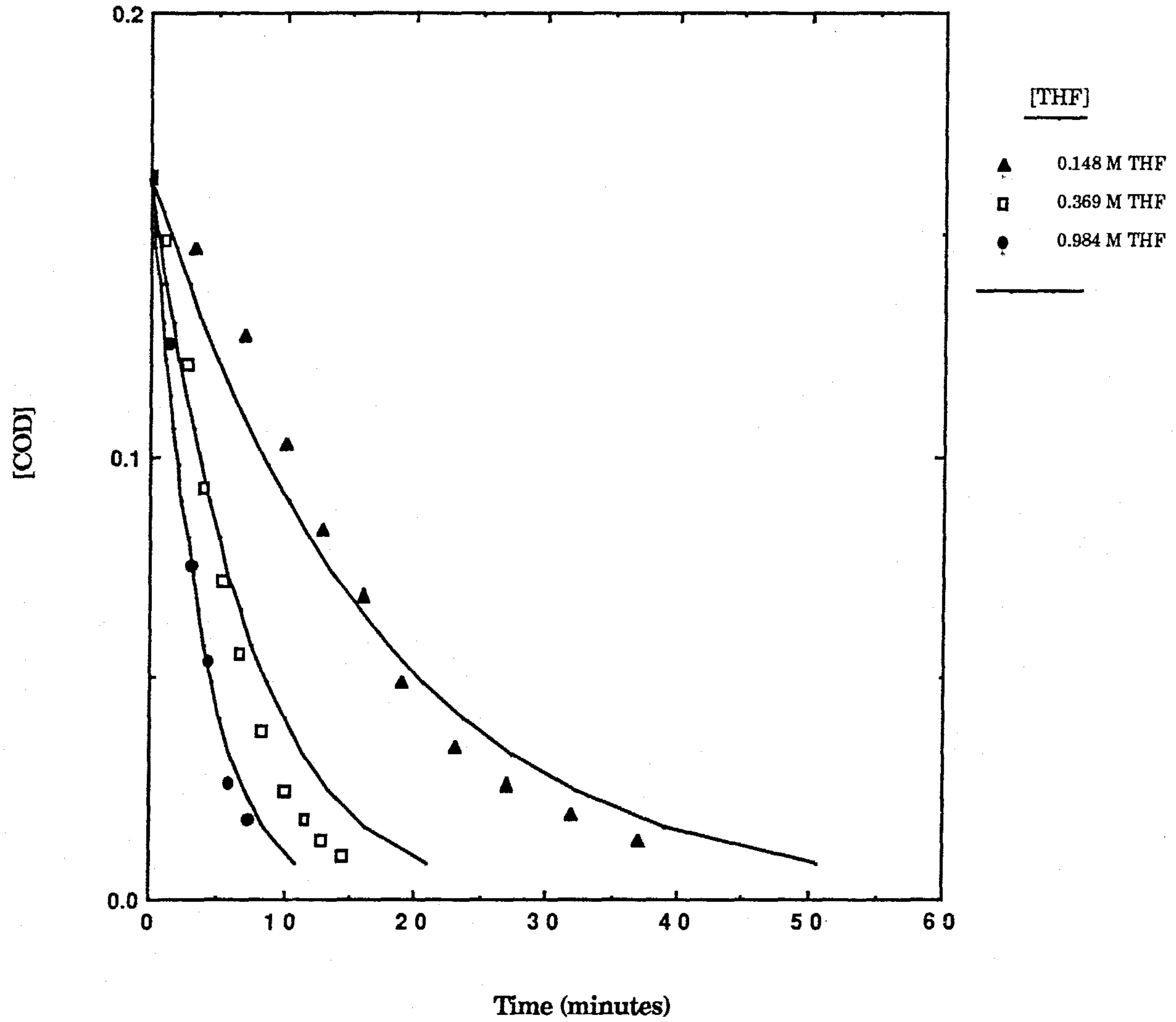

Figure 10. COD Polymerization Kinetics — Theory vs. Experiment. For conditions described in the text, the data points for the metathesis polymerization of COD with catalyst **1** are plotted at three different concentrations of the reversibly-binding ligand THF. The solid curves have been generated using kinetic parameters $k_2 = 12$ min^{-1}, $k_1/(k_2 + k_{-1}) = 4.3$ M^{-1}, and $K_f = 15.4$ M^{-1}.

Summary of Mechanism

The investigation into the metathesis polymerization of 8-membered cycloolefin ring monomers with the tungsten carbene **1** has generated the following findings:

(1) A phenomenon referred to as "cycloextrusion" occurs in monomers having a -C=C-C=C- diene moeity in the ring. A mechanism has been proposed which rationalizes the geometry and the statistics of this cycloextrusion process. The cycloextrusion is highly concentration dependent and is subject to substituent effects.

(2) The stereochemistry determined for the polyacetylene produced from the room temperature "neat" polymerization of COT with catalyst **1** is accounted for by the polymerization mechanism in which the ring-opening metathesis reaction generates new double bonds with a high degree of *trans* specificity. Secondary metathesis ("back-biting") of the double bonds present in the polymer tail is *not* a predominant side-reaction, as this process would tend to scramble the *cis-trans* stereochemistry and lead to the thermodynamically favored all-*trans* polyacetylene.

(3) The reactivity of the tungsten carbene catalyst **1** can be mediated gradually and predictably by introduction of a reversibly binding ligand. Thermodynamic and kinetic constants have been studied for this binding formation-dissociation reaction, and it has been found that the binding involves one and only one ligand molecule. The reactivity of the tungsten carbene in metathesis polymerization can effectively be varied by orders of magnitude employing this strategy. The application of a reversible-binding ligand has been realized in terms of allowing greater processability during the "neat" polymerization of cyclooctatetraene into polyacetylene, and the increased air stability of the catalyst in the presence of reversibly binding ligands.

(4) The kinetic results of metathesis polymerization with the tungsten carbene catalyst **1** in the presence of a reversibly binding ligand are consistent with a rapid equilibrium which involves catalyst and monomer (but not reversibly-binding ligand), followed by a second step which regenerates the catalyst and does not involve free monomer. That is, this metathesis polymerization reaction has been effectively modeled employing the scheme for enzyme kinetics with a competitive inhibitor.

REFERENCES

(1) For reviews of ring-opening metathesis, see (a) Ivin, K. J. *Olefin Metathesis*; Academic Press: London, 1983. (b) Grubbs, R. H. In *Comprehensive Organometallic Chemistry*; Wilkinson, G. E., Ed.; Permagon Press: Oxford, 1982; Vol. 8, pp 499-551.

(2) Thron-Csanyi, E.; Timm, H. *J. Molec. Catal.* **1985**, *28*, 37.

(3) Amass, A. J.; Zurimendi, J. A. *Polymer* **1982**, *23*, 211.

(4) Thron-Csanyi, E. *J. Molec. Catal.* **1985**, *28*, 49.

(5) Ceausescu, E. *J. Molec. Catal.* **1985**, *28*, 351.

(6) Ceausescu, E.; Cornilescu, A.; Nicolescu, E.; Popescu, M.; Coca, S.; Belloiu, C.; Dimonie, M.; Gherorghui, M.; Dragutan, V.; Chipara, M. *J. Molec. Catal.* **1985**, *28*, 337.

(7) Gilliom, L. R.; Grubbs, R. H. *J. Am. Chem. Soc.* **1986**, *108*, 733.

(8) Klavetter, F. L.; Grubbs, R. H. *J. Am. Chem. Soc.* **1988**, *110*, 7807.

(9) Reppe, W.; Schichting, O.; Klager, K.; Toepel, T. *Ann.* **1948**, *560*, 1.

(10) Gasteiger, J.; Gream, G.; Huisgen, R.; Konz, W.; Schnegg, U. *Chem. Ber.* **1971**, *104*, 2412.

(11) Schaverien, C.; Dewan, J.; Schrock, R. R. *J. Am. Chem. Soc.* **1986**, *108*, 2771.

(12) Elution through alumina serves to selectively remove inorganics (residual catalyst).

(13) Hall, L. D.; Sanders, J. K. *J. Am. Chem. Soc.* **1980**, *102*, 5703.

(14) Benzene formation during acetylene polymerization has been known for decades: Ikeda, S.; Tamaki, A. *Polym. Lett.* **1966**, *4*, 605.

(15) Bates, F.; Baker, G. *Macromolecules* **1983**, *16*, 704.

(16) Program developed at the California Institute of Technology by Richard E. Barrens and Dennis A. Dougherty.

(17) Schrock, R. R.; DePue, R. T.; Feldman, J.; Schaverien, C. J.; Dewan, J. C.; Liu, A. H. *J. Am. Chem. Soc.* **1988**, *110*, 1423.

(18) Fray, G. I.; Saxton, R. G. *The Chemistry of Cyclooctatetraene and Its Derivatives*; Cambridge Univ. Press: Cambridge, 1978.

(19) Catalyst **1** ring-opens neither benzene nor 1,3-cyclohexadiene, nor readily reacts with cyclohexene (unpublished results, this laboratory).

(20) *Cis-trans* thermal isomerization at room temperature is relatively slow [Chien, J. C.; Karasz, F. E.; Wnek, G. E. *Nature* **1980**, *285*, 390]. However, local exothermicities involved in the polymerization of "neat" COT may be sufficient to induce some isomerization.

(21) It is not known at this time whether or not the ring opening of the tungstacyclobutane to form the new carbene involves associative coordination of COT; however, the fact that only one THF molecule binds to the catalyst center suggests that the tungstacyclobutane would be too sterically crowded to permit binding to another COT molecule.

(22) Final stereochemistry may be in part due to thermal isomerization.

(23) Günther, H. *NMR Spectroscopy*; John Wiley & Sons: New York, 1980; p 242.

(24) Reference 23, p 243.

(25) Kress, J.; Osborn, J.; Greene, R.; Ivin, K.; Rooney, J. *J. Am. Chem. Soc.* **1987**, *109*, 899.

(26) The integrated form of Equation 2 was used to calculate [M] as a function of time.

Appendix A

Data for THF•Carbene Binding

0 ºC

Co	THFo	Obs'd Shift	Calc'd Shift	% C Bound	% THF Bound
0.0486	0.0490	821.5	821.9	58.27	57.79
0.0482	0.146	835.9	835.4	87.48	28.94
0.0464	0.607	840.3	840.0	97.43	7.44
0.0390	2.473	840.3	840.9	99.40	1.57

10 ºC

Co	THFo	Obs'd Shift	Calc'd Shift	% C Bound	% THF Bound
0.0486	0.0490	817.8	818.3	50.71	50.30
0.0482	0.146	833.0	832.5	81.78	27.06
0.0464	0.607	839.4	839.0	95.96	7.33
0.0390	2.473	839.9	840.4	99.04	1.56

40 ºC

Co	THFo	Obs'd Shift	Calc'd Shift	% C Bound	% THF Bound
0.0308	0.0306	803.4	803.2	18.29	18.41
0.0305	0.152	820.5	820.3	54.77	11.01
0.0287	0.857	836.0	836.0	88.18	2.95
0.0247	2.457	837.4	839.5	95.62	0.96
0.0164	12.28	843.0	841.5	99.09	0.13

60 ºC

Co	THFo	Obs'd Shift	Calc'd Shift	% C Bound	% THF Bound
0.0308	0.0306	799.5	798.9	9.02	9.08
0.0305	0.152	811.2	810.6	33.53	6.74
0.0287	0.857	829.9	830.3	74.87	2.51
0.0247	2.457	835.7	837.3	89.67	0.90
0.0164	12.28	842.6	841.1	97.95	0.13

Appendix B

Data for COD Kinetics in the Presence of THF

$[\text{Catalyst}]_o = 0.0184$ M
$[\text{COD}]_o = 0.163$ M

[THF]	Minutes	[COD]
0.148	0	0.163
	1.3	0.126
	3.0	0.075
	4.4	0.054
	5.9	0.026
	7.4	0.018
0.369	0	0.163
	1.1	0.150
	2.7	0.121
	4.1	0.093
	5.4	0.072
	6.8	0.055
	8.5	0.037
	10.2	0.024
	11.6	0.018
	13.0	0.013
	14.5	0.010
0.984	0	0.163
	3.3	0.147
	7.0	0.127
	10.0	0.103
	13.0	0.083
	16.0	0.068
	19.0	0.049
	23.0	0.034
	27.0	0.026
	32.0	0.020
	37.0	0.013
1.97	0	0.163
	7.0	0.147
	13.0	0.134
1.97	22.0	0.088
	30.0	0.073
	38.0	0.049
	46.0	0.023
4.67	0	0.163
	17.0	0.139
	29.0	0.119
	56.0	0.075
	70.0	0.054
7.13	0	0.163
	38.0	0.127
	70.0	0.095
	105	0.060
	120	0.044
	143	0.033
	164	0.023
9.59	0	0.163
	32.0	0.145
	82.0	0.114
	132	0.073
	173	0.047
	210	0.034
12.3	0	0.163
	60.0	0.140
	120	0.106
	175	0.073
	230	0.047

Appendix C

Hypothetical Data for **Two** THF Molecules Bound to Carbene

$$C + 2L \rightleftharpoons CL_2$$

$$[C] = C_o - [CL_2]$$

$$[L] = L_o - [CL_2]$$

$$K_f = \frac{[CL_2]}{[C]\,[L]^2}$$

$$\%\,\textbf{Bound} = \frac{\delta_{obs} - \delta_{free}}{\Delta\delta} = B$$

$$K_f = \frac{B}{L_o^2 + 4C_o(C_o + L_o)B^2 - 4C_oB^3 - (L_o^2 - 4L_oC_o)B}$$

This equation for the binding constant is clearly inconsistent with the observed data for % bound (comparison to results from 25 °C):

Obs'd % Bound	**Calc'd K for bis-THF adduct**
17.7	1850
71.0	120
95.8	4.2
99.5	1.6

Appendix D

Rate Equations for Various Mechanisms Describing COD Polymerization

Scheme VI

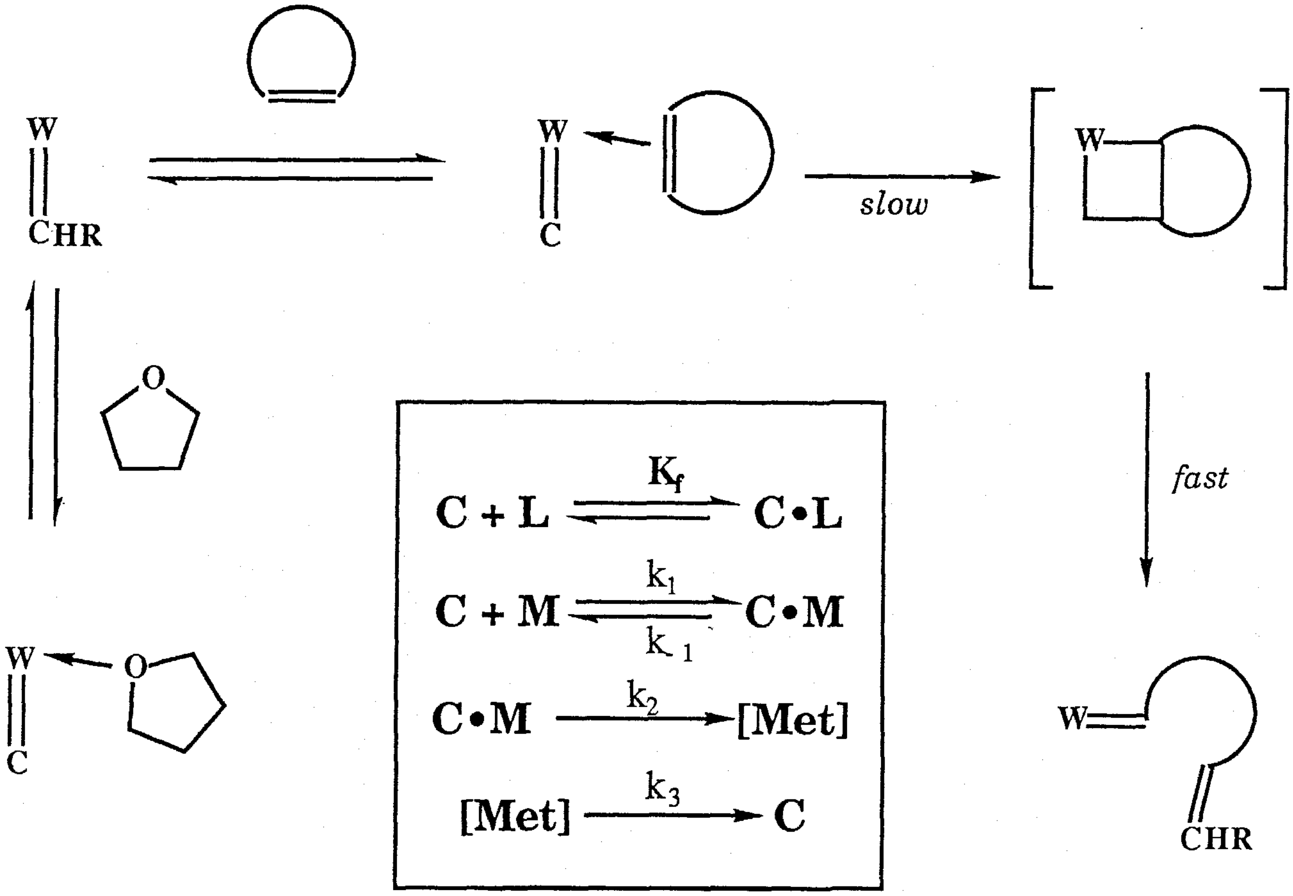

$$\boxed{\begin{array}{l} C + L \overset{K_f}{\rightleftharpoons} C\bullet L \\ C + M \underset{k_{-1}}{\overset{k_1}{\rightleftharpoons}} C\bullet M \\ C\bullet M \xrightarrow{k_2} [\mathrm{Met}] \\ [\mathrm{Met}] \xrightarrow{k_3} C \end{array}}$$

$$\textbf{Rate} = \frac{k_1k_2C_o[M]}{(K_f[L] + 1)(k_2 + k_{-1}) + k_1[M]}$$

Scheme VII

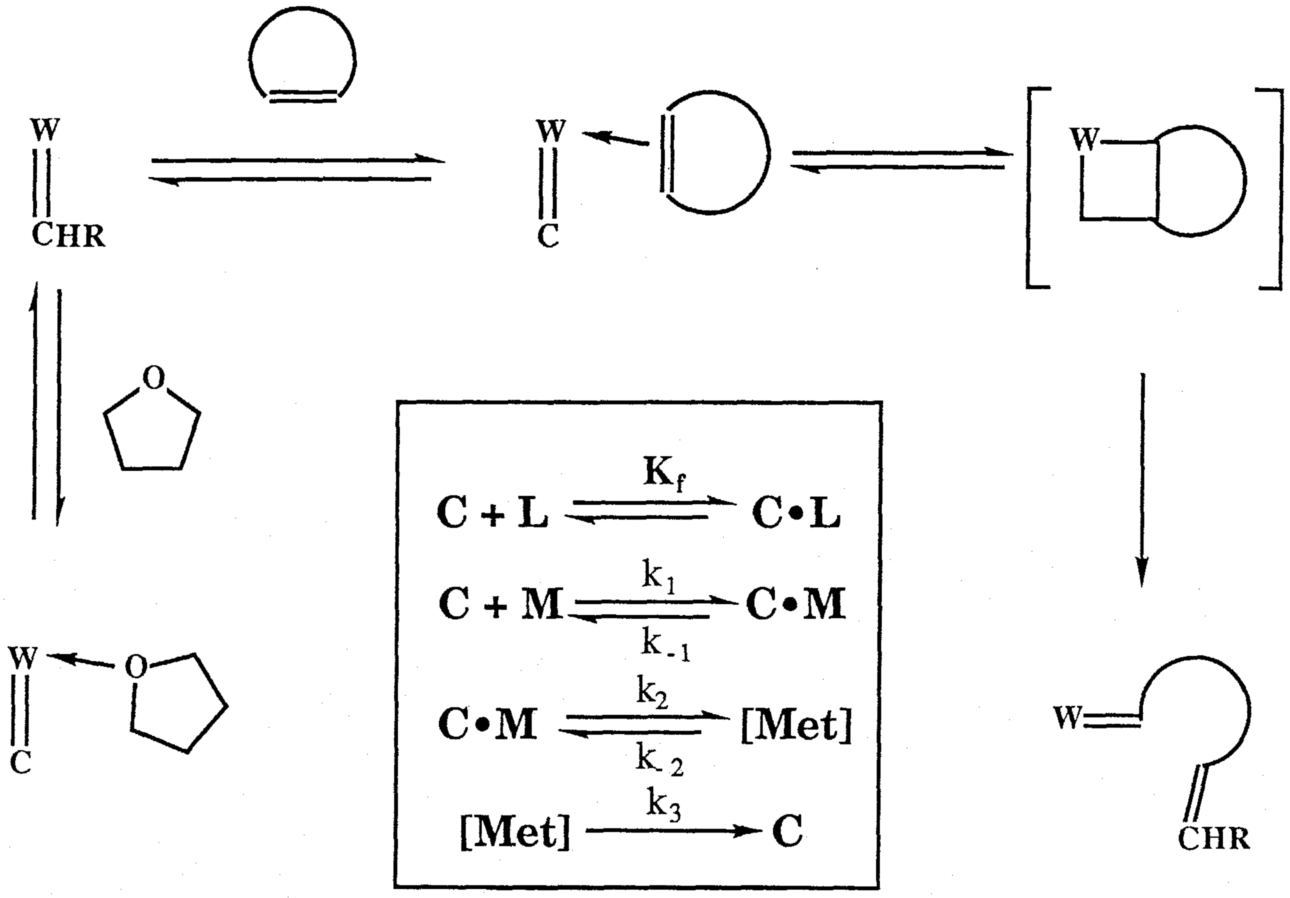

$$C + L \underset{}{\overset{K_f}{\rightleftharpoons}} C{\bullet}L$$

$$C + M \underset{k_{-1}}{\overset{k_1}{\rightleftharpoons}} C{\bullet}M$$

$$C{\bullet}M \underset{k_{-2}}{\overset{k_2}{\rightleftharpoons}} [Met]$$

$$[Met] \xrightarrow{k_3} C$$

$$\text{Rate} = \frac{k_1k_2k_3C_o[M]}{(\mathbf{K}_f[L] + 1)[k_{-1}(k_{-2} + k_3) + k_2k_3] + k_1[M](k_2 + k_{-2} + k_3)}$$

$$\text{or Rate} = \frac{k_1k_2'C_o[M]}{(\mathbf{K}_f[L] + 1)(k_2' + k_{-1}) + k_1[M]} \quad \text{where } k_2' = k_2\left(\frac{k_3}{k_{-2} + k_3}\right)$$

Scheme VIII

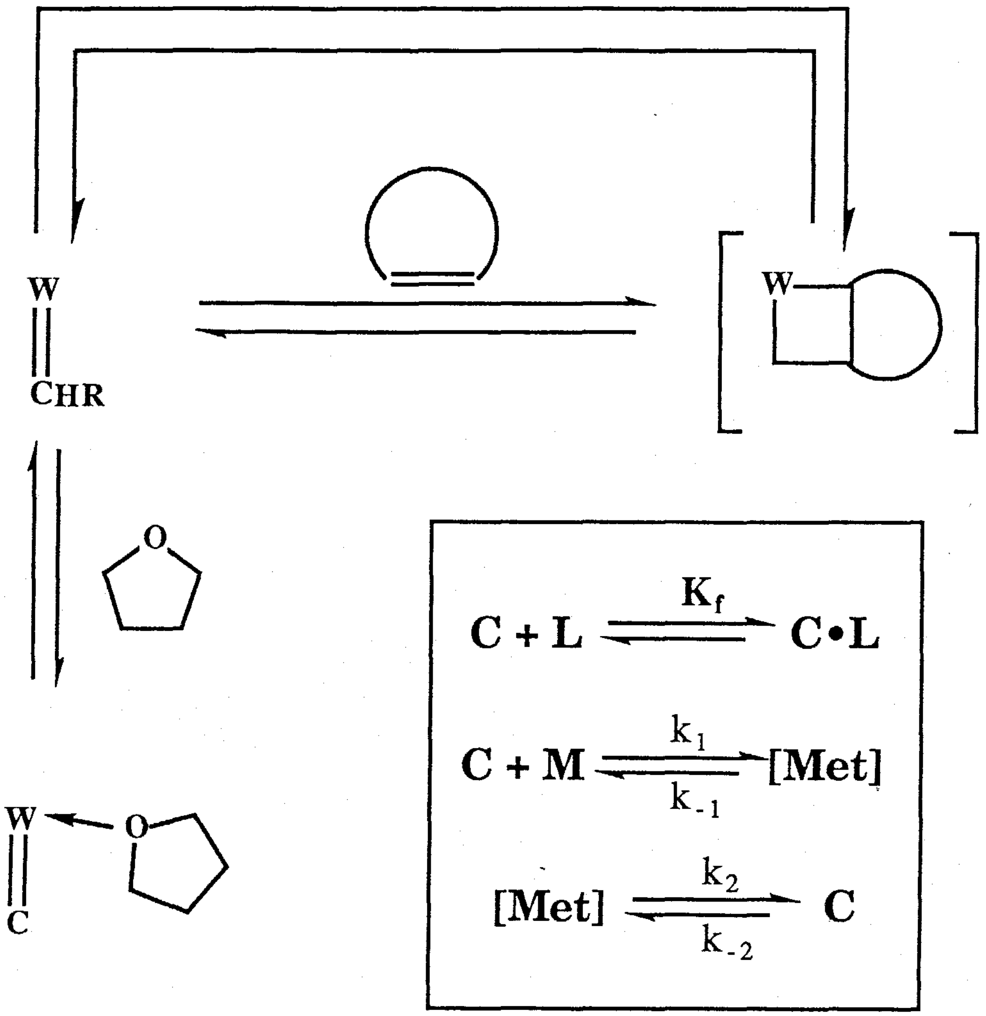

$$C + L \underset{}{\overset{K_f}{\rightleftharpoons}} C{\bullet}L$$

$$C + M \underset{k_{-1}}{\overset{k_1}{\rightleftharpoons}} [Met]$$

$$[Met] \underset{k_{-2}}{\overset{k_2}{\rightleftharpoons}} C$$

$$\textbf{Rate} = \frac{(k_1k_2[M] - k_{-1}k_{-2})C_o}{(\mathbf{K}_f[L] + 1)(k_2 + k_{-1}) + k_{-2} + k_1[M]}$$

Scheme IX

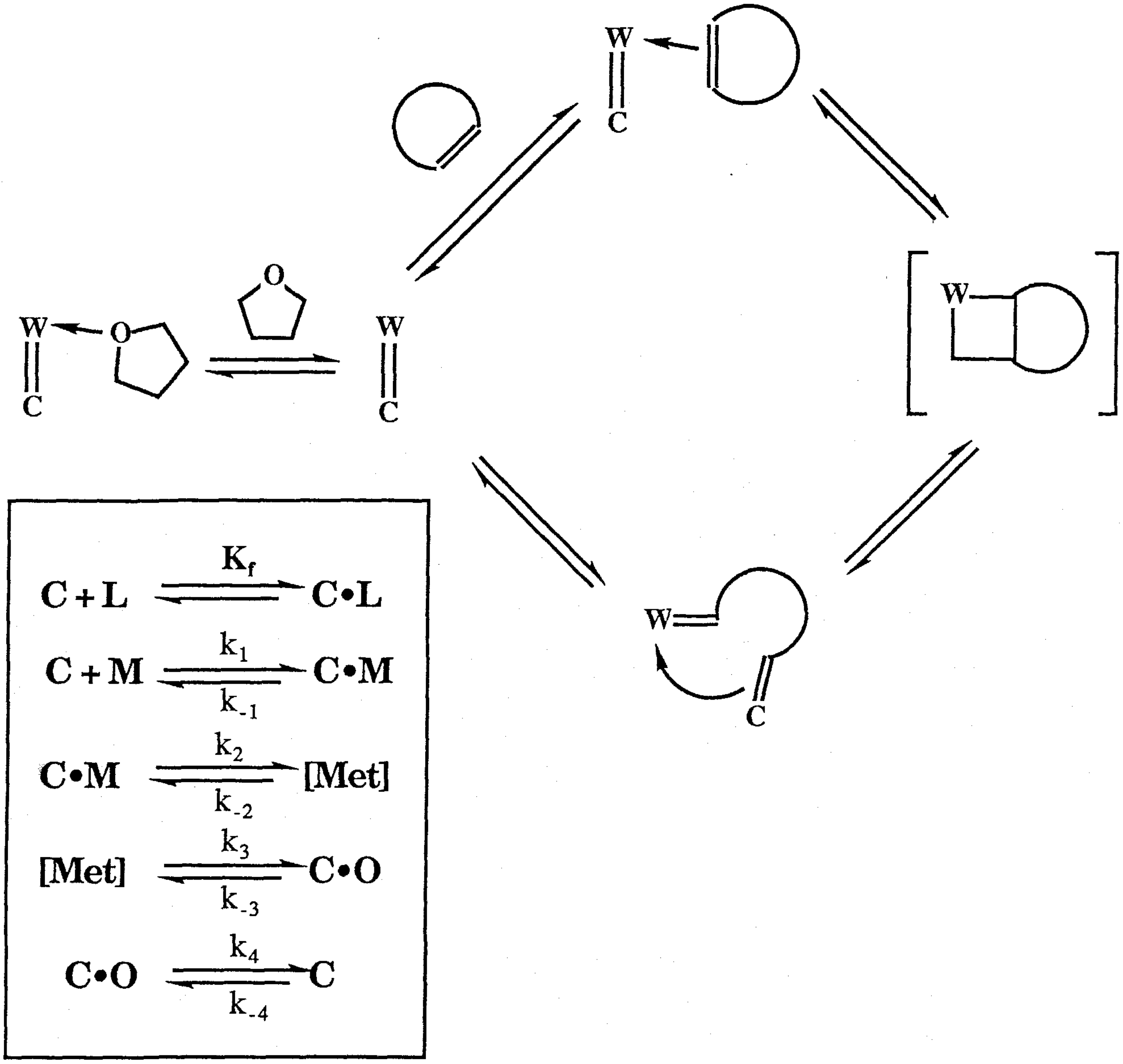

$$C + L \overset{K_f}{\rightleftharpoons} C\bullet L$$

$$C + M \underset{k_{-1}}{\overset{k_1}{\rightleftharpoons}} C\bullet M$$

$$C\bullet M \underset{k_{-2}}{\overset{k_2}{\rightleftharpoons}} [Met]$$

$$[Met] \underset{k_{-3}}{\overset{k_3}{\rightleftharpoons}} C\bullet O$$

$$C\bullet O \underset{k_{-4}}{\overset{k_4}{\rightleftharpoons}} C$$

$$\text{Rate} = \frac{(k_1k_2k_4[M] - k_{-1}k_{-3}k_{-4})C_o}{\left(1 + \frac{k_2}{k_3 + k_{-2}}\right)(k_{-1}k_{-4} + k_1k_4[M]) + k_{-1}k_{-4}(\mathbf{K}_f[L] + 1)}$$

Chapter 5

Novel Linear Polyacetylene Copolymers

ABSTRACT

Metathesis polymerization of 1,3,5,7-cyclooctatetraene (COT) yields an intractable, silvery conducting polymer (polyacetylene). Metathesis polymerization of 1,5-cyclooctadiene (COD) affords a rubbery, transparent insulating polymer (poly-butadiene). What material results upon co-polymerization?

Since COD and COT undergo metathesis polymerization at similar rates, the resulting copolymer should have a random distribution of ring-opened COD (=C-C-C-C=C-C-C-C=) and ring-opened COT (=C-C=C-C=C-C=C-C=) units along the polymer backbone. The greater the concentration of COD in the COD/COT monomer mixture, the more sites of saturation randomly inserted in the polymer backbone. By controlling the COD/COT ratio, copolymers with varying conjugation lengths are produced. Raman spectroscopy, UV-Vis, NMR, electrical conductivity, and non-linear optical measurements all indicate a progression of conjugation length in the copolymer with increasing mole fraction COT in the COD/COT mixture. As an important control study, copolymers formed from norbornene (NBE) and COT — *which undergo metathesis polymerization at very different rates* — have also been investigated.

INTRODUCTION

Polyacetylene is a conducting polymer which has received much attention in the past decade.[1] This material, once doped, has a conductivity up to 10^5 ohm^{-1}/cm,[2] comparable to values of highly conductive metals. Some advantages often cited for using polyacetylene instead of metals include the light weight and room-temperature processability associated with polymers. Indeed, polyacetylene is a light weight material, having a density ranging from 1.2 g/cc to below 0.1 g/cc, depending upon method of preparation.[1] Although polyacetylene once formed is an intractable material, strategies have been advanced which allow much processability during the stages of polyacetylene formation.[3]

One of the aspects of conducting polymers, and polyacetylene in particular, largely under-realized is the preparation of polymer blends and copolymers. The physical blending of two different polymers can be used to dramatically alter the solubility, thermal, mechanical, optical, and electrical properties of materials. Even more drastic variations in the physical properties can be effected through copolymerization, where two or more monomer types are present in the same polymer chain. The topology of copolymer chains range from linear to comb-like (graft copolymers), so that in concept at least, the experimenter can manipulate the copolymer's structure and control many of the physical properties.

Polyacetylene blends and graft copolymers have been prepared.[4] By combining polyacetylene with highly visco-elastic polymers such as polybutadiene or polystyrene, experimenters hoped to render polyacetylene more tractable and more soluble. The formation of linear copolymers with polyacetylene has largely been limited to copolymerization of acetylene with some alkyl- or dialkyl-substituted acetylene.[5]

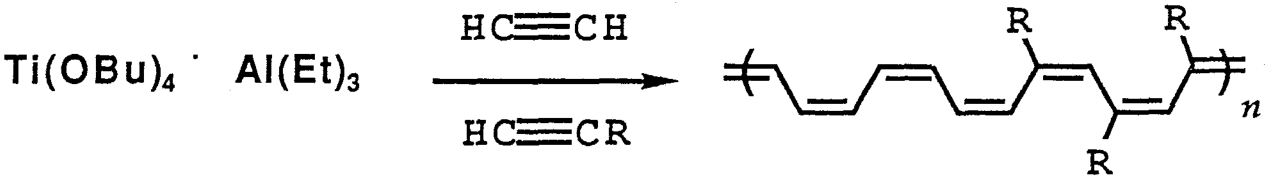

All such efforts to improve the mechanical or solubility properties of polyacetylene through blending or copolymerization, however, have compromised its highly desirable electrical conductivity.

The preparation of linear copolymers in particular may involve considerable experimental control. The monomers can either be polymerized either sequentially or simultaneously. In sequential polymerization, one monomer type is first exhaustively polymerized, then a second monomer type is added and exhaustively polymerized. This methodology forms chains containing long sequences of the different monomer types, and for this reason is referred to as a "block" copolymer. In the simultaneous polymerization of monomers, the distribution of monomer units along the chain is determined by their relative rates of reaction. For example, if monomer **A** polymerizes much more rapidly than does monomer **B**, then a highly blocked copolymer will be formed. If, however, monomers **A** and **B** polymerize at the same rate, the distribution of **A** units and **B** units along the copolymer chain will be governed by statistics, and a random copolymer will be formed. Thus, whereas only block copolymers are formed when the copolymerization is subject to procedural control (sequential polymerization), either block or random copolymers can be prepared through kinetic control.

In the following research, the author combines the methodology for preparing polyacetylene through metathesis polymerization of 1,3,5,7-cyclooctatetraene,[6] with the strategy of preparing copolymers through kinetic control, to produce novel linear polyacetylene copolymers in both random and block form.

EXPERIMENTAL

General considerations. Materials were stored and handled in a nitrogen filled Vacuum Atmospheres drybox outfitted with a refrigeration unit. Solution NMR spectra were recorded on a JEOL FX-90Q (89.60 MHz ^{1}H) or a JEOL GX-400 (399.65 MHz ^{1}H) instrument equipped with variable temperature thermostatting (±0.2 °C). Analytical gas chromatography was performed on a Shimadzu GC-mini 2 flame ionization instrument equipped with a 0.24 mm x 25 m SE-30 capillary column. Conductivities were measured in an inert atmosphere using a 4-point probe arrangement in order to negate contact resistance. Thermogravimetric analysis was performed on a Perkin Elmer TGA-7 instrument under nitrogen puge, at a scanning rate of 30 °C per minute.

Materials. Cyclooctatetraene (COT) was prepared by Reppe cyclotetramerization of acetylene.[7] COT was fractionally distilled (45 °C, 25 mm Hg), filtered through neutral alumina, and vacuum distilled from CaH_2. Purity was confirmed by GC analysis before use (>99.9%). Purified COT was stored under nitrogen, below its melting point, protected from light. Norbornene (Aldrich, 99%), 1,5-cyclooctadiene (Aldrich, 99%) and 1,3-cyclooctadiene (Aldrich, 98%) were purified by vacuum distillation from CaH_2. Solvents were vacuum distilled from benzophenone ketyls, except for methylene chloride and carbon tetrachloride which were vacuum distilled from P_2O_5. Catalyst 1 was synthesized as previously reported.[8] Iodine used in the doping experiments was sublimed prior to use and stored under argon.

Preparation of comonomer solutions. Comonomer solution were prepared by mixing appropriate amounts of COT with the second monomer (1,5-cyclooctadiene or norbornene) in stoppered glass vials. Mixing and subsequent storage were carried out in the drybox. The procedure for polymerization of these comonomer solutions is as previously described for the polymerization of "neat" COT.[6]

Dilute solution competition kinetics. Catalyst **1** (6.3 mg, 8.5 µmol) was dissolved in d_8-THF (0.05 mL) in an NMR tube before capping with a septum.

Precisely 5.0 equivalents of 1,5-cyclooctadiene (5.2 μL, 42.4 μmol) and 5.0 equivalents of COT (4.8 μL, 42.4 μmol) were injected from septum-capped vials *via* syringe into the NMR tube, after brief vigorous shaking a spectrum was recorded (~30 seconds) to obtain initial 1,5-cyclooctadiene (COD) and COT concentrations referenced to the residual solvent peak. Polymerization rates at 25 °C were -d[COD]/dt = 3.3×10^{-5} M/min and -d[COT]/dt = 2.1×10^{-5} M/min. At 60 °C the initial rates are -d[COD]/dt = 2.4×10^{-4} M/min and -d[COT]/dt = 3.1×10^{-4} M/min.

Optical spectroscopy. COD/COT copolymer films having thickness ~0.1 mm were prepared according to the procedure developed for poly-COT "neat" polymerization,[6] and placed in the optical path of the spectrometer. Once prepared, the films were immediately investigated, with no attempt to protect them from the atmosphere during analysis. For the dilute solution spectra, films were placed (and shaken) in sufficient quantities of methylene chloride so as to dissolve the entire sample.

Raman spectroscopy. Spectra were obtained for excitation wavelength 488 nm from a Argon ion laser source. One to three scans (reflected from film's surface) were taken using a power of 300-330 mWatts; signal-to-background was approx. 40:1. Reproducibility was within 3 cm^{-1}, and each sample was referenced to known absorption frequencies of a CCl_4 sample. Optical filters were placed in front of the target sample so as to limit external dispersion effects. Samples were polymer films enveloped between two thin glass plates (biological cover slips). No attempt was made to cool the sample during analysis. In the range of 600-2200 cm^{-1}, two major peaks with maximums 1113 cm^{-1} and 1491 cm^{-1} are observed.

Electron paramagnetic spectroscopy. Film shavings were placed in quartz tubes under inert atmosphere. Microwave power was varied from 1 mW to 70 mW to probe for signal saturation. The time constant used was 0.064 seconds, with a typical scan range / rate of 50 G / 4 minutes. The resonance of spins in all samples occurred at ~3380 G, corresponding to free spins. The copolymer film produced from a 20% COD / 80% COT mixture was heated under nitrogen for 5 minutes outside the cavity, and a spectrum of this partially isomerized film recorded. Spin concentrations were referenced to known standards.

Conductivity measurements. All films were saturatively doped with iodine either by immersion in an iodine/CCl_4 solution for 1 hour, or by vapor-phase infusion of the iodine over a period of 24 hours. Excess iodine was removed by submitting the films to high vacuum or by rinsing the film with fresh CCl_4. Film conductance was measured using a 4-point probe apparatus, and thickness was obtained with a micrometer. Dopant uptake in each case was determined by mass differential in film before and after doping.

RESULTS AND DISCUSSION

Choice of Comonomers.

A method for preparing high quality films of polyacetylene through the ring-opening metathesis polymerization (ROMP) of COT has been experimentally developed (see Chapter 3, this thesis), and the reaction has been investigated to yield a greater mechanistic understanding and more control of the polymerization reaction of cycloolefins with catalyst **1** (see Chapter 4, this thesis).

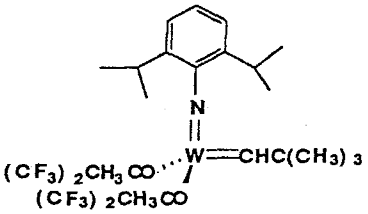

1

Homopolymers formed upon metathesis polymerization of cyclooctatetraene (COT), 1,5-cyclooctadiene (COD), and norbornene (NBE) are shown in Scheme I.

The metathesis polymerization mechanism should allow for the preparation of linear copolymers. For example, COD and COT have similar molecular structures, similar ring strain, and consequently should undergo metathesis polymerization at similar rates. Therefore, a random copolymer would be formed from copolymerization of COD and COT. Conjugated units of COT are interrupted by random insertion of COD units, and thus as shown in Scheme II the average number of consecutive COT units (**b**) [and consequently the conjugation length of polyene segments] is controlled by the COD/COT ratio. A block copolymer should be formed from NBE and COT. Norbornene has a much greater ring strain than does COT, and the near-instantaneous polymerization of NBE first produces a long block (repeat length **k**) of norbornene units (Scheme II). As norbornene concentration in the reaction mixture rapidly tapers off, COT begins to polymerize. The much slower polymerization of COT produces the final block (repeat length **m**) of consecutive COT units. Even at high NBE/COT ratios in the monomer mixture, the great difference in rates of polymerization ensures that a long block of consecutive COT units will be formed.

Homopolymerization

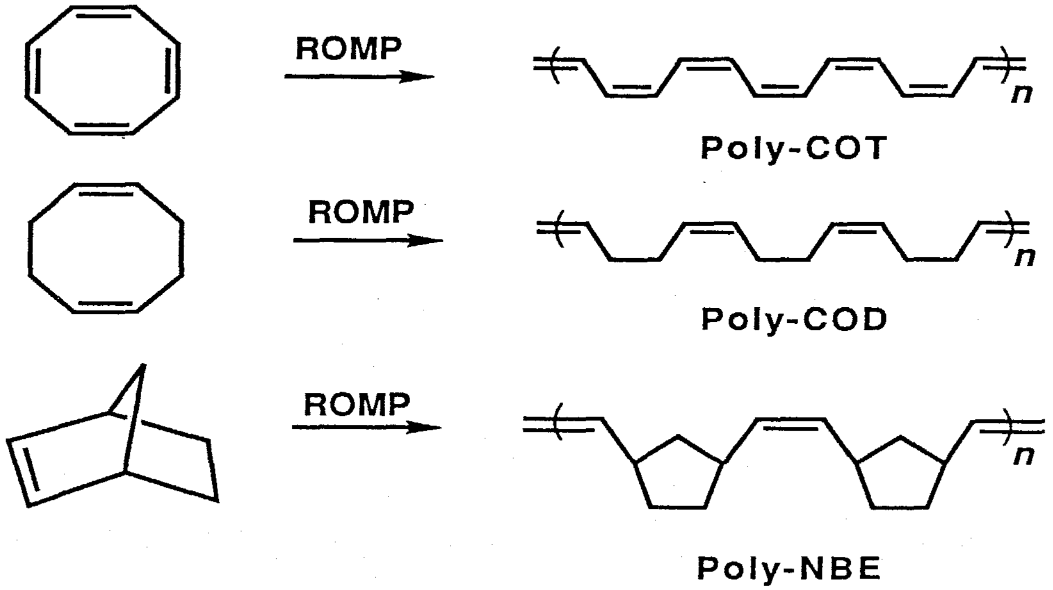

Scheme I: Polymers formed upon ring-opening metathesis of COT, COD, and NBE.

Copolymerization

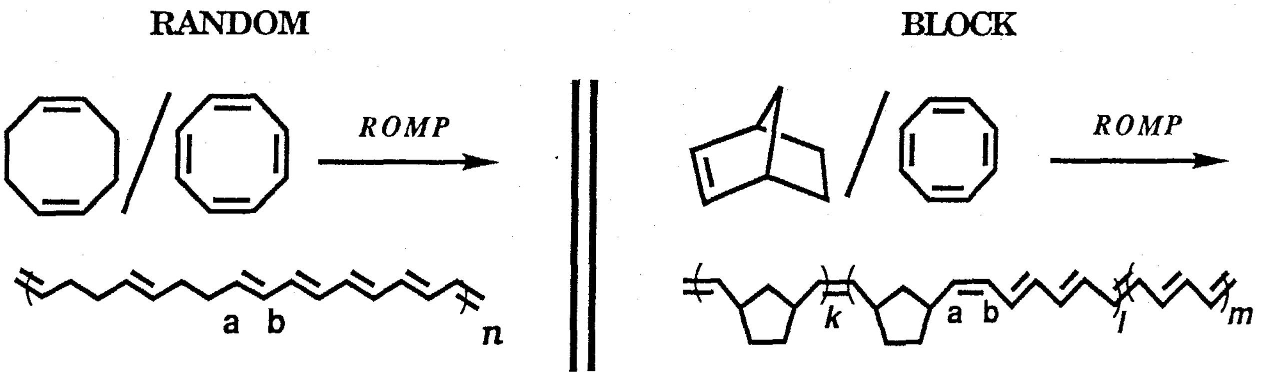

Scheme II: Linear copolymers from ring-opening metathesis of COD/COT or NBE/COT mixtures.

Dilute Solution Competition Studies.

Norbornene polymerizes much more rapidly than either COD or COT. In fact, at room temperature the polymerization of NBE with catalyst **1** is nearly instantaneous in all solvents studied. The relative rates of metathesis polymerization for COD and COT were examined by dilute solution competition studies. It is found that in tetrahydrofuran (THF) solutions at 25 °C, COD polymerizes more rapidly than does COT by a factor of 1.6 (Figure 1).[9] At 60 °C, the polymerization rate ratio -d[COD]/dt : -d[COT]/dt is reduced to 1.3 (see Figure 2), suggesting that a random distribution function for this COD/COT copolymer would be applicable.

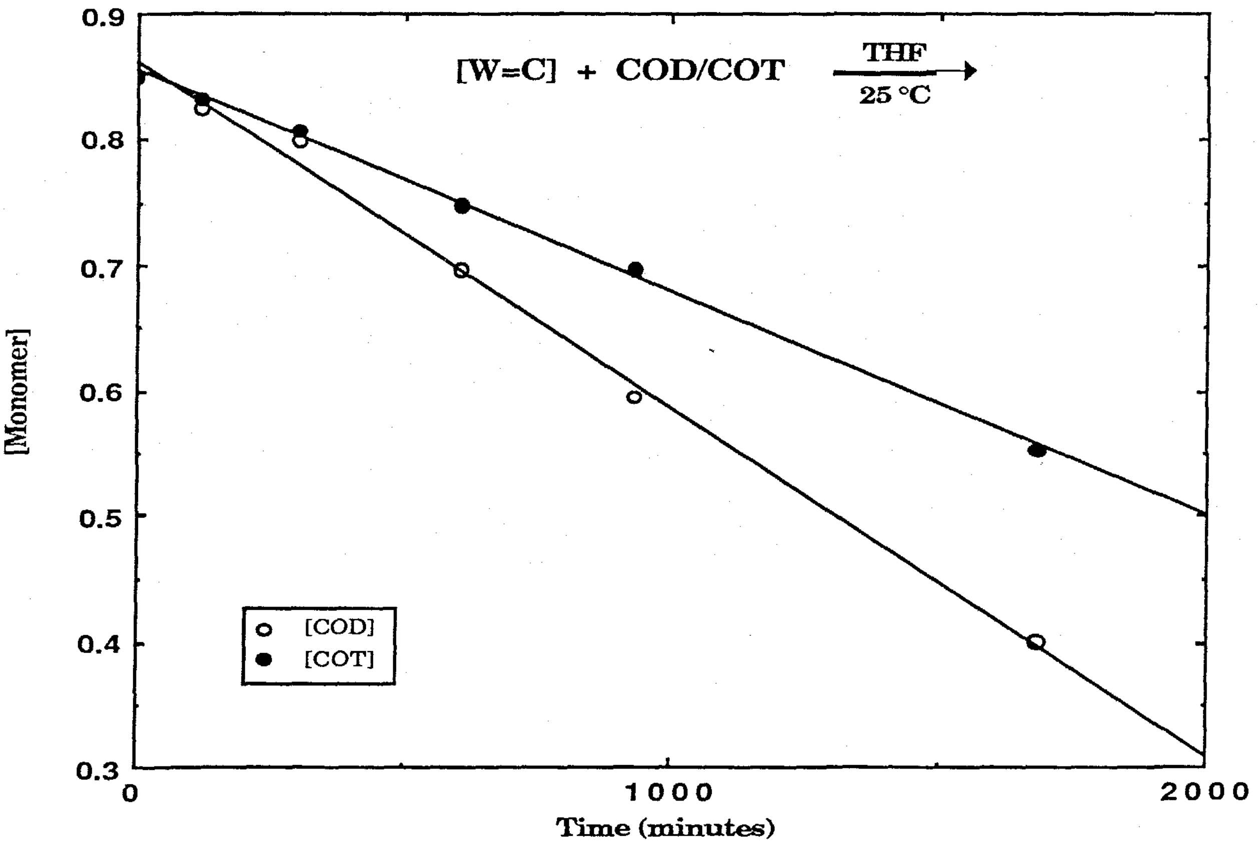

Figure 1. COD/COT Dilute Solution Competition Kinetics @ 25 °C

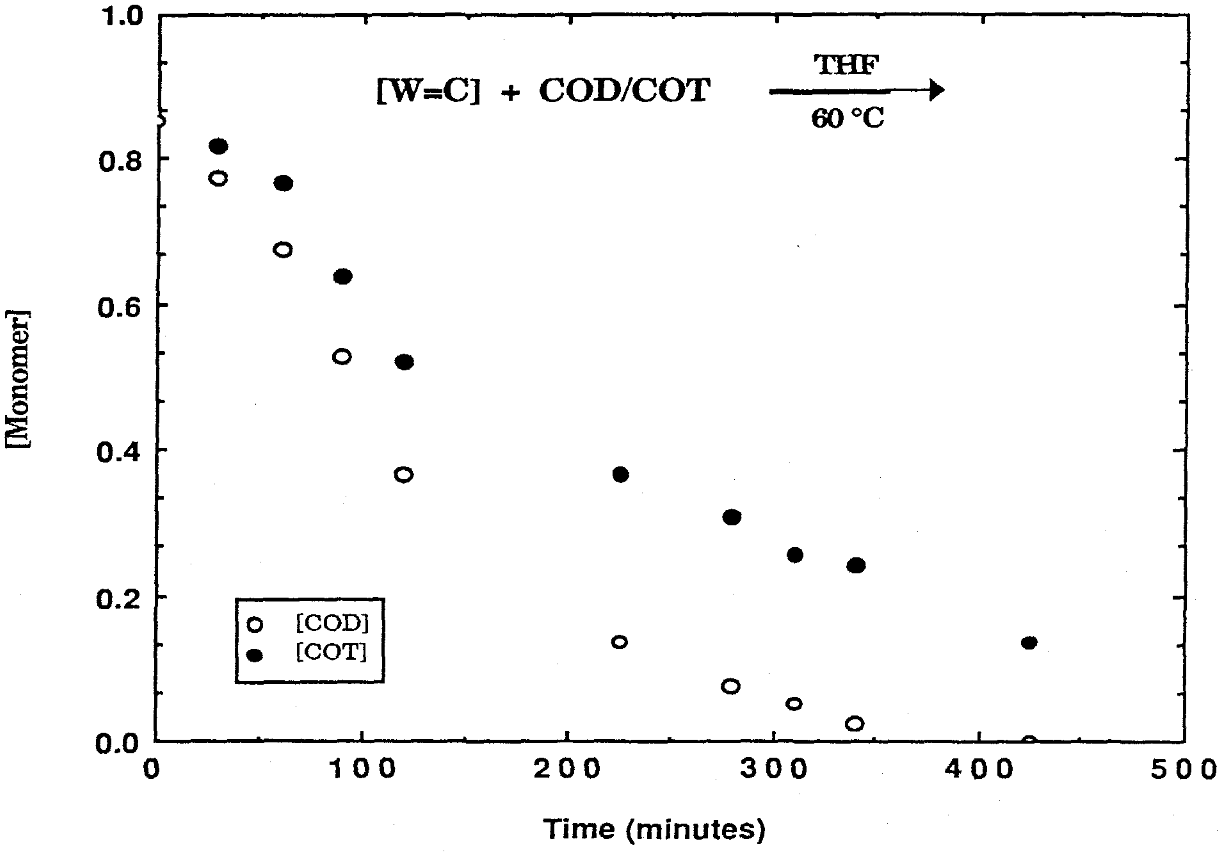

Figure 2. COD/COT Dilute Solution Competition Kinetics @ 60 °C

Distribution of Polyene Sequences for a Random (or Nearly Random) COD/COT Copolymer.

For a purely random copolymer, the probability density function describing the lengths of segments along a polymer chain is solely dependent upon (1) the ratio of concentrations for the various monomer types, and (2) the polymer chain length. If the segment lengths are normalized to the chain length, then even the chain length does not factor into the probability density; whether the copolymer is monodisperse of polydisperse in chain lengths is irrelevant.

For a random copolymer containing two different monomer units such as COD and COT, the segment density function S(n) is expressed as

$$S(\mathbf{n}) = X_1{*}P(E)_1 + X_2{*}P(E)_2$$

or $$S(\mathbf{n}) = [L - \mathbf{n} - 1][(1 - f)^2(f)^{\mathbf{n}}] + [2][(1 - f)(f)^{\mathbf{n}}] \qquad \textit{Eq. 1}$$

where
$\mathbf{n}$ = Number of consecutive COT units per segment
$P(E)_1$ = Probability of a segment containing exactly $\mathbf{n}$ consecutive COT units sandwiched between 2 COD units
$P(E)_2$ = Probability of a segment containing exactly $\mathbf{n}$ consecutive COT units at chain's end, with 1 COD unit following
X_1 = Number of permutations per chain for $P(E)_1$
X_2 = Number of permutations per chain for $P(E)_2$
L = Length (number of monomer units) per chain
f = Fraction of COT {[COT] / ([COT] + [COD])}
$S(\mathbf{n})$ = Total number of segments per chain having exactly $\mathbf{n}$ consecutive COT units

Perhaps of more interest than the number of segments per chain having exactly **n** consecutive COT units, S(**n**), is the total number of COT units involved in such S(**n**) segments, denoted as U(**n**). For example, 3.5 segments per chain having exactly 4 consecutive COT units would mean that the total number of COT units involved in segments having 4 consecutive COT units, U(4), is 3.5*4 = 14. If in addition it is found that there are precisely 0.5 segments per chain having exactly 14 consecutive COT units, then U(14) is 0.5*14 = 7, so that in this example U(4) = 2*U(14). For analytical techniques where the "signal" intensity is directly proportional to the number of carbons, this parameter U(**n**) provides a useful and valid comparison of expected signal intensity vs. segment length **n**. It should be noted that the segment length **n** is simply 4 times the conjugation length in these COD/COT copolymers, since each ring-opened COT unit contains 4 conjugated double bonds. Shown in Figure 3 is a plot of U(**n**) *vs.* **n** (chain length arbitrarily chosen as 150 monomer units). A more complete series of U(**n**) *vs.* **n** curves is included in **Appendix A**. Also, Monte Carlo simulations have been performed to verify that even for COD/COT copolymers formed during conditions in which COD polymerizes twice as fast as COT, the polyene profiles are still well-described by the purely random model for all non-extreme ratios of COD/COT (**Appendix B**).

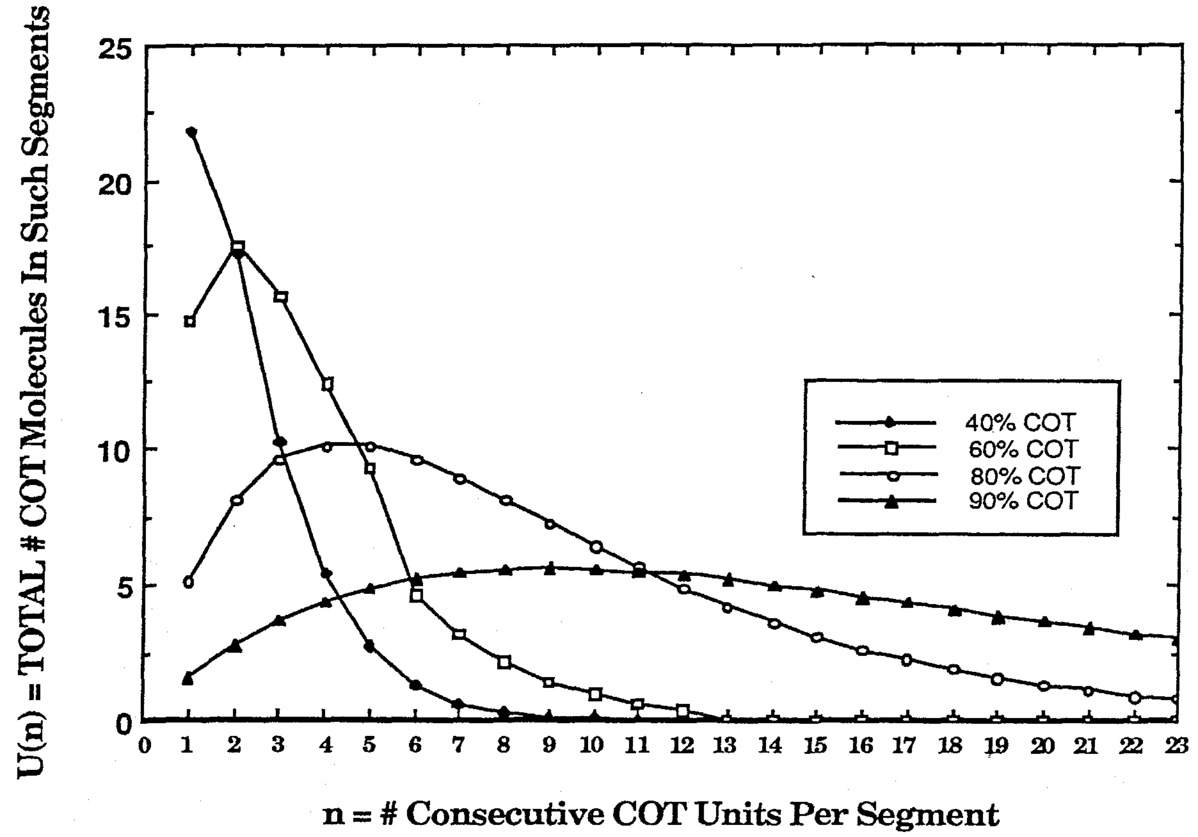

Figure 3. Calculated Polyene Densities for Purely Random COD/COT Copolymers.

Investigation of Polyacetylene Copolymer Films.

Optical Spectroscopy. The difference between the COD/COT copolymers and the NBE/COT copolymers is strikingly apparent. In the COD/COT copolymers, the appearance ranges from colorless to shiny silver. For the NBE/COT copolymers, films containing only 10% poly-COT are still shiny silver-gold indicating the presence of long conjugated segments, and confirming that the NBE/COT copolymers are indeed highly blocked.

Rather than having absorption peaks, the copolymer films exhibit a rather sharp absorption band edge (Table 1). In all the COD/COT copolymer films, there are polyene segments of very short length which have high energy transitions. There also exists the possibility of valence band to *excited* conduction band states, so that even for a single conjugation length, the polyene will absorb at several frequencies.

The COD/COT copolymers are soluble in select organic solvents (CH_2Cl_2, THF) for films containing up to about 40% poly-COT; the solution spectra for 20% COT / 80% COD and 40% COT / 60% COD copolymer films are shown in Figure 4. The vibratitional fine structure in the electronic transitions translate to energies of 1300 - 1900 cm^{-1}, corresponding to the polyene C=C vibrational transition.

Vibronic Spectroscopy. Because the vibrational transitions are strongly coupled to the electronic transitions, polyacetylene is subject to rather pronounced Raman vibronic excitations. The energies of these excitations are subject to dispersion and have been shown to demonstrate a definite dependence upon excitation wavelength; still, the vibronic absorption profiles ("peaks") are much narrower than for the optical transitions, and Raman spectroscopy remains the method of choice for characterization of conjugation lengths in long polyenes.

Table 1: Random COD/COT Copolymer Film Characteristics

% COT in Mixture	Appearance of Film	Approx. Optical Band Edge (nm)	Raman C=C peak (half-height range in cm^{-1})
0	colorless	<350	1659-1673
10	yellow	430	
20	orange	450	1517-1538
30	red-orange	470	
40	orange-red	540	1509-1544
50	red	580	
60	dark red	610	1494-1544
70	magenta (shiny)	670	
80	silver-magenta	760	1483-1542
90	dark silver		1479-1545
100	bright silver		1463-1531

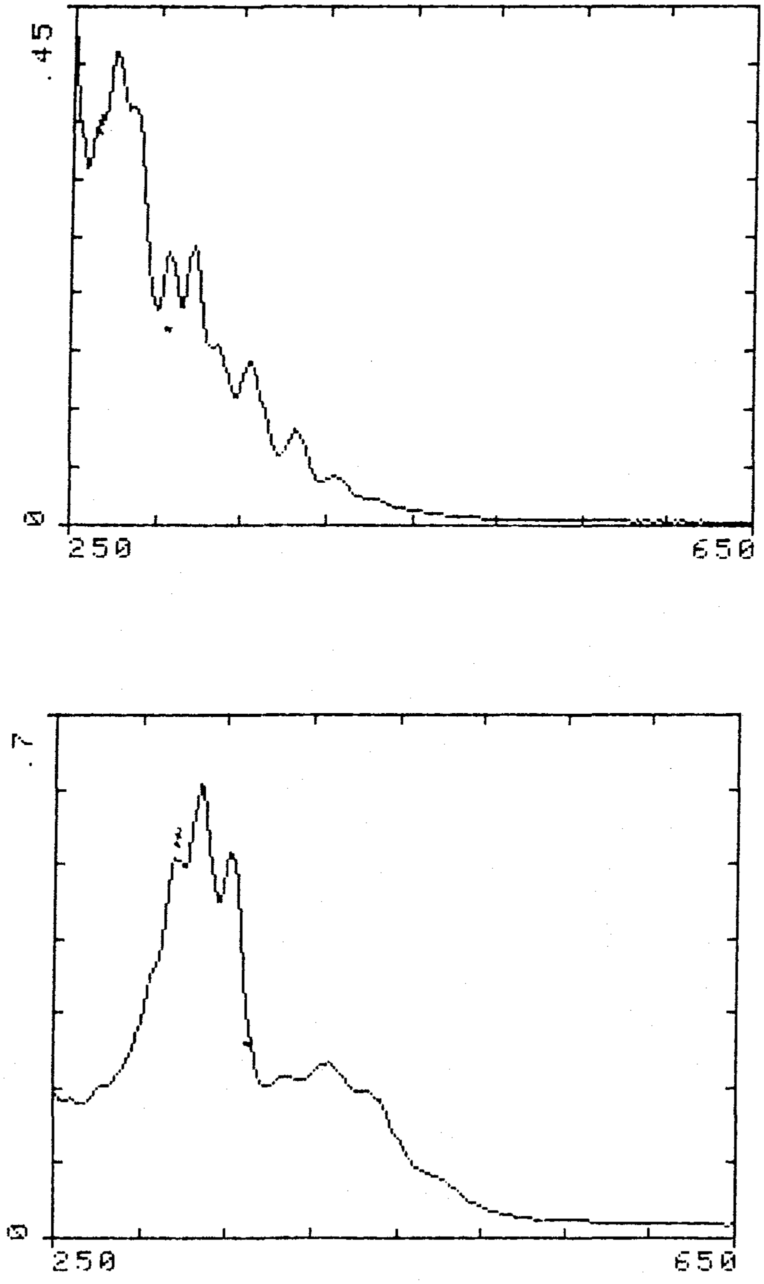

λ (cm-1)	Relative absorbance
274	0.41
286	0.36
308	0.24
322	0.24
336	0.15
356	0.14
382	0.08
406	0.04

λ (cm-1)	Relative absorbance
260	0.19
320	0.51
334	0.61
352	0.51
410	0.23

Figure 4. Optical spectra for CH_2Cl_2 solutions of COD/COT copolymer films. The top curve shows the spectrum for a 20% COT copolymer, and on bottom is the spectrum for a 40% COT copolymer. Note that with increasing COT, there is greater relative absorption in the lower energy visible region due to the longer polyenes.

The Raman profiles for the C=C absorption of the conjugated segments is shown in Figure 5 for both the COD/COT and the NBE/COT copolymer films. A laser excitation wavelength of relatively high energy (488 nm) was chosen so as to accentuate absorption of the finite (moderately short) conjugation lengths. Spectra show that upon increasing COT content in the COD/COT polymerization mixture, Raman C=C peaks of the resulting copolymer films broaden due to additional low-energy absorptions (Table 1); that is, *more long conjugation segments are being formed.* In pure poly-COT film, where each chain is absolutely uninterrupted by incorporation of saturation so that only long polyenes are present, there is a marked decrease of high-energy (short conjugation length) absorption. The same effect is observed in the NBE/COT copolymer films, implying that even in the 20% NBE / 80% COT copolymers, random insertion of perhaps even a trace of norbornene into the polyacetylene blocks can and does affect the conjugation length.

Electron Paramagnetic Resonance Spectroscopy. Electron paramagnetic resonance (EPR) reveals information about the spin concentration and spin mobility in materials. For normal short polyenes, EPR yields no signal, as spins (unpaired electrons) are created only by overcoming the high energy barrier for bond breaking, and once formed the highly reactive spins instantly dimerized unless immobilized in some frozen matrix. However, for polyacetylene spins are formed in high concentration during *cis-trans* isomerization.[10]

The spins formed in polyacetylene have been extensively studied, and are best described as neutral solitons. The wavefunction of this soliton is thought to spread out over approximately 16 carbon atoms along the backbone,[11] with greatest electron density at the center of the distribution and a node at every other carbon (this nodal distribution is in accord with simple valence bond theory). The mobility of the soliton is very much dependent upon the local *cis-trans* structural environment of the chain, with long *trans* polyacetylene sequences supporting the greater soliton mobility.

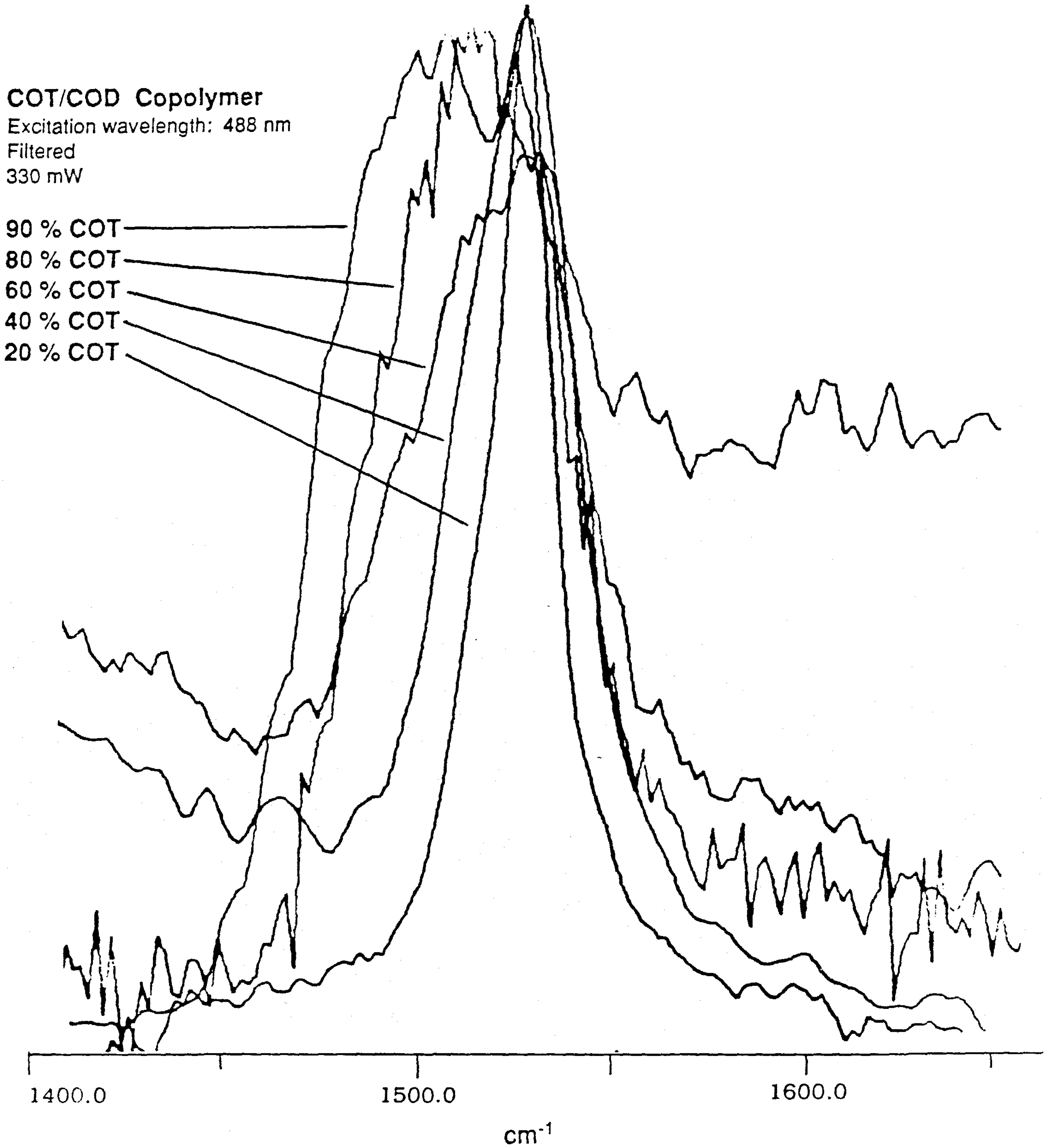

Figure 5a. Raman spectra of COD/COT copolymer films.

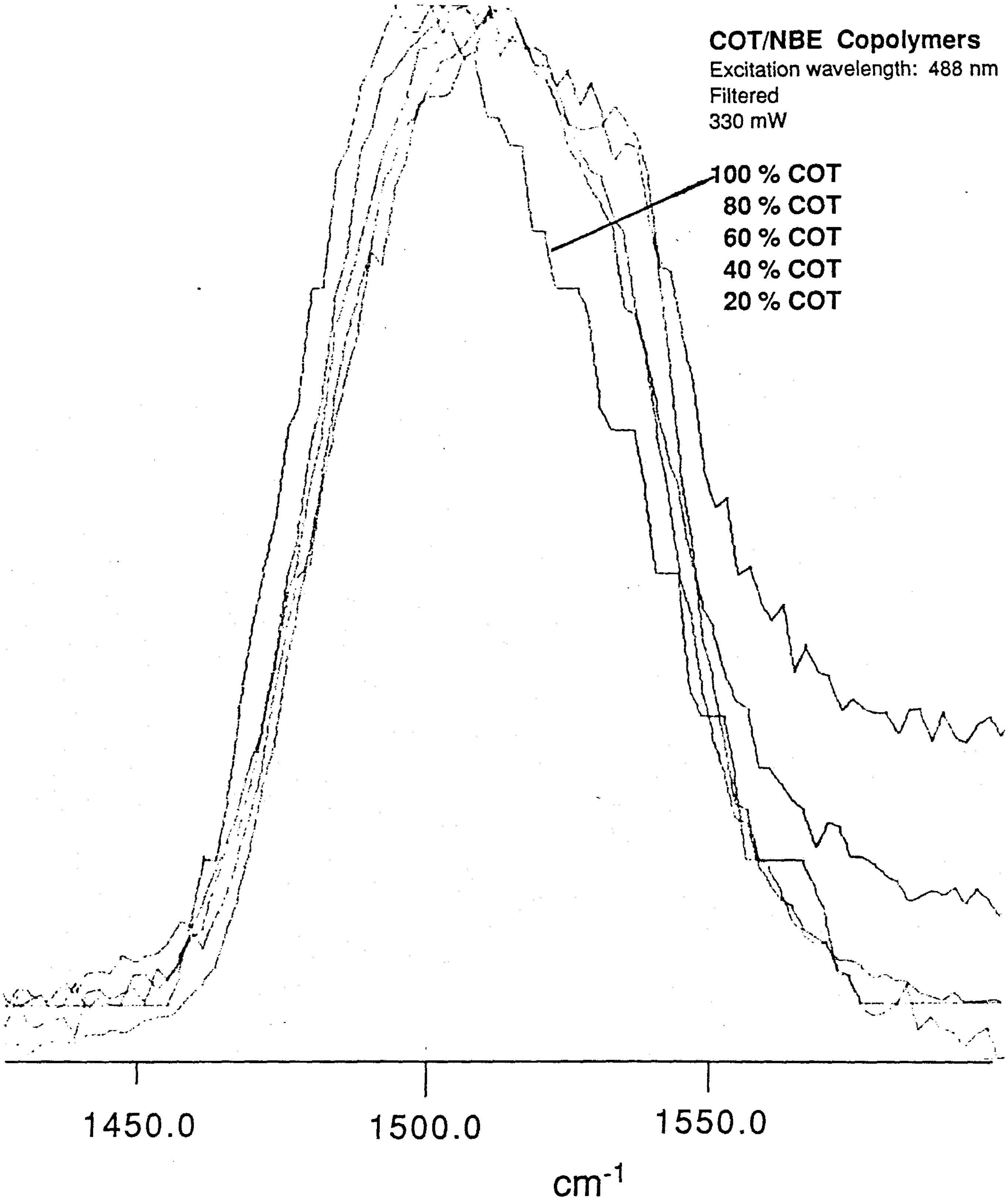

Figure 5b. Raman spectra of NBE/COT copolymer films.

The COD/COT random copolymers have been investigated by EPR (see Table 2), and the results are consistent with an increasing conjugation length for greater poly-COT content. For films containing 20% or less poly-COT no EPR signal is detected, indicative of short polyenes. As the percentage of poly-COT is increased, not only does the spin concentration increase, but also the line width of the peak undergoes substantial motional narrowing. One can conclude that even though a soliton may be created on a given polyene segment, by increasing the conjugation length of the segment the very nature of the soliton (its mobility) is altered.

Table 2: EPR Data for COD/COT Copolymer Films

% COT	Hpp (G)	[Spins / mg] * 10^{15}
10	----	----
20	----	----
40	20.0	0.08
60	13.5	0.05
80	7.50	0.67
100	5.40	1.87
80 (after isomerization)	4.10	4.01

It has already been demonstrated that pristine poly-COT film has approximately 70% of its double bonds in the *cis* configuration,[6] and it seems likely that this value would be similar for the polyene segments in the copolymers. By thermally inducing *cis-trans* isomerization, the films should undergo an increase in spin concentration and decrease in EPR line width (increased soliton mobility) according to previous results seen with pure polyacetylene. This thermal isomerization has been demonstrated by EPR for the 20% COD / 80% COT copolymer.

Conductivity. Upon oxidation (p-type doping) with iodine, polyacetylene loses electrons from its valence band and becomes conductive. Polyacetylene — prepared by any method — always exhibits a maximum iodine uptake of approximately 160% by weight, giving an elemental composition of $(CHI_{.16})_n$. However, the conductivity and dopability for shorter polyenes has been a subject riddled with speculation, until now. Conductivities of the block and random copolymers have been measured for the iodine-doped films (Figure 6).

The top curve of the first graph represents the logarythmic conductivity vs. COT content in the NBE/COT mixture. At 100% COT, the film is pure polyacetylene. At 80% COT, the films consist of 80% polyacetylene in 20% insulating matrix — polynorbornene. In fact, the conductivity curve is governed by general percolation theory, where the percolation threshhold — the metal to insulator transition — occurs at 15-20% of the conductor in the insulator matrix.

In contrast, the top curve of the second graph depicts logarythmic conductivity vs. polyacetylene content for the random copolymer films (*note the different abscissa scale*). By the point to where the polyacetylene content has dropped to 60%, the material is insulating.

(1) At 60% polyacetylene in the <u>block</u> films, the material has a very substantial conductivity.

(2) At 60% polyacetylene in the <u>random</u> films, the material is insulating.

In the random copolymers, the polyacetylene consists of a distribution of much shorter conjugation lengths, only a portion of which are conductive. In fact, the dopant uptake (lower curve in each graph) shows that in the block copolymers the iodine uptake is approximately proportional to polyacetylene content. All the polyacetylene is getting oxidized and contributing to conduction. In the random copolymer, however, the 60% polyacetylene film takes up no detectable amount of iodine; the short conjugation lengths are not getting oxidized. The experimental conclusion is that conjugation length does indeed affect conductivity, a point which has been the subject of considerable debate among polyacetylene scientists.

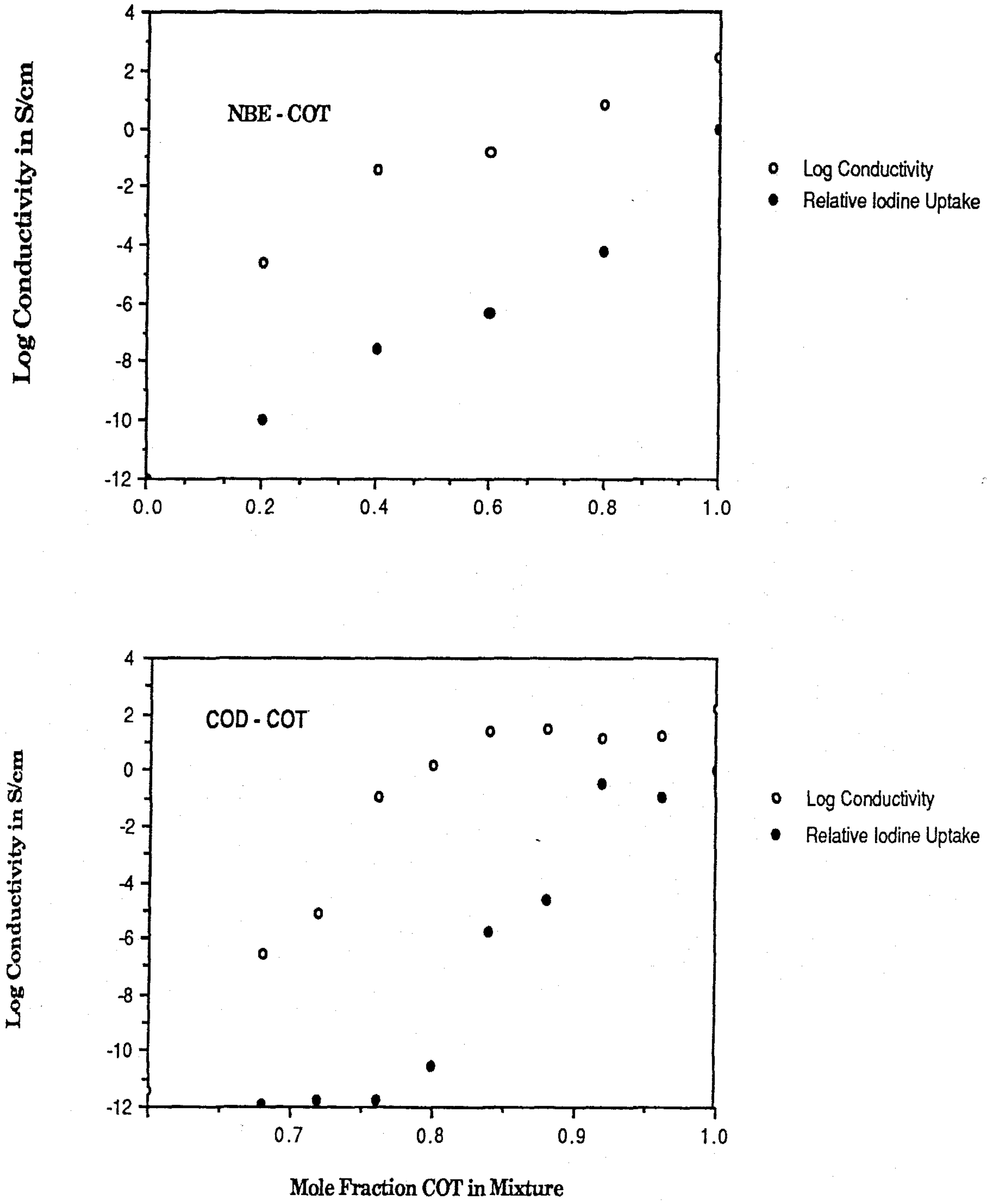

Figure 6: Conductivities and Dopant Uptake of NBE-COT Block and COD-COT Random Polyacetylene Copolymer Films.

Another important point is that the conductivity of the random films can be varied over 10 orders of magnitude from the insulating regime, through the semi-conducting regime, to metal-like conductivities merely by varying the film's composition from 60% to 80% polyacetylene.

Nuclear Magnetic Resonance Spectroscopy. The COD/COT copolymer films — up to about 40% poly-COT — can be dissolved in solvents such as THF and CH_2Cl_2. Upon increasing COT content in the co-monomer polymerization mixture from 20% to 40%, ^{1}H NMR of the dissolved films reveals a new (downfield) broad peak (Figure 7), again indicative of longer conjugation segments with increasing COT content. For reference, the proton shift of grafted polyacetylene occurs at about 7.1 ppm.[12]

Non-linear Optical Spectroscopy. Figure 8 reveals non-linear optical measurements of χ^3 as a function of COT incorporation into the COD/COT copolymers. With increasing COT, the χ^3 value increases exponentially. Measurements were performed on solutions of the COD/COT copolymer in THF.[13] The *cis-trans* structure of the polyene segments needs to be investigated before this data can be compared to other investigations of non-linear optical properties as a function of conjugation length.

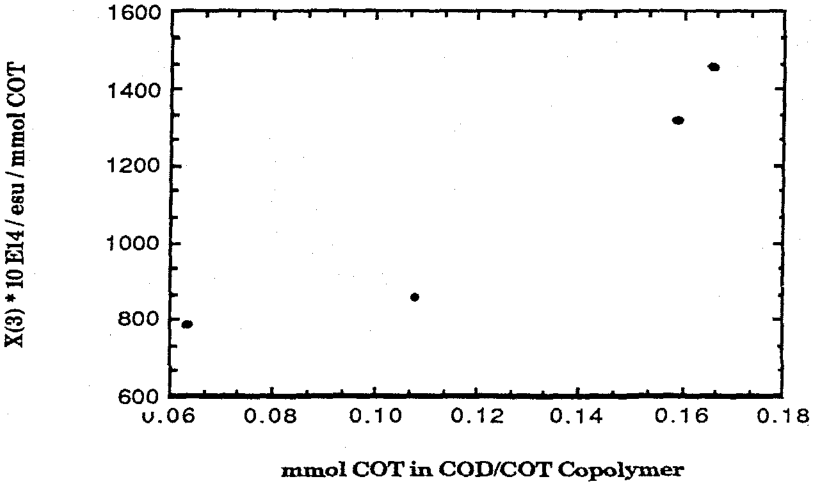

Figure 8: Third Harmonic Generation in COD/COT Copolymer Solutions.

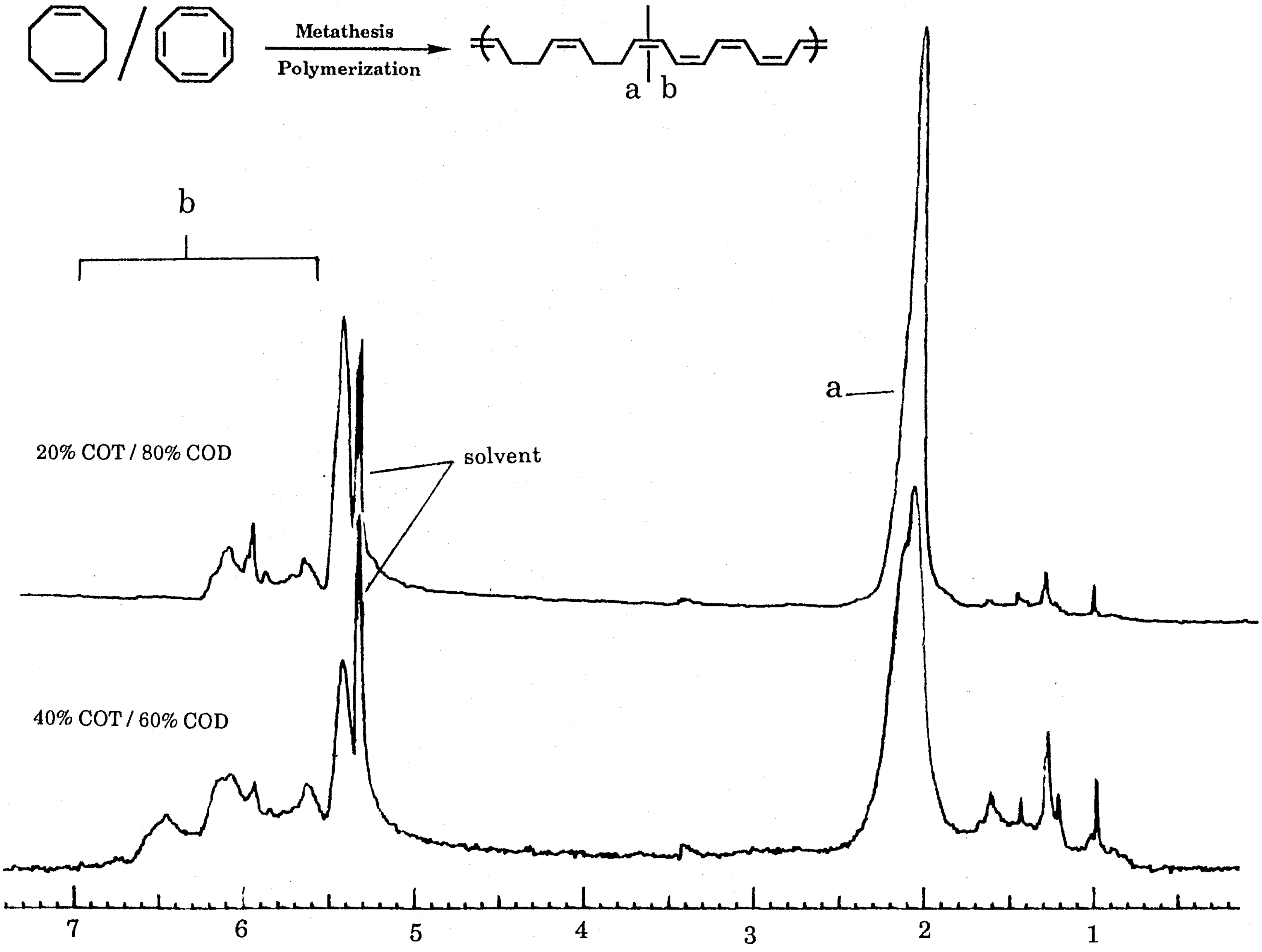

Figure 7. ^{1}H NMR of COD/COT copolymer films.

Atmospheric Stability. The NBE/COT block copolymers seem to be more susceptible to atmospheric degradation than pure poly-COT film, perhaps due to the increased porosity that the copolymerization imparts to the material. The stability of the COD/COT random copolymers has been followed by optical spectroscopy. Shown in Figure 9a are the transmission spectra of the copolymer films taken prior to atmospheric exposure, and shown in Figure 9b are the transmission spectra of the same copolymer films after 14 days exposure to air. As previously suggested by the dopant uptake studies, the longer chain polyenes are more susceptible to oxidation and consequently more susceptible to atmospheric degradation.

Thermal Stability. Thermogravimetric analysis was performed on various compositions of the COD/COT copolymer films in a nitrogen atmosphere to probe their relative stabilities. All films, ranging from pure poly-COT to pure poly-COT, begin decomposing rapidly as the temperature reaches 470 - 500 °C; however, the percent residue ("graphitization yield") after prolonged pyrolisis varies markedly (Table 3). It is interesting that the films undergo decomposition at similar temperatures in both poly-COT and poly-COD films, whereas the nature of the C-C bond is very different for these two polymers.[14]

Table 3: Graphitization of COD/COT Copolymer Films

% COT	Graphitization Yield (Percent by Weight)
0	0
20	2
40	6
60	9
80	16
100	21

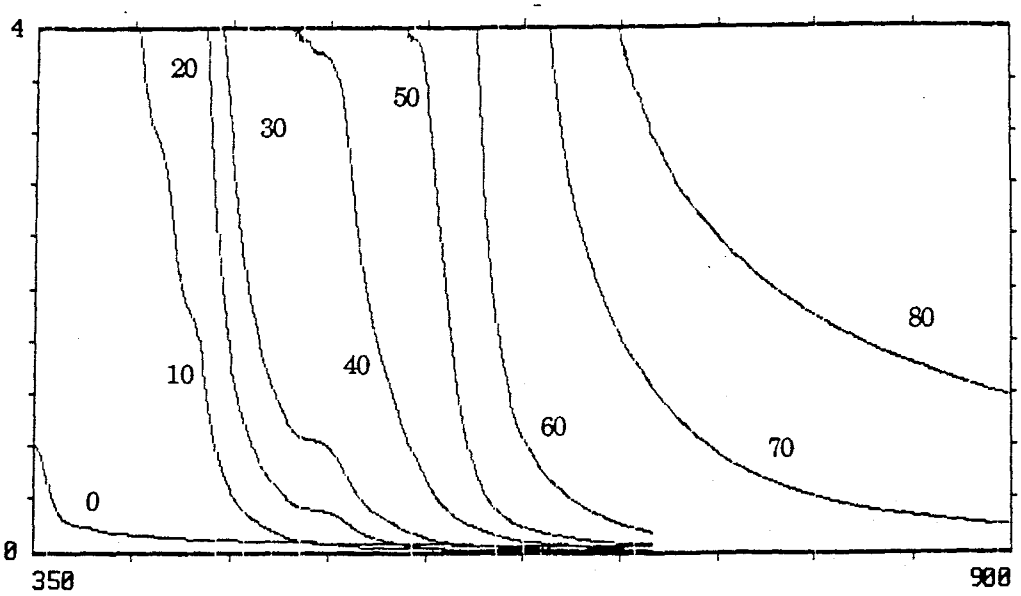

Figure 9a. Optical spectra of COD/COT random copolymer films, taken immediately following preparation. Numbers in figure are percent COT in films.

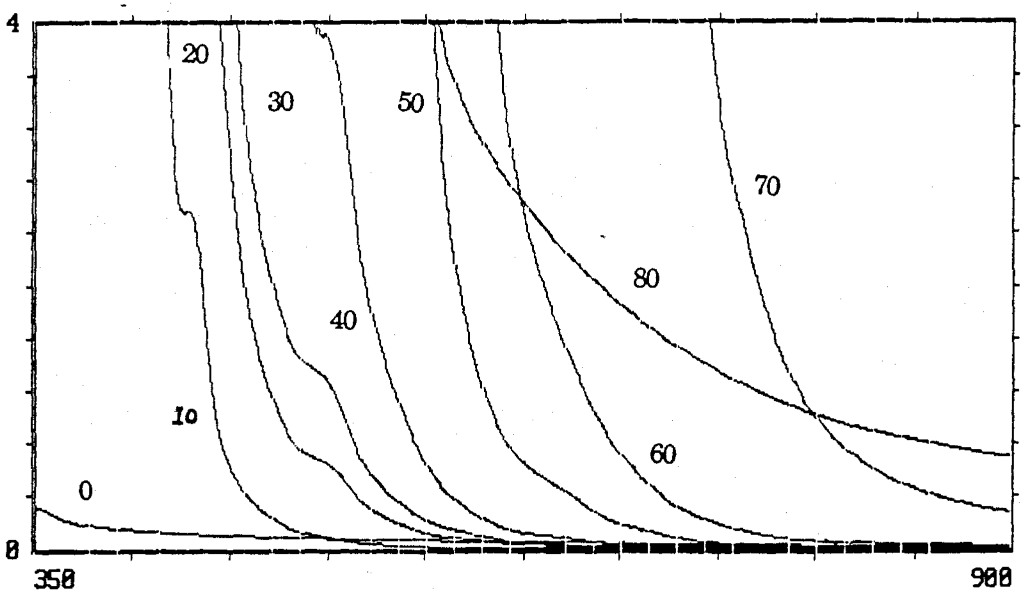

Figure 9b. Optical spectra of same COD/COT copolymer films as in Figure 9a, taken after two weeks exposure to atmosphere. The absorption profiles of the copolymer films containing a low percentage of COT remain virtually unchanged; however, with high COT content and therefore longer polyenes, these copolymer films become more susceptible to degradation.

SUMMARY

Cyclooctatetraene undergoes ring-opening metathesis with other cycloolefins to form linear copolymers in either random or block fashion, dependent upon choice of monomer. Mechanical, electrical, and optical properties are varied by controlling the ratio of COT to comonomer. The random copolymerizations provide a facile route into finite polyenes ranging from very short conjugation lengths to "infinite" conjugation lengths ("neat" COT polymerizes to give polyacetylene). These random copolymers can be tailored to have iodine-doped conductivities ranging from the insulator regime to the metallic regime, again dependent upon mole fraction COT. This approach to the synthesis of polyene sequences spanning the range of conjugations lengths maintains a high degree of experimental control. Continued investigation into these new materials should lead to a greater understanding of finite conjugation sequences and conducting polymers in general.

REFERENCES

(1) For an excellent compilation of polyacetylene research, see Chien, J. C. W. *Polyacetylene*; Academic Press: Orlando, FL, 1984.

(2) Basescu, N.; Liu, Z.-X.; Moses, D.; Heeger, A. J.; Naarmann, H.; Theophilou, N. *Nature* **1987**, *327*, 403.

(3) *Handbook of Conducting Polymers*; Skotheim, T. A., Ed.; Marcel Dekker, Inc.: New York, 1986; Vols. 1 and 2.

(4) (a) Aldissi, M.; Bishop, A. R. *Synth. Met.* **1986**, *14*, 13. (b) Aldissi, M. *Synth. Met.* **1986**, *13*, 87. (c) Bates, F.; Baker, G. *Macromolecules* **1983**, *16*, 1013. (d) Bates, F.; Baker, G. *Macromolecules* **1983**, *16*, 704. (e) Bolognesi, A.; Catellani, M.; Destri, S.; Porzio, W. *Polymer* **1986**, *27*, 1128.

(5) (a) Gibson, H. W.; Pochan, J. M. *Encyclopedia of Polymer Science and Engineering*; Wiley-Interscience: New York, 1985; Vol. 1, pp 87-130. (b) Deits, W.; Cukor, P.; Rubner, M.; Jopson, H. *Synth. Met.* **1982**, *4*, 199.

(6) Klavetter, F. L.; Grubbs, R. H. *J. Am. Chem. Soc.* **1988**, *110*, 7807.

(7) Reppe, W.; Schichting, O.; Klager, K.; Toepel, T. *Ann.* **1948**, *560*, 1.

(8) Schaverien, C.; Dewan, J.; Schrock, R. R. *J. Am. Chem. Soc.* **1986**, *108*, 2771.

(9) It is interesting to note that in the previous chapter of this thesis (Chapter 4) it was found that COD homopolymerizes at a rate 15 times faster than the COD in a COD/COT copolymerization. It is possible that the ring-opened COT unit appended to the tungsten carbene (W=C-C=C-C=C-C=C-C=C-) is retarding the polymerization rate by deactivating the tungsten center (that is, by releasing electron densio the highly electronegative metal d orbitals involved in metathesis.

(10) (a) Shirakawa, H.; Ito, T.; Ikeda, S. *Makromol. Chem.* **1978**, *179*, 1565. (b) Chien, J. C. W.; Karasz, F. E.; Wnek, G. E.; MacDiarmid, A. G.; Heeger, A. J. *J. Polym. Sci., Polym. Lett. Ed.* **1980**, *18*, 45. (c) Bernier, P.; Linaya, C.; Rolland, R.; Aldissi, M. *Polymer* **1980**, *21*, 7.

(11) (a) Su, W. P.; Schrieffer, J. R.; Heeger, A. J. *Phys. Rev. Lett.* **1979**, *42*, 1698. (b) Rice, M. J. *Phys. Lett.* **1979**, *71A*, 152. (c) Takayama, H.; Lin-Liu, Y.; Maki, K. *Phys. Rev. B* **1980**, *21*, 2388.

(12) Bates, F.; Baker, G. *Macromolecules* **1983**, *16*, 704.
(13) Marder, S.; Perry, J.; Klavetter, F.; Grubbs, R. *Materials* **1989**, *1*, 171.
(14) Poly-bromocyclooctatetraene, which contains the much weaker C-Br bond, undergoes substantial weight loss beginning at 150 °C (unpublished results, this laboratory).

Appendix A

Conjugation Length Profiles for Various Compositions of COD/COT Copolymers

For the compositions of COD/COT copolymers containing 10%, 20%, 40%, 60%, 80%, and 90% poly-COT, the statistical distribution of conjugation lengths has been calculated according to the formulas

$$S(\mathbf{n}) = [L - \mathbf{n} - 1][(1 - f)^2(f)^{\mathbf{n}}] + [2][(1 - f)(f)^{\mathbf{n}}] \qquad (1)$$

$$U(\mathbf{n}) = S(\mathbf{n})*\mathbf{n} \qquad (2)$$

where $\mathbf{n}$ = Number of consecutive COT units per segment
L = Length (number of monomer units) per chain
f = Fraction of COT {[COT] / ([COT] + [COD])}
$S(\mathbf{n})$ = Total number of segments per chain having exactly **n** consecutive COT units
$U(\mathbf{n})$ = Total number COT molecules involved in segments having exactly **n** consecutive COT units

For all of these calculations, the polyene segment conjugation length is four times the number of consecutive COT units, or 4**n**. The chain length for all the profiles was arbitrarily chosen to be 150 monomer units.

If it is the case that only 1 neutral soliton can exist on a given polyene segment, then data such as electron paramagnetic spectroscopy spin intensities, for example, would best correlate with S(n) profiles, which describe the number of segments of various conjugation lengths. However, for characterization methods sensitive to the total number of olefinic carbon atoms in a given conjugation length (for example, ^{13}C NMR with pulse-delayed integration), the U(n) profiles will provide a better description of the expected signal intensities.

Figure 10. 15 COT Monomer Units Per Chain (10% COT)

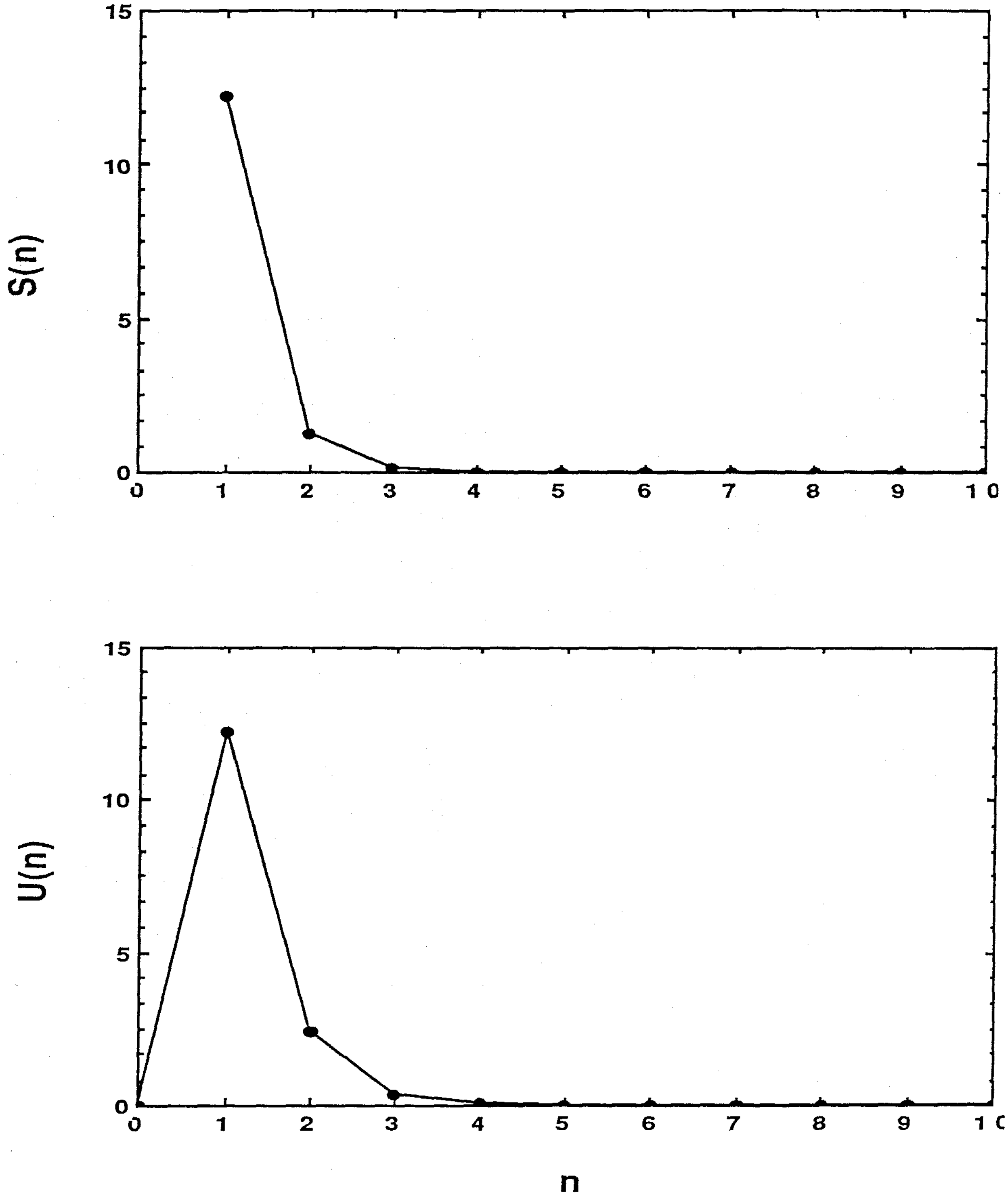

Figure 11. 30 COT Monomer Units Per Chain (20% COT)

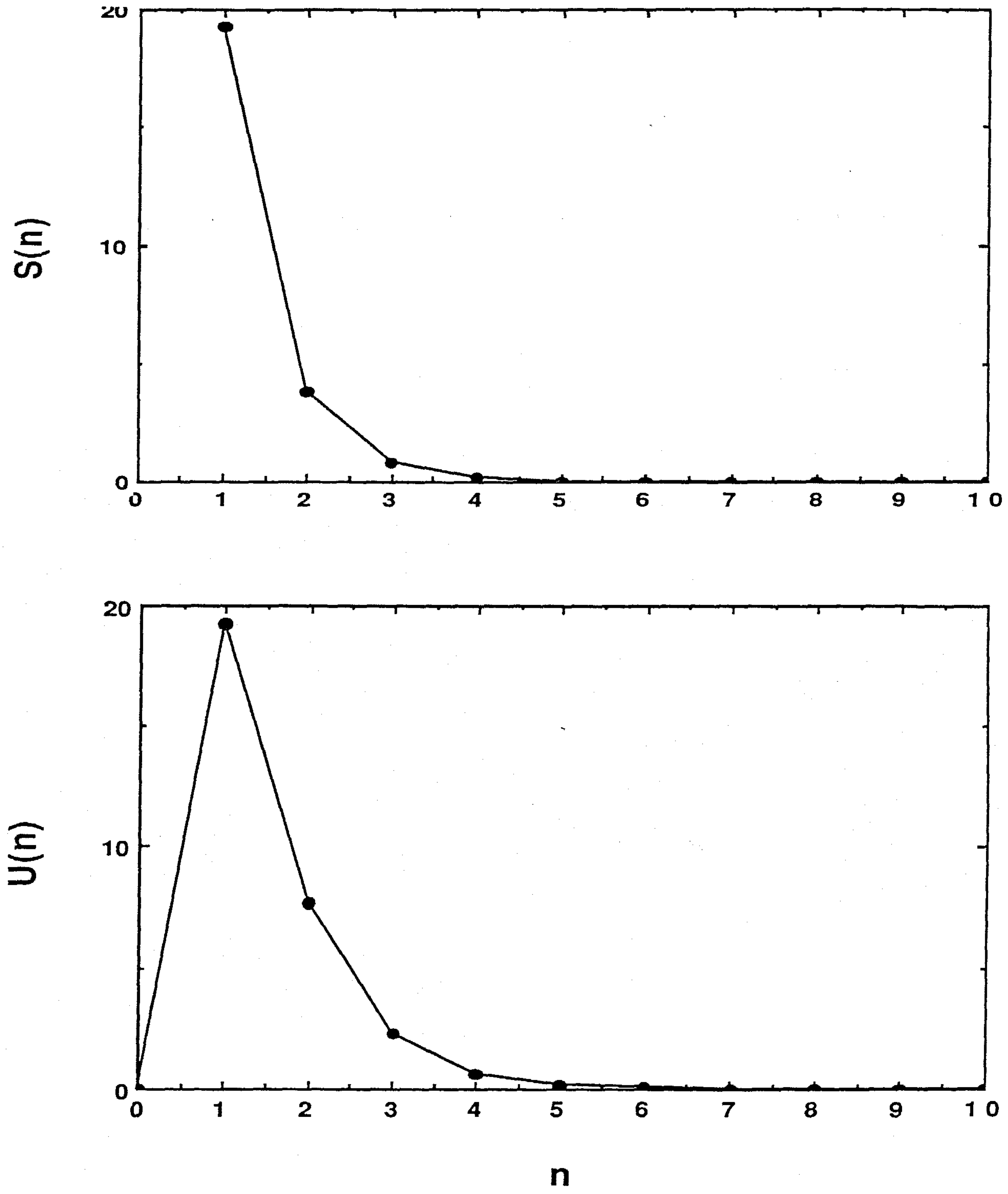

Figure 12. 60 COT Monomer Units Per Chain (40% COT)

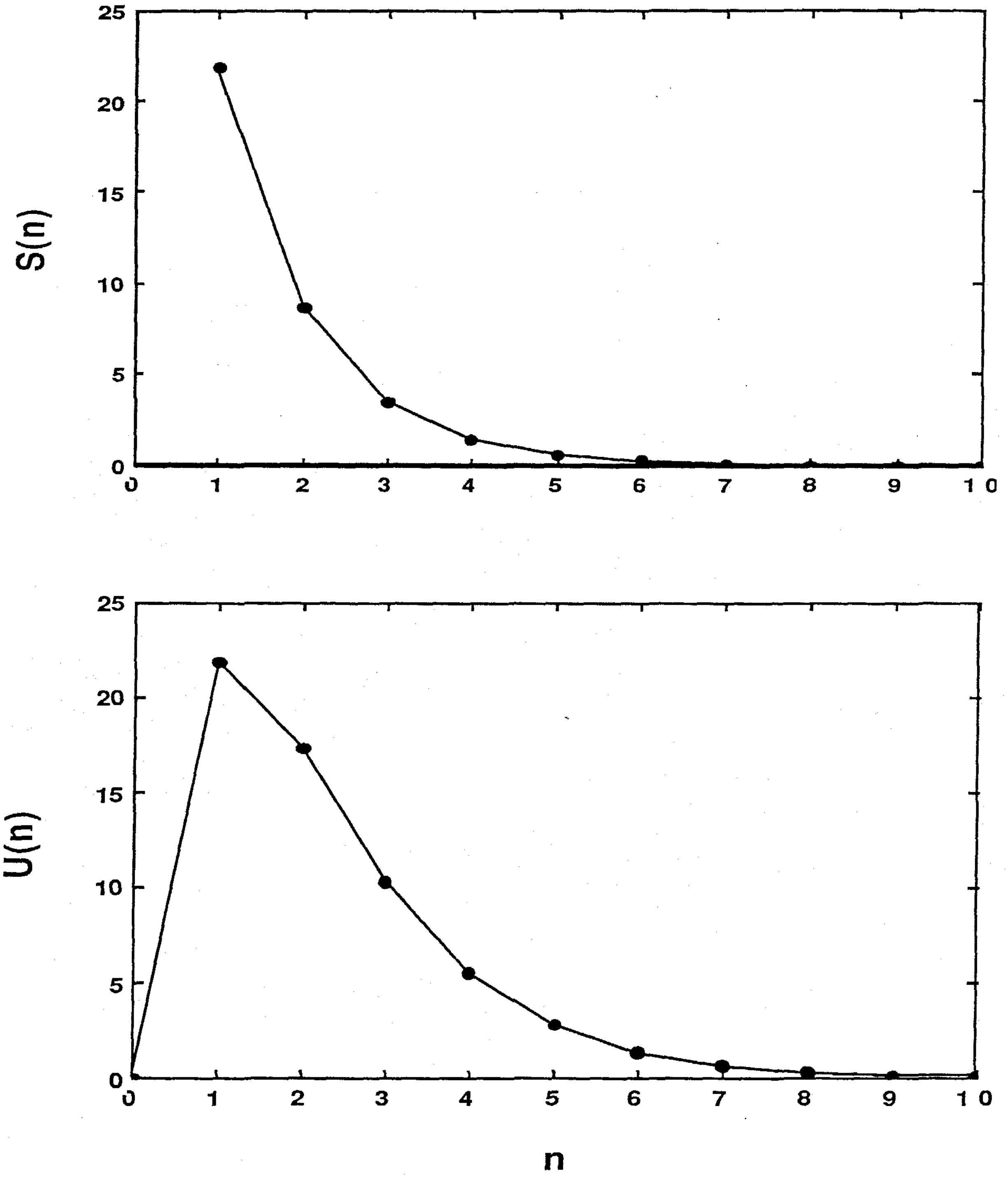

Figure 13. 90 COT Monomer Units Per Chain (60% COT)

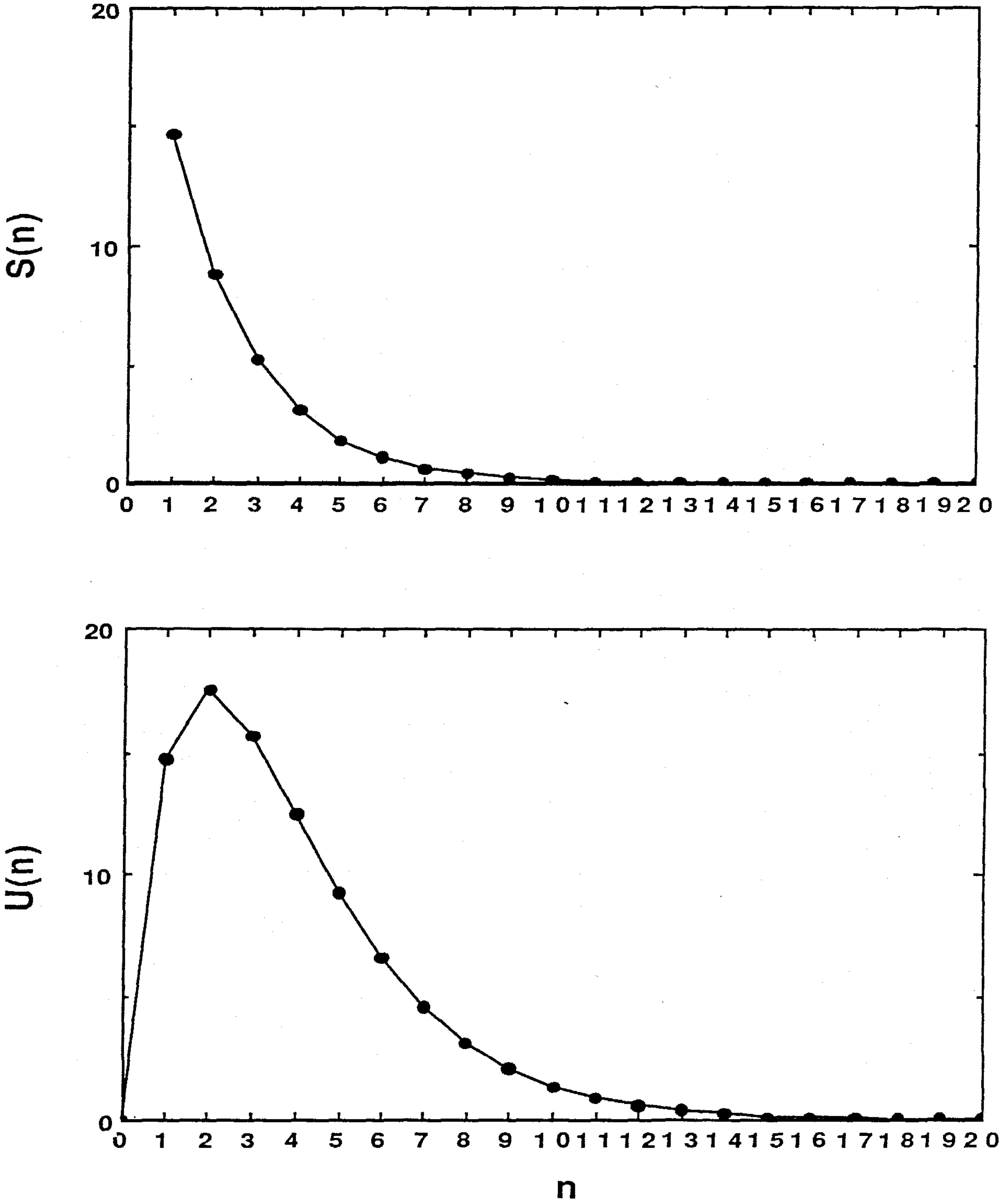

Figure 14. 120 COT Monomer Units Per Chain (80% COT)

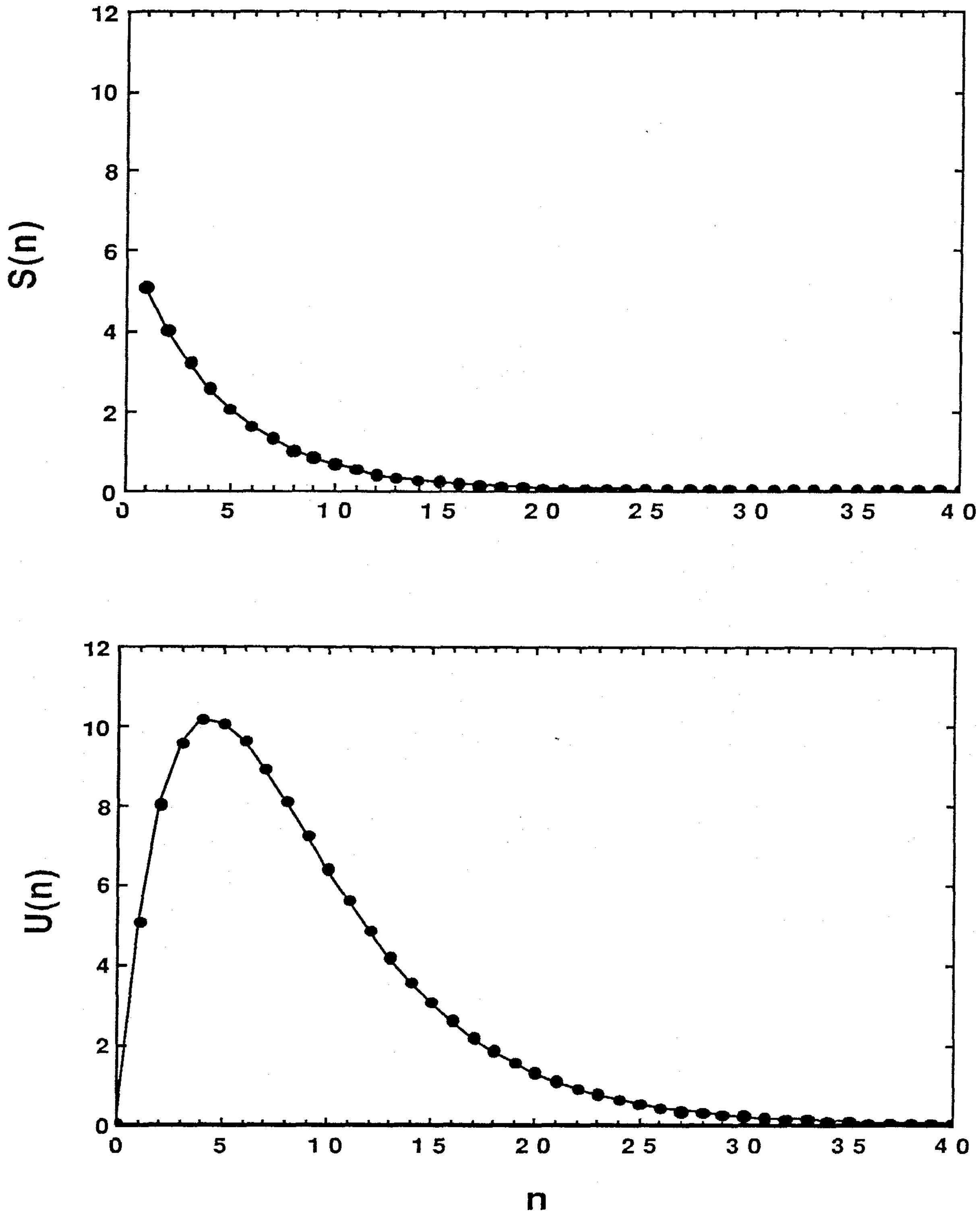

Figure 15. 135 COT Monomer Units Per Chain (90% COT)

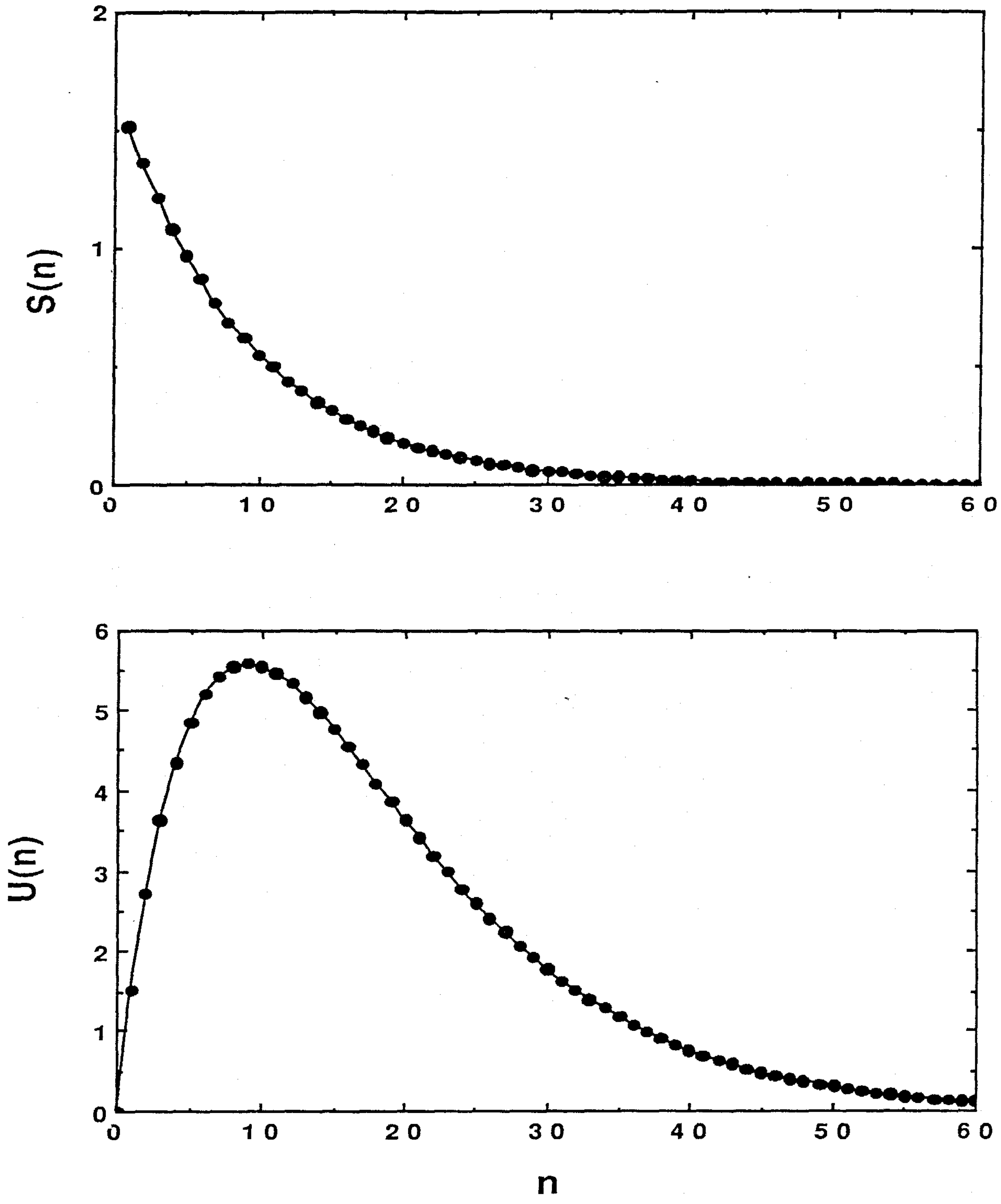

Appendix B

Monte Carlo Simulations for COD/COT Copolymers (Varying COD/COT Rates)

The following program generates the density profiles in Figure 16 (COD and COT react at equal rates) and Figure 17 (COD reacts twice as fast as COT).

```
5   REM: MONTE CARLO SIMULATION OF A COD/COT COPOLYMERIZATION.
10  DIM D(500), T(500)
20  INPUT "# COD, COT MOLECULES"; W,E
25  REM: W + E = CHAIN LENGTH AND SHOULD CONVENIENTLY BE ~150.
30  INPUT "HOW MANY TIMES FASTER DOES COD REACT THAN COT?";F
40  INPUT "# RANDOM SEEDS, TRIALS PER SEED";P,X
45  REM: MONTE CARLO CALCULATIONS BEGIN HERE
50  FOR U = 1 TO P
60  RANDOMIZE
70  FOR G = 1 TO X
80  A = W:B = E
90  PRINT G
110 FOR H = 1 TO A+B
120 N = F*A+B: PA=F*A/N
140 V=RND
150 IF V<PA, THEN 230
160 REM: COT HAS POLYMERIZED, STATEMENTS 170, 220 EXECUTED
170 B=B-1: D(K)=D(K)+1:K=0:J=J=1
220 GOTO 280
230 REM: COD HAS POLYMERIZED, STATEMENT 240 EXECUTED
240 A=A-1: T(J)=T(J)+1:J=0:K=K+1
280 NEXT H
290 IF J>0 THEN 320
300 D(K)=D(K)+1
310 GOTO 330
320 T(J)=T(J)+1:J=0:K=0
340 NEXT G
350 NEXT U
360 REM: REST OF PROGRAM IS OUTPUT OF CALCULATIONS
370 LPRINT "MONTE CARLO SIMULATION OF  COPOLYMERIZATION":LPRINT:LPRINT
390 LPRINT "COD REACTS";F;"TIME(S) FASTER THAN COT":LPRINT P;"SEEDS &";X;"TRIALS
    PER SEED"
410 LPRINT W;"COD MOLECULES &"; E; "COT MOLECULES":LPRINT "N = # CONSECUTIVE
    COT MOLECULES"
430 LPRINT:LPRINT:LPRINT:LPRINT "N" ; TAB(10) ; "COD SEGMENTS"; TAB(25) ; "COT
    SEGMENTS";TAB(40);"TOTAL COD";TAB(55);"TOTAL COT":LPRINT
460 I=I+1
470 Z = INT (T(I)/P/X*I*100)/100:Z1 = INT (D(I)/P/X*I*100)/100
490 LPRINT I; TAB(10); INT(D(I)/P/X*100)/100; TAB(25); INT     (T(I)/P/X*100) / 100; TAB(40);
Z1; TAB(55); Z
500 Q=Q+Z:Q1=Q1+Z1
520 IF (Q+Q1)>(.99*(W+E)) THEN 540
530 GOTO 460
540 PRINT "COT TOTAL =";Q:PRINT "COD TOTAL =";Q1:END
```

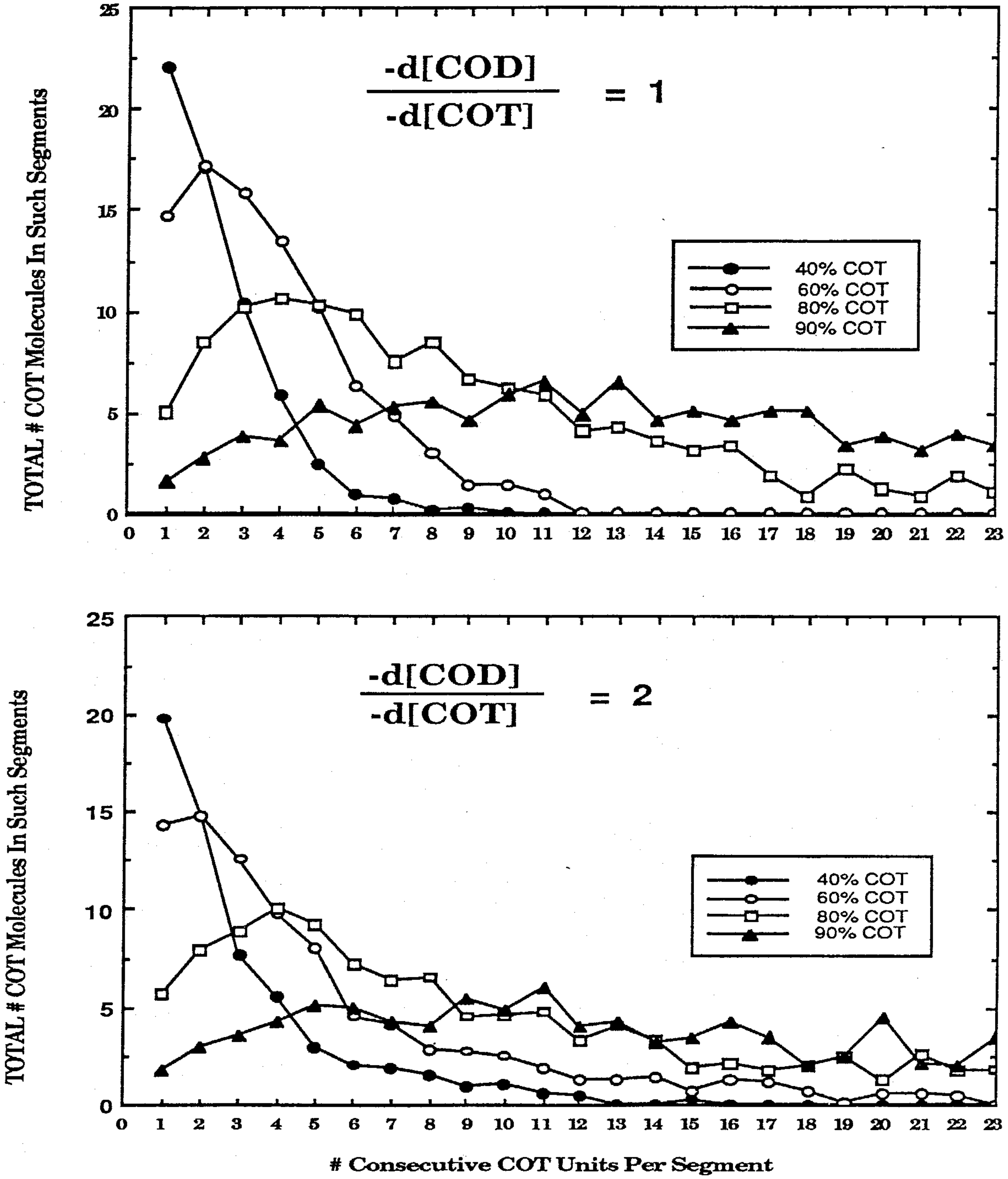

Figure 16 (top) and Figure 17 (bottom): COD/COT Monte Carlo Simulations. The top curve illustrates polyene density profiles for a purely random copolymer, as generated through Monte Carlo computations (see Figure 3 — polyene densities calculated through probability formulas — for comparison). In the bottom curve in which COD reacts twice as fast as COT, still a highly random copolymer is formed.